FINAL REPORT

IN SITU BIORESTORATION OF NITRATE CONTAMINATED WATER WELLS

Volume 2

MODELING STUDIES

Project Investigators:

M. Yavuz Corapcioglu and W. Michael Stallard

Department of Civil Engineering
Texas A&M University
College Station, TX 77843-3136

Phone (409) 845-9782
e-mail yavuz@acs.tamu.edu

December 1995

ABSTRACT

The investigation of a technique for protecting a downstream drinking water well from nitrate contamination of groundwater is presented. A recirculating nitrate treatment well system is proposed in which groundwater is drawn into the well, denitrified in the treatment chamber, and returned to the top of the aquifer. Well hydraulics were experimentally examined in a two-dimensional aquifer model, and ambient groundwater velocities of 1 to 3 m/day were simulated in combination with well recirculation rates of 25 to 200 ml/min. An on-line feed control system was developed for testing the treatment barrier associated with well recirculation and biological denitrification. The impacts of carbon feed, groundwater flow, nitrate loading, and well recirculation on the performance of system operation were also investigated.

Hydraulic problems identified with experimental apparatus included blow-through of contaminant at the well intake by high ambient groundwater velocities and submergence by the well hydraulics of depth-distributed contaminant plumes without interception. The problems associated with biological denitrification were found to be possible permeability loss by screen fouling and blinding of soil pores by overfeed of carbon. These identified problems were corrected by maintaining a greater well recirculation rate and adjusting carbon feed at stoichiometric ratio of nitrate load to the well.

This study has demonstrated that the recirculating nitrate treatment well system may be a feasible process for protecting drinking water wells from groundwater contamination in a sandy unconfined aquifer. Experimental results provide guidance in identifying parameters that could possibly affect the performance of the treatment system. On the basis of experimental results, the procedures of system design were also developed for evaluating the feasibility of the proposed methodology.

TABLE OF CONTENTS

LIST OF FIGURES

FIGURE   Page

LIST OF TABLES

CHAPTER I

INTRODUCTION

BACKGROUND

Groundwater is one of the most precious natural resources in the United States. It has been estimated that approximately 100 million people, about fifty percent of the total U.S. population, and ninety percent of those who live in rural areas, are dependent on groundwater for drinking proposes (Bitton and Gerba, 1984). However, nitrate contaminants from natural and man made sources are causing an ever more increasing decline in the quality of this resource. According to the U. S. Environmental Protection Agency, approximately 5% of both public and private drinking water wells in the United States exceed the USEPA maximum nitrate contaminant limit in drinking water (USEPA, 1990). In some areas, 20% of drinking wells tested showed excessive levels of nitrates ranging up to 20 times the recommended limit (Anderson, 1987). High nitrate concentration in drinking water has been recognized as causing certain health problems such as gastric cancer (Fraser and Chilvers, 1981), stomach cancer (Hillet et al., 1973), birth defects (Dorsch, et al., 1984), nitrate poisoning of infants (infant cyanosis or methemoglobinemia, a potentially fatal disease of infants) (Super et al., 1981). In order to protect public health, the U.S. Environmental Protection Agency (EPA) has established a drinking water standard of maximum contaminant level of 10 mg per liter as nitrogen or 45 mg per liter as nitrate.

The major sources of nitrates in groundwater come from: effluent from septic tanks, leaky sewer lines, artificial fertilizers, geological deposits of nitrate salts, farm animal

waste, and waste water disposal. Among these sources, artificial fertilizer is the most common nitrate source found in groundwater contamination (Bourchard et al., 1992). Due to the prevalence of potential sources, nitrate is becoming one of the most commonly identified groundwater contaminants (Spalding and Exner, 1993). This is particularly true of the unconfined aquifer in agricultural areas. Shallow drinking wells, especially those in the alluvial aquifer, are more easily contaminated with nitrogen fertilizers. These wells may pose a major health risk to those who live in rural areas and use groundwater for drinking.

Nitrate is a very mobile species in groundwater. It does not adsorb on soil. Once nitrate enters an aquifer, it remains in the groundwater unless it is removed or transformed by biological denitrification processes (Smith and J. Duff, 1988). Firestone (1982) gave the four general requirements for denitrification: (1) nitrate or nitrite as terminal electron acceptors; (2) the presence of suitable denitrifying bacteria; (3) suitable electron donors; and (4) anaerobic conditions or restricted oxygen availability. These conditions, however, are rarely met in a natural environment for many aquifers. Thurman (1985) has surveyed one hundred groundwater aquifers in the U.S.A. and reported that the average dissolved organic carbon (DOC) was only 0.7 mg/l for the sandstone, limestone, sand and gravel aquifers. The content of organic carbon is not enough to removal high nitrate level. A study by Foster et al. (1985) also gave the same conclusion that if the concentration of NO_3-N in the groundwater exceeds the concentration of DOC in the groundwater, some nitrate will still be left in aquifer.

The natural rate of denitrification is not sufficient to remove the high concentration of nitrate due to the limits of the available organic carbon in the many aquifers. An artificial treatment method is required to remove nitrate from the groundwater. Nitrate in the groundwater can be removed by a physical and /or chemical method (such as an ion exchange, a membrane separation, and an electrodialysis) and by a biological method (such as denitrification) (Hamon and Fustec, 1991).

The main advantages for using physical-chemical processes are that these processes are simple and time required to remove nitrate is shorter. However, these processes only separate nitrate from one liquid phase to another liquid phase. The further treatment or disposal of the byproducts needs for these processes. The biological process, on the other hand, transforms nitrate to nitrogen gas by denitrifying bacteria. The by-products of this biochemical reaction are simple carbon dioxide and water. Thus, the biological process appears to be more economical than physical-chemical process because this process does not need disposal of byproduct.

Many researchers (Kruithof et al., 1985, Mercado et al., 1988) have studied the use of an underground denitrification technique to remove nitrate from groundwater. They injected organic carbon into the aquifer by a recharge well and pumped treated water from a pump well. They found this method can remove up to 50% of the nitrate from the raw groundwater. Furthermore, this method is independent of any seasonal temperature variations. The disadvantage of this underground process is the clogging of the aquifer pore spaces with gaseous products of aquifer and dead biological matter. Kruithof et. al. (1985) concluded from the field experiment that the underground denitrification methods offer some potential, but, in practice, they will be dependent on the prevention of the clogging problems.

PROPOSED TREATMENT SYSTEM SCHEME

A new treatment system, called the "Recirculating Groundwater Remediation Well (RGRW) System", is proposed to protect the drinking water wells from migrating nitrate contamination. The system consists of one or more large diameter treatment wells that have two screen sections. The nitrate contaminated groundwater is brought into the lower screen section of the treatment well by a pump. In the well, which itself is used as a bioreactor for denitrification, anoxic condition is maintained and soluble organic chemicals

are supplied into the well as an acceptable electron donor and energy source for denitrifying bacteria. The denitrified water is reinjected into the aquifer from the upper screen section of the well, thereby inducing a vertical circulating flow near the well that will create a hydraulic barrier to stop the nitrate contaminated groundwater from reaching the downstream drinking water well. A scheme of the proposed system is shown in Figure 1

OBJECTIVES

The objectives of this research are as following:

(1) Develop a numerical model to help design and operation of the recirculating nitrate treatment well system;

(2) Evaluate the model by comparison of simulated results with analytic solutions and experimental data;

(3) Determine the critical factors which may affect the design and operation of the treatment well; and

(4) Use the models to evaluate the overall performance of the recirculating nitrate treatment well system.

To achieve these objectives, the problems will be studied in three categories:

(1) Hydraulic behavior of flow pattern surrounding the groundwater recirculating treatment well with and without (negligible) natural groundwater;

(2) Nitrate transport under different operation conditions of the treatment well; and

(3) Microbial denitrification in the aquifer near the outside of the treatment well as well as within the treatment well.
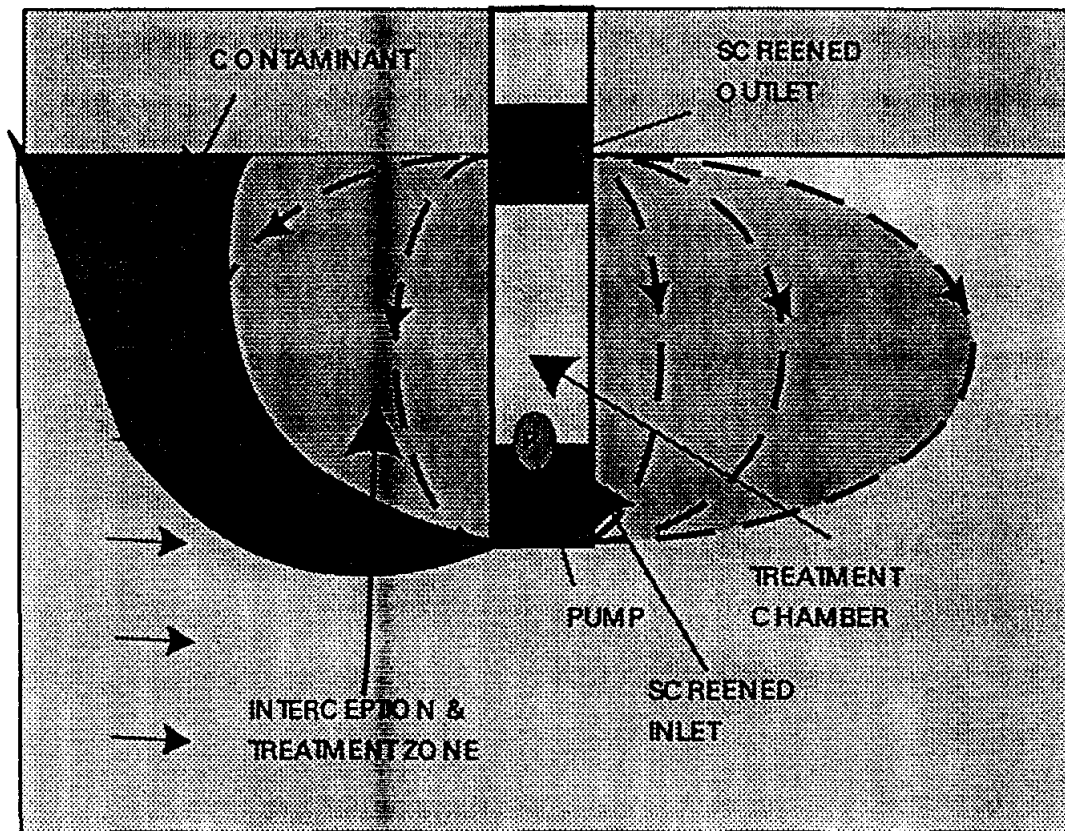
Figure 1. Schematic of a recirculating groundwater remediation well system.

CHAPTER II

LITERATURE REVIEW

BRIEF REVIEW OF DENITRIFICATION

Denitrification is a biological process in which nitrate and nitrite are reduced to nitrogen gas. There are two types of enzyme systems involved with the reduction of NO_3-N: assimilatory and dissimilatory. Assimilatory nitrate reduction converts nitrate into ammonia; ammonia is then used by the cells in biosynthesis. If ammonia is already present, the assimilation of nitrate need not occur to satisfy cell requirement (Grady and Lim, 1980). Dissimilatory nitrate reduction or denitrification involves the conversion of nitrate nitrogen, NO_3-N to a gaseous nitrogen species. If methanol is used as an electron donor, denitrification can be represented as a two-step process as shown in equations (2-1) and (2-2) (Polprasert and Park, 1986).

The first step is the conversion of nitrate to nitrite.

$$NO_3^- + \tfrac{1}{3}CH_3OH \Rightarrow NO_2^- + \tfrac{2}{3}H_2O + \tfrac{1}{3}CO_2 \tag{2-1}$$

The second step involves the reduction of nitrite to nitrogen gas:

$$NO_2^- + \tfrac{1}{2}CH_3OH \Rightarrow \tfrac{1}{2}N_2 + \tfrac{1}{2}CO_2 + \tfrac{1}{2}H_2O + OH^- \tag{2-2}$$
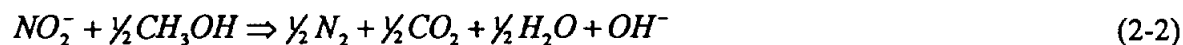
The overall transformation is obtained by combing equations (2-1) and (2-2) as

$$NO_3^- + \tfrac{5}{6}CH_3OH \Rightarrow \tfrac{1}{2}N_2 + \tfrac{7}{6}H_2O + \tfrac{5}{6}CO_2 + OH^- \tag{2-3}$$
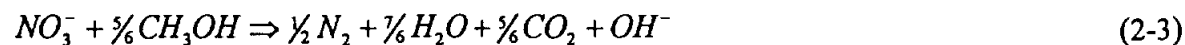
Equation (2-3) can be split into the following reduction half-reaction (equation (2-4)) and oxidation half-reaction (equation (2-5)) as

$$NO_3^- + 6H^+ + 5e^- \Rightarrow 0.5N_2 + 3H_2O \qquad (2\text{-}4)$$

$$\tfrac{5}{6}CH_3OH + \tfrac{1}{6}H_2O \Rightarrow \tfrac{5}{6}CO_2 + 5H^+ + 5e^- \qquad (2\text{-}5)$$

It is clear from equations (2-4) and (2-5) that nitrate gains electrons and is reduced to nitrate gas and the carbon source loses electrons and is oxidized to carbon dioxide. Therefore, nitrate is the electron acceptor and the carbon source is the electron donor.

A typical synthesis denitrification can be written as (McCarty et al, 1969)

$$4CH_3OH + 3NO_3^- + 3H^+ + CO_2 \Rightarrow 3C_5H_7O_2N + 19H_2O \qquad (2\text{-}6)$$
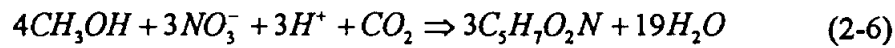
Based on the laboratory studies, 25 to 30 percent of the amount of methanol that is required for energy is needed for synthesis. McCarty et al. (1969) gave the following empirical equation to describe the overall nitrate removal reaction.

$$NO_3^- + 1.08CH_3OH + H^+ \Rightarrow 0.065C_5H_7O_2N + 0.47N_2 + 2.44H_2O + 0.76CO_2^- \qquad (2\text{-}7)$$
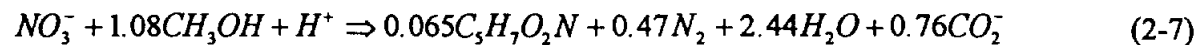
If ethanol is used as a carbon source for denitrification, the similar stoichiometric relationship can be written as

Assimilation reaction

$$97NO_3^- + 50C_2H_5OH \Rightarrow 46N_2 + 75CO_2 + 84H_2O + 97OH^- + 5C_5H_7O_2N \qquad (2\text{-}8)$$

Dissimilation reaction

$$2NO_3^- + 5C_2H_5OH \Rightarrow 6N_2 + 10CO_2 + 9H_2O + 12OH^- \qquad (2\text{-}9)$$
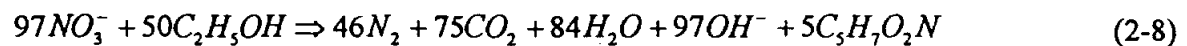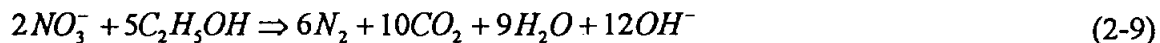
In nature, soil and sediments contain about 10^8 to 10^{10} total bacteria per gram of dry solids (Alexander, 1977). The bacterium capable of denitrification range from a fraction of a percent to 95 percent of the total population, depending on the O_2, carbon, NO_3, and the levels of the soil (Focht and Verstraete, 1977). Generally, the bacteria responsible for denitrification are facultative capable of utilizing nitrate nitrogen (NO_3-N) as a terminal electron acceptor for microbial respiration when molecular oxygen(O_2) is not present. Denitrifying genera can be catalogued as heterotrophs (that use the organic energy source as a source for cellular) and autotrophs (that obtain carbon from inorganic carbon dioxide as a source for cellular carbon). Payne (1977) lists 15 denitrifying genera including *Achromobacter, Aerobacter, Alcaligenes, Bacillus, Brevibacterium, Flavobacterium, Lactobacillus, Micrococcus, Proteus, Pseudomonas, and Spirillum*, et al. Most of these denitrifying genera are heterotrophic and facultative anaerobes (Payne, 1981).

Many environmental factors have a significant effect on the rate of denitrified growth and nitrate removal. The most important of these factors include carbon source, oxygen, temperature, pH, et al.

The availability of organic carbon compounds is one of most important factors which affects the rate of nitrate reduction in the groundwater. Many laboratory and field data (Smith and Duff, 1988, Bradley et al, 1992) have clearly shown that there is a significant relationship between the denitrifying activity and the organic carbon content: if the organic carbon level is below a certain level, the denitrifying activity will cease. Dahab and Lee (1988) have reported that when using methanol as carbon source to complete denitrification, the most favorable ratio of carbon to nitrate nitrogen is 1.5 to 2. If using

ethanol as a carbon source, the optimum ratio of C/N was found to be 1.25 in soil column studies (Hamon and Fustec, 1991). The denitrifying activity is also related to the types of organic carbon. It has been noted that different organic compounds which support equal rates of denitrification may give different mole fractions of N_2O in the products. This suggests that there may exert differential effects on the reductass involved (Knowles, 1982).

Because nitrate reduction serves as an alternative means of microbial respiration, there has been considerable interest in the influence of oxygen upon the responsible enzyme system. Studies by Payne (1973) indicated that when NO_3 is used as the terminal electron acceptor, the energy yield per mole of organic material respired is approximately 60% of that yield under O_2 as the terminal electron acceptor. Therefore the use of oxygen as the final electron acceptor is more energetically favored than the use of nitrate in denitrification. In the saturated zone, bacteria will first use O_2 to oxidize organic carbon until the oxygen supplies become limiting, then the bacteria switches to use NO_3 as the electron acceptor. Decreasing the O_2 concentration results in an increase of NO_3 reduction. Misra et al (1974) showed that the reduction rate of a NO_3 increased 10 times while the gaseous O_2 concentration decreased from 20% to 0.5%.

Temperature is also very important factor for assessing the overall efficiency of the denitrification process. It can exert an effect upon the biological system in two ways: by affecting the rates of enzymatically catalyzed reactions and by affecting the rate of diffusion of substrates to the cell. For denitrification, the favored temperature ranges from 5°C to 35 °C. In the low-temperature range, soil denitrification decreases greatly, but is, nevertheless, measurable even at 0 to 5°C (Bailey and Beauchamp, 1973). Misra et al. (1974) observed that the first-order constant for NO_3 reduction changes from 0.0016 hr^{-1} at 19.5°C to 0.035 hr^{-1} at 34.5°C. Tchobanglous and Burton (1991) suggested that quantifying temperature effects can be expressed as $K_1 = K_o \theta^{(T_1 - T_2)}$, where K_1 and K_0 are the reaction

rate coefficients at temperatures T_1 and T_2, respectively, and θ is the thermal coefficient. For most biochemical operations T_2 is chosen as 20°C. Novak (1974) has proposed another equation to account for the effects of temperature. It can be written as: $K_1 = K_0 e^{[c(T_1 - T_2)]}$, where c is the temperature coefficient.

pH is another important factor in denitrification. The highest denitrification rate is within the range of 7.0 to 8.0 (Parker et al, 1975). Klemrdtsson et al. (1977) noted that in the acid peat, the low pH of 3.5 can be a factor which prevents the occurrence of denitrification.

Some nutrients such as P, S, K, Ma, Ca are also important requirements for denitrifying bacteria growth. Spector (1956) suggested that the average favorable ratio of C:N:P:S for cellular composition is 100:20:4:1. Study by Champ et al. (1979) indicated that most groundwater contains adequate concentrations of the necessary nutrients to support biosynthesis.

REVIEW OF NITRATE TRANSPORT MODELS

Understanding the movement of nitrate in the aquifer and predicting the concentration of nitrate at a water supply well are essential for managing the potential of nitrate pollution of groundwater. Most theoretical descriptions of the NO_3 transport in porous media are based on the convection- diffusive equation with a reaction term.

$$\frac{\partial N}{\partial t} = D\frac{\partial^2 N}{\partial X^2} - V\frac{\partial N}{\partial X} - F(N,C,X,t) \qquad (2\text{-}10)$$

where N is the concentration of NO_3 in the groundwater, D is the dispersion concentration, V is the average pore water velocity, and F (N, C, X, t) is the reaction term.

In formulating the reaction term, one must consider the rate of nitrate reduction as a function of the NO_3 concentration (electron acceptor), available organic matter (electron

donor) and environmental conditions, such as temperature, pH, dissolved oxygen and bacterial population.

Early researchers (Broadbent and Clark, 1965, Focht, 1974) assumed that the rate of NO_3 reduction is independent of NO_3 concentration and the rate of NO_3 reduction can be considered a zero-order or first-order reaction. Starr and Parlange (1976) analyzed their steady-state column experiment data and showed that some of those data can be explained by zero-order kinetics. Reddy et at. (1978) also found that NO_3 reduction followed zero-order kinetics in fifteen flooded-soils amended with 0.5% rice straw and 100 ppm NO_3-N. Kanwar et al. (1980) used a zero-order miscible displacement model to describe NO_3 reduction and observed reasonable agreement between predicted and experimental breakthrough curves and the NO_3 concentration profile in the column. Other researchers (Bouldin et al. 1974, Stanford et al., 1975), however, measured NO_3 reduction and found that the NO_3 loss rate from denitrification was best described by first-order kinetics. Cho (1971), Misra et al. (1974), used the Laplace transform technique to solve convection-dispersion equation with a first-order reaction term. The analytic solutions were obtained by assuming homogeneous soil system subject to one-dimensional steady state flow regimes.

Later researchers (Betlach and Tiedie, 1981, McConnaughey, 1981) found use of simple terms is justified only if during the whole of transport process concentrations stay within the certain ranges. Denitrification rate is a zero-order at high NO_3 concentration (unlimited uptake) and is a first-order at low concentration (Nitrate limitation). A more elaborate model was presented by Cho and Mills(1979) in which a nonlinear Monod-type kinetic term is used to describe a single species reactive nitrate transport in a porous media. The specific growth rate can be written as

$$\mu = \frac{\mu_{max} N}{K_N + N} \tag{2-11}$$

where μ_{max} is the maximum specific growth rate, (1/T), N is the concentration of nitrate (M/L_3). K_n is the saturation constant (M/L_3), which is defined as the nitrate concentration at which the specific growth rate is equal to half of the maximum growth rate.

A single species Monod-model does not consider carbon effects and may be suitable in some special field or laboratory cases but not in general cases. Burford and Bremner (1975) measured the NO_3 reduction rate and found the rate of NO_3 reduction in the porous media not only depends on the NO_3 concentration, but also on the availability of oxidizable carbon compounds. There was a good correlation between denitrification rate and available carbon compounds. Their experimental data support their conclusion that NO_3 reduction under anaerobic condition was largely controlled by the availability of readily decomposible carbon compound. Several forms have been proposed to describe more than one substrate or nutrient substrate limited cases. Roels (1983) suggested the following form to represent reaction term:

$$r_N = \frac{1}{Y_N}\left(\min\left[\frac{\mu_{mc}C}{K_c + C}\right]; \left[\frac{\mu_{mn}N}{K_n + N}\right] \right) \qquad (2\text{-}12)$$

where μ_{mc} and μ_{mn} are maximum specific growth rates applying to carbon and nitrate respectively. Kc and Kn are the saturation constants for carbon and nitrate respectively.

The dual-Monod model is a more often used form which successfully describes microbial growth as simultaneously limited by both carbon and nitrate substrates. The model can be expressed as (Widdowson et al., 1988, Lindstrom, 1992)

$$r_N = \frac{\mu_{max}}{Y_N}\left[\frac{C}{K_c + C}\right]\left[\frac{N}{K_n + N}\right] \qquad (2\text{-}13)$$

In the past few years a more sophisticated model has been published that incorporate microbial growth, the transport of organic carbon and nitrate (e.g., MacQuareie et al., 1990, Widdowson et al., 1988 and Kinzelbach and Schaffr, 1991). These models are able to describe the interactive transport of organic carbon (electron donor), nitrate (electron acceptor) and microbial mass in the water phase and biological phase of microorganisms, including the possibility of the diffusion-limited exchange processes between the mobile pore water and bacteria. The model proposed by Widdowson et al. (1988) is based on the microcolony concept that assumes small isolated colonies of microbes have the form of a cylindriary plate which attached to the surface of the aquifer sediments. There is a diffusion boundary layer to separate the pore buck liquid from the colony surface. Generally, the boundary layer diffusion process is rapid compared to concentration changes in the bulk fluid. Therefore, it is assumed pseudo steady state conditions across the boundary layer. The model takes into account the kinetic of substrate and nitrate transport from the water phase to the microcolonies.

All of the above models provide insight into the details of the biochemistry of the sequential nitrate reduction in the aquifer. However, these models consider only natural denitrification in the aquifer and do not include the effects of the artificial treatment reactor. The models can not be directly used to design the recirculating groundwater nitrate treatment well system. One of the objectives of this dissertation will be to develop a model which more realistically describes denitrification in the aquifer as well as in the treatment reactor and will help us to design and operate the treatment well system.

CHAPTER III

SEMIANALYTICAL MODEL FOR ESTIMATION OF CAPTURE
ZONES OF A RGRW IN AN UNCONFINED AQUIFER

One of the important considerations in the design and operation of a Recirculating Groundwater Remediation Well (RGRW) system is its hydraulic characteristics, which include flow patterns and capture zones. A capture zone is defined as the area surrounding a well in which all the water will be removed by the well in a certain period of time. Traditional two dimensional capture models for the analysis and the design of pump system are not suitable to analyze the RGRW system because those models are based on Dupuit's assumption, i.e., the vertical flow is negligible (Bear and Jacobs 1965, Javandel and Tsang, 1986, Lee and Wilson, 1986). In the presence of natural groundwater flow, the flow pattern of RGRW is three dimensional and there is no radial symmetry around the well axis. To solve these complex flow patters, a three-dimensional capture model is necessary to develop for analysis of the vertical flow patterns around the wells. Recently, Herrling et al. (1991) used the Galerkin finite element method to solve the three-dimensional flow patterns around the vertical circulation well in the confined aquifer with a regional flow gradient. Philip and Walter (1992) employed the linear superposition method to solve the flow field in the confined aquifer. Both of those models are suitable for a confined aquifer. In practice, flow in unconfined aquifers may more often be encountered in potential waste sites. Therefore, developing a three-dimensional model for calculating vertical recirculation flow patterns in unconfined aquifers is necessary.

MATHEMATICAL ANALYSIS

Governing Flow Equation

An unconfined aquifer of infinite lateral extent resting on an impermeable horizontal layer is illustrated in Figure 2. It is assumed that:

(1) The aquifer is an unconfined aquifer with a Constant thickness;

(2) The aquifer is homogeneous, isotropic, and infinite in horizontal extent;

(3) The elastic property of the medium and the temporal variability of the piezometric head are negligible;

(4) Natural groundwater flow is a constant and uniform;

(5) Pumping rate is constant; and

(6) Drawdown at the well is much smaller than the thickness of the aquifer and the hydraulic head.

The governing flow equation may be stated by substituting Darcy's Law into the conservation of mass equation in a radial coordinate system.

$$\frac{\partial^2 \phi}{\partial r^2} + \frac{1}{r}\frac{\partial \phi}{\partial r} + \frac{\partial^2 \phi}{\partial z^2} = 0 \tag{3-1}$$

where ϕ is the piezometric head, r is the radial distance from the pumping well, and z is the vertical coordinate. The boundary and initial conditions of the equation are given as following:

$$\frac{\partial \phi}{\partial t} - \frac{K}{\varepsilon}\left[\left(\frac{\partial \phi}{\partial r}\right)^2 + \left(\frac{\partial \phi}{\partial z}\right)^2 - \frac{\partial \phi}{\partial z}\right] = 0 \qquad \text{at the water table} \tag{3-2}$$

$$\phi = d + s \qquad \text{at the water table} \tag{3-3}$$
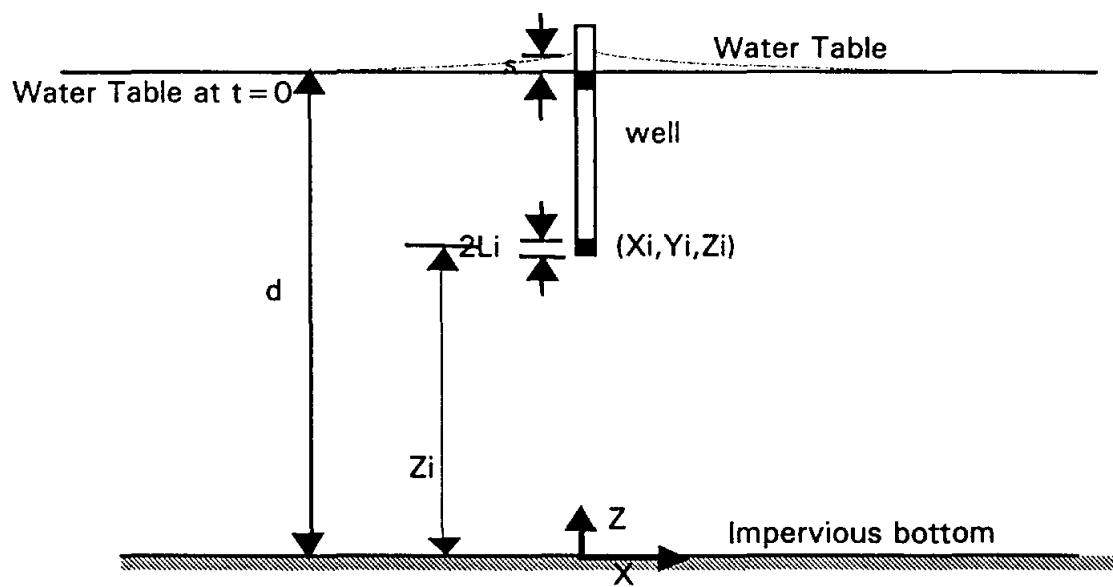
Figure 2. Schematic of a partially penetrating recirculating well in an unconfined aquifer.

$$\frac{\partial \phi(r, z = 0, t)}{\partial z} = 0 \qquad \text{at the impervious aquifer bottom} \quad (3\text{-}4)$$

$$s(r = \infty, z, t) = 0 \qquad \text{at } r \to \infty \qquad\qquad (3\text{-}5)$$

$$s(r, z, t = 0) = 0 \qquad \text{at } t = 0 \qquad\qquad (3\text{-}6)$$

$$\lim_{r \to 0} \left(-2\pi K(2l_i) \frac{\partial \phi}{\partial r} \right) = Q \qquad \text{along the } z_i\text{-}l_i < z < z_i + l_i \qquad (3\text{-}7)$$

where ε is the porosity; K is the hydraulic conductivity of the isotropic aquifer; s is the drawdown; d is the aquifer depth; 2L is the length of the screened interval of the well; Z_i is the depth of the center of the well screened interval ; Q is the discharge; and t is the time.

It is quite difficult to obtain an analytic solution of the equation (3-1) satisfying the given boundary conditions in terms of the head ϕ as a function of r, z, t and d because the boundary condition along a free surface is nonlinear and is posed on the unknown water table. Dagan (1966) used small perturbation technique to solve this problem by assuming that the drawdown at the well is much smaller than the thickness of the aquifer and that the hydraulic head can be expressed as a small perturbation expansion $\phi = \phi_0 + \delta\phi_1 + \delta^2\phi_2 + \cdots$ where $\delta = Q/Kd^2$ is a small parameter. This technique may lead to the first order linearized approximation of the water table. Then the Green function was used to solve the linearized equation. The solution of equation (3-1) is given as (Dagan, 1966)

$$\phi = \frac{Q}{4\pi K} \left\{ \frac{1}{\left[r_i^2 + (z+z_i)^2\right]^{1/2}} + \frac{1}{\left[r_i^2 + (z-z_i)^2\right]^{1/2}} \right.$$

$$-\frac{2}{d}\int_0^\infty \frac{\cosh\lambda\left(1-\frac{z_i}{d}\right)\cosh\lambda\left(1+\frac{z}{d}\right)e^{-\frac{\lambda K \tanh\lambda}{\varepsilon d}t}}{\sinh\lambda\cosh\lambda} J_0\left(\lambda\frac{r_i}{d}\right)\,d\lambda$$

$$\left. +\frac{2}{d}\int_0^\infty \frac{e^{-\lambda}\cosh\left(\frac{\lambda z_i}{d}\right)\cosh\left(\frac{\lambda z}{d}\right)}{\sinh\lambda} J_0\left(\lambda\frac{r_i}{d}\right)\,d\lambda \right\} \qquad (3\text{-}8)$$

where J_0 is zero order Bessel's function. This solution is valid in the vicinity of as well as at large distances from the well (Dagan, 1966).

Hydraulic Head Caused by a Well with a Finite Length Screen

Considering a well with a screen of finite length 2L partially penetrating a very thick homogenous isotropic aquifer, we assume that the discharge Q_i is uniformly distributed along the well screen, so that the strength of an elementary line sink of the length $d\xi$ is $dQ_i = (Q_i/2l_i)d\xi$. Then

$$d\phi = \frac{Q_i}{8\pi l_i K} \left\{ \frac{1}{\left[r_i^2 + (z+z_i+\xi)^2\right]^{1/2}} + \frac{1}{\left[r_i^2 + (z-z_i-\xi)^2\right]^{1/2}} \right.$$

$$-\frac{2}{d}\int_0^\infty \frac{\cosh\lambda\left(1+\frac{z_i}{d}\right)\cosh\lambda\left(1+\frac{z}{d}\right)e^{-\frac{\lambda K \tanh\lambda}{\varepsilon d}t}}{\sinh\lambda\cosh\lambda} J_0\left(\lambda\frac{r_i}{d}\right)\,d\lambda \qquad (3\text{-}9)$$

$$\left. +\frac{2}{d}\int_0^\infty \frac{e^{-\lambda}\cosh\lambda\left(\frac{z_i+\xi}{d}\right)\cosh\left(\frac{\lambda z}{d}\right)}{\sinh\lambda} J_0\left(\lambda\frac{r_i}{d}\right)\,d\lambda \right\}d\xi$$

By integrating along the segment ($-l_i < \xi < +l_i$) of the well, and transforming to Cartesian coordinates, we can obtain the hydraulic head caused for a well with a finite length screen in an unconfined aquifer as

$$
\begin{aligned}
\phi = \frac{Q}{8\pi K l_i} \Bigg\{ & \ln \frac{z+z_i+l_i+\left[(z+z_i+l_i)^2+(x-x_i)^2+(y-y_i)^2\right]^{\frac{1}{2}}}{z+z_i-l_i+\left[(z+z_i-l_i)^2+(x-x_i)^2+(y-y_i)^2\right]^{\frac{1}{2}}} \\
& +\ln \frac{z-z_i+l_i+\left[(z-z_i+l_i)^2+(x-x_i)^2+(y-y_i)^2\right]^{\frac{1}{2}}}{z-z_i-l_i+\left[(z-z_i-l_i)^2+(x-x_i)^2+(y-y_i)^2\right]^{\frac{1}{2}}} \\
& -\int_0^\infty \frac{\cosh\lambda\left(1+\frac{z_i}{d}\right)\sinh\left(\frac{\lambda l_i}{d}\right)\cosh\lambda\left(1+\frac{z}{d}\right)e^{-\frac{\lambda K\tanh\lambda}{\varepsilon d}t}}{\lambda\sinh\lambda\cosh\lambda} J_0\left(\lambda\frac{r_i}{d}\right) d\lambda \\
& +\int_0^\infty \frac{e^{-\lambda}\sinh\left(\frac{\lambda l_i}{d}\right)\cosh\left(\frac{\lambda z_i}{d}\right)\cosh\left(\frac{\lambda z}{d}\right)}{\lambda\sinh\lambda} J_0\left(\frac{\lambda}{d}\sqrt{(x-x_i)^2+(y-y_i)^2}\right) d\lambda \Bigg\}
\end{aligned}
$$

(3-10)

Steady-state Velocity Field of a RGRW

Under steady-state conditions, $t \to \infty$, the third term on the right hand side of equation (3-10) yield to zero. The velocity at any point in the flow domain is found by differentiation of the head field.

$$
V_x = -\frac{K}{\varepsilon}\frac{\partial\phi}{\partial X}
$$

(3-11)

$$
V_y = -\frac{K}{\varepsilon}\frac{\partial\phi}{\partial Y}
$$

(3-12)

$$
V_z = -\frac{K}{\varepsilon}\frac{\partial\phi}{\partial Z}
$$

(3-13)

Since the solution (3-10) satisfies the differential linear equation of (3-1), the superposition principle can be used to determinate the velocity field. For a RGRW, which has two screen intervals with extraction induced in one interval and injection induced in the other, the velocity field may be determined by adding the individual velocity contribution from each interval. The combination of velocity fields of the uniform ambient groundwater flow with point sources and sinks in a steady-state floe field may be determined as following:

$$
V_x = V_{ox} - \sum_{i=1}^{n} \frac{Q(x-x_i)}{8\pi l_i \varepsilon} \left\{ \frac{1}{\sqrt{(x-x_i)^2+(y-y_i)^2+(z+z_i+l_i)^2}\left(\sqrt{(x-x_i)^2+(y-y_i)^2+(z+z_i+l_i)^2}+z+z_i+l_i\right)} \right.
$$

$$
- \frac{1}{\sqrt{(x-x_i)^2+(y-y_i)^2+(z+z_i-l_i)^2}\left(\sqrt{(x-x_i)^2+(y-y_i)^2+(z+z_i-l_i)^2}+z+z_i-l_i\right)}
$$

$$
+ \frac{1}{\sqrt{(x-x_i)^2+(y-y_i)^2+(z-z_i+l_i)^2}\left(\sqrt{(x-x_i)^2+(y-y_i)^2+(z-z_i+l_i)^2}+z-z_i+l_i\right)}
$$

$$
- \frac{1}{\sqrt{(x-x_i)^2+(y-y_i)^2+(z-z_i-l_i)^2}\left(\sqrt{(x-x_i)^2+(y-y_i)^2+(z-z_i-l_i)^2}+z-z_i-l_i\right)}
$$

$$
\left. - \int_0^\infty \frac{e^{-\lambda}\sinh\left(\frac{\lambda l_i}{d}\right)\cosh\left(\frac{\lambda z_i}{d}\right)\cosh\left(\frac{\lambda z}{d}\right)}{d\sinh\lambda} \frac{J_1\left(\frac{\lambda}{d}\sqrt{(x-x_i)^2+(y-y_i)^2}\right)}{\sqrt{(x-x_i)^2+(y-y_i)^2}} d\lambda \right\} \qquad (3\text{-}14
$$

$$
V_y = V_{oy} - \sum_{i=1}^{n} \frac{Q(y-y_i)}{8\pi l_i \varepsilon} \left\{ \frac{1}{\sqrt{(x-x_i)^2+(y-y_i)^2+(z+z_i+l_i)^2}\left(\sqrt{(x-x_i)^2+(y-y_i)^2+(z+z_i+l_i)^2}+z+z_i+l_i\right)} \right.
$$

$$
- \frac{1}{\sqrt{(x-x_i)^2+(y-y_i)^2+(z+z_i-l_i)^2}\left(\sqrt{(x-x_i)^2+(y-y_i)^2+(z+z_i-l_i)^2}+z+z_i-l_i\right)}
$$

$$
+ \frac{1}{\sqrt{(x-x_i)^2+(y-y_i)^2+(z-z_i+l_i)^2}\left(\sqrt{(x-x_i)^2+(y-y_i)^2+(z-z_i+l_i)^2}+z-z_i+l_i\right)}
$$

$$
- \frac{1}{\sqrt{(x-x_i)^2+(y-y_i)^2+(z-z_i-l_i)^2}\left(\sqrt{(x-x_i)^2+(y-y_i)^2+(z-z_i-l_i)^2}+z-z_i-l_i\right)}
$$

$$
\left. - \int_0^\infty \frac{e^{-\lambda}\sinh\left(\frac{\lambda l_i}{d}\right)\cosh\left(\frac{\lambda z_i}{d}\right)\cosh\left(\frac{\lambda z}{d}\right)}{d\sinh\lambda} \frac{J_1\left(\frac{\lambda}{d}\sqrt{(x-x_i)^2+(y-y_i)^2}\right)}{\sqrt{(x-x_i)^2+(y-y_i)^2}} d\lambda \right\} \qquad (3\text{-}15
$$

$$V_z = V_{OZ} - \sum_{i=1}^{m} \frac{Q_i}{8\pi l \epsilon_i} \left\{ \frac{1}{\sqrt{(x-x_i)^2 + (y-y_i)^2 + (z+z_i+l_i)^2}} - \frac{1}{\sqrt{(x-x_i)^2 + (y-y_i)^2 + (z+z_i-l_i)^2}} \right.$$

$$+ \frac{1}{\sqrt{(x-x_i)^2 + (y-y_i)^2 + (z-z_i+l_i)^2}} - \frac{1}{\sqrt{(x-x_i)^2 + (y-y_i)^2 + (z-z_i-l_i)^2}}$$

$$\left. + \int_0^\infty \frac{e^{-\lambda} \sinh\left(\frac{\lambda l_i}{d}\right) \cosh\left(\frac{\lambda z_i}{d}\right) \sinh\left(\frac{\lambda z}{d}\right)}{d \sinh \lambda} J_0\left(\frac{\lambda}{d}\sqrt{(x-x_i)^2 + (y-y_i)^2}\right) d\lambda \right\} \quad (3\text{-}16)$$

where J1 is the first order Bessel's function.

Equations (3-14), (3-15) and (3-16) describe the velocity component in an unconfined aquifer caused by a RGRW system. For an anisotropic system, we can use the scaling technique to transform all dimensional parameters in the anisotropic domain into an equivalent isotropic domain. First step is the determination of the scaling factors. All the dimensional parameters and hydraulic conductivity are scaled into the equivalent isotropic domain by multiplying the scaling factors. The equivalent isotropic hydraulic conductivity and scaling factors are given by (Bear, 1972):

$$\beta_x = \sqrt[6]{\frac{K_y K_z}{K_x^2}} \quad (3\text{-}17)$$

$$\beta_y = \sqrt[6]{\frac{K_x K_z}{K_y^2}} \quad (3\text{-}18)$$

$$\beta_z = \sqrt[6]{\frac{K_x K_y}{K_z^2}} \quad (3\text{-}19)$$

$$K = \sqrt[3]{K_x K_y K_z} \quad (3\text{-}20)$$

where K is the equivalent isotropic hydraulic conductivity; K_x, K_y, K_z represent the hydraulic conductivity in the x, y, z direction, respectively. β_x, β_y, β_z are the scaling factors in x, y, z coordinates, respectively. Then, we solve the equivalent isotropic problem using the scaled parameters and equivalent isotropic hydraulic conductivity. Finally, by dividing the calculated isotropic solution by the scaling factor, we obtain the solution for an anisotropic aquifer.

NUMERICAL IMPLEMENTATION

Particle Tracking

Once velocities are determined, a particle tracking technique can be used to delineate the contaminant pathline (the route that an individual particle of contaminant follows through the aquifer) and determine the advection of the contaminant front. The pathline traveled by the contaminant particle is divided into increment's dl. The distance traveled by a particle travel at time step may be written as

$$dX = V_{cx} \, dt = V_x \, dt / R\varepsilon \tag{3-21}$$

$$dY = V_{cy} \, dt = V_y \, dt / R\varepsilon \tag{2-22}$$

$$dZ = V_{cz} \, dt = V_z \, dt / R\varepsilon \tag{3-23}$$

$$d\ell = \sqrt{dX^2 + dY^2 + dZ^2} = \sqrt{V_x^2 + V_y^2 + V_z^2} \, dt / R\varepsilon \tag{3-24}$$

where dX ,dY and dZ are the projections of $d\ell$ on the x ,y and z axis, respectively; V_{cx}, V_{cy}, and V_{cz} are the components of the contaminant particle velocity in the x, y, and z

directions, respectively; V_x, V_y, and V_z are the components of the groundwater velocity in the x, y and z directions, respectively; and R is the retardation factor.

If we assume that the contaminant adsorption is represented by a linear adsorption, R is given by

$$R = 1 + \rho_b k_b / \varepsilon \tag{3-25}$$

where ρ_b is the bulk density of the porous medium; and k_d is the distribution coefficient.

Substituting equations (3-14), (3-15) and (3-16) into equations (3-21), (3-22), (3-23) and (2-24), and integrating them, we obtain a pathline. In practice, analytical integration of the equations (3-21), (3-22), (3-23) and (3-24) seem to be impossible. So numerical integration technique is used to solve the equations.

Pathline and Capture Zone Delineation Procedure

A computer program has been developed to delineate the contaminant pathline and determine the advection of the contaminant front. First, the velocity is determined by equations (3-14), (3-15) and (3-16) at the initial particle location X^n, Y^n, Z^n, and a temporary new position X^*, Y^* and Z^* of the particle along the pathway is determined by

$$X^* = X^n + V_\alpha(X^n, Y^n, Z^n) \Delta t / 2 \tag{3-26}$$

$$Y^* = Y^n + V_\alpha(X^n, Y^n, Z^n) \Delta t / 2 \tag{3-27}$$

$$Z^* = Z^n + V_\alpha(X^n, Y^n, Z^n) \Delta t / 2 \tag{3-28}$$

Next, the velocity at position X*, Y* and Z* is determined. This velocity can be used for a new estimate for the entire time step. The recalculated new position can be determined by the modified velocity as

$$X^{n+1} = X^n + V_\alpha(X^*, Y^*, Z^*)\Delta t \tag{3-29}$$

$$Y^{n+1} = Y^n + V_\alpha(X^*, Y^*, Z^*)\Delta t \tag{3-30}$$

$$Z^{n+1} = Z^n + V_\alpha(X^*, Y^*, Z^*)\Delta t \tag{3-31}$$

Thus, starting from the initial position of the particle at t=0, we can determine successive locations of the particle at later times. It can be expected that accurate results depend on the value of increment $\Delta \ell$. The value of $\Delta \ell$ is determined in calculation process that the certain criteria must be satisfied. One condition is that $\Delta \ell$ must not exceed the maximum $\Delta \ell_{max}$ prescribed step length. Also the directional change of velocity over the displacement length must not be greater than a prescribed tolerance. When this criterion is not satisfied, the value of $\Delta \ell$ is reduced by 1/2 and the calculation is repeated with the reduced distance increment. The iteration is continued till the criterion is satisfied.

The advection of the contaminant front at any given time can be calculated by keeping track of the travel times of contaminant particles released from the contaminant sources. By joining these points in a sequential order, we can estimate the advective transport of the contaminant front.

The pathline computation continues till one of following termination criteria is met.

(1) Checking if the assigned value of travel time has been exceeded;

(2) Checking if the boundaries of the flow region has been encountered;

(3) Checking if the particle is entrapped into the well; and

(4) Checking if a stagnation point has been encountered.

CODE STRUCTURE

The theoretical approach described in the above previous section was implemented in a FORTRAN 77 computer code running on the VAX/VMS mainframe computer at TEXAS A&M University. The code name is called 3DRGRW. A simplified flow chart of the code is presented in Figure 3. The simulated results will be discussed in the next chapter.
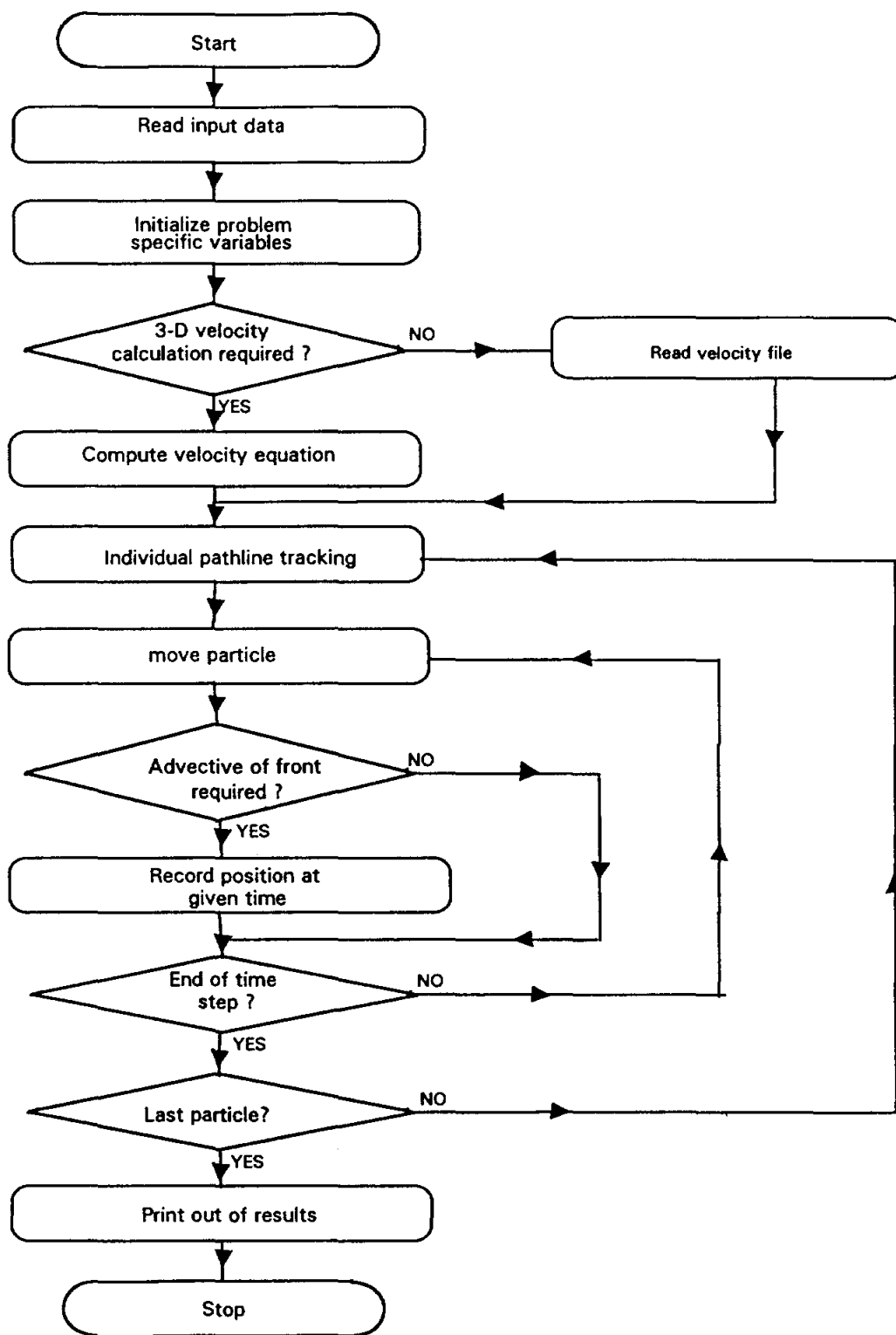
Figure 3. Simplified flow chart for 3DRGRW module.

CHAPTER IV

SEMIANALYTICAL MODEL RESULTS AND DISCUSSIONS ON WELL HYDRAULICS

The principle of the three dimensional, semi-analytical model used to analyze the vertical circulation flow around the RGRW system has been described in Chapter III. In this chapter we will discuss the results of the simulation.

MODEL VERIFICATION

To test the validity of the semi-analytic model, the streamlines calculated by computer program are compared with the fully analytical solutions. Two test cases are considered. The first case involves a situation where water is injected into an unconfined aquifer by a fully penetrating injection well. The aquifer hydraulic parameter as following: thickness aquifer D = 10 m (32.81 ft); hydraulic conductivity K = 1×10^{-5} m/s (3.28×10^{-5} ft/s); the porosity ε = 0.3; radius of the well r_w = 0.1 m (0.33 ft) and the injected rate Q = 1000 m^3/day (3.53×10^4 ft^3/day). For this problem, the velocity at any point in the flow field is one dimensional in the radial direction. A analytic solution describing the position of the contaminant front as a function of time is as following:

$$r = \sqrt{r_w^2 + \frac{Q}{\pi}\frac{t}{D\varepsilon}}$$

(4-1)

Figure 4 shows the advection front predicted by the analytical solution and the computer program at 100, 200, 400 and 800 days. The solid curves represent the position of the advection front predicted by the analytic solution. The points in the figure are the particle positions calculated by the computer program. The dashed curves
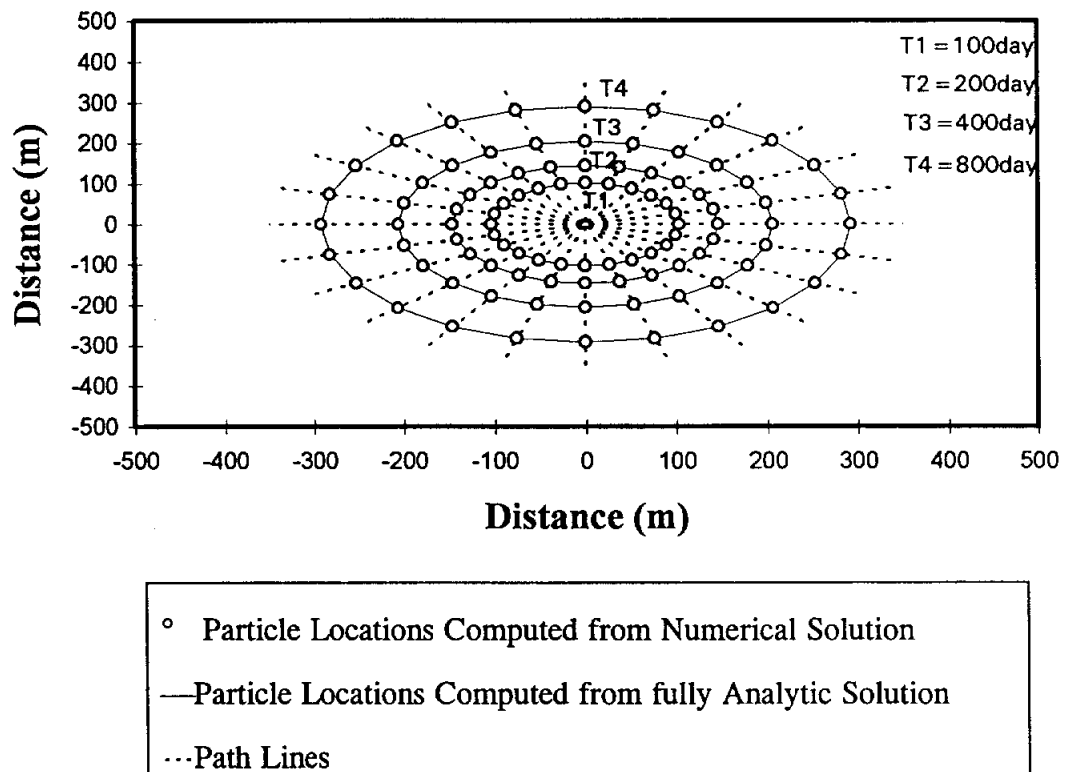
Figure 4. Comparison of particle locations and pathlines calculated by the computer program with the analytic solutions for a radial flow around a fully penetrating well. (1 m = 3.28 ft)

represent the pathlines. The solution obtained by the computer program matches the analytic solution quite well.

The second case involves an injection well and a withdrawal well with equal flow rate Q located at point (d,0) and (-d,0), respectively. The case of the fully penetrating wells without regional flow in the confined aquifer is a two-dimensional problem in the xy plane. The streamline function ψ can be written as (Bear, 1972):

$$\psi = m \tan^{-1} \frac{-2yd}{x^2 + y^2 - d^2}$$ (4-2a)

where $m = Q/2\pi D$ and D is the aquifer thickness.

For streamline function ψ = constant; and tan ψ/m =c, the fully analytic solution for streamlines can be written as:

$$x^2 + \left(y + \frac{d}{c}\right)^2 = \left(d\sqrt{1 + 1/c^2}\right)^2$$ (4-2b)

The general computer program was modified for application to this two dimensional case. Figure 5 shows a comparison between streamlines computed by the computer program and a fully analytic solution. The aquifer and well characteristics are the pumping rate Q =100 ft^3/day; the hydraulic conductivity K= 1x10^{-3} ft/s; the distance between two wells d=10 ft; and the thickness of the confined aquifer d=10 ft.

RESULTS OF THE MODEL AND SENSITIVITY ANALYSIS

Flow Patterns without Natural Groundwater Flow

The flow field around the RGRW without the natural groundwater flow was simulated by the 3DRGRW model. The hypothetical unconfined aquifer with the geometry is shown in Figure 2. The aquifer thickness is 120 ft; with the aquifer porosity
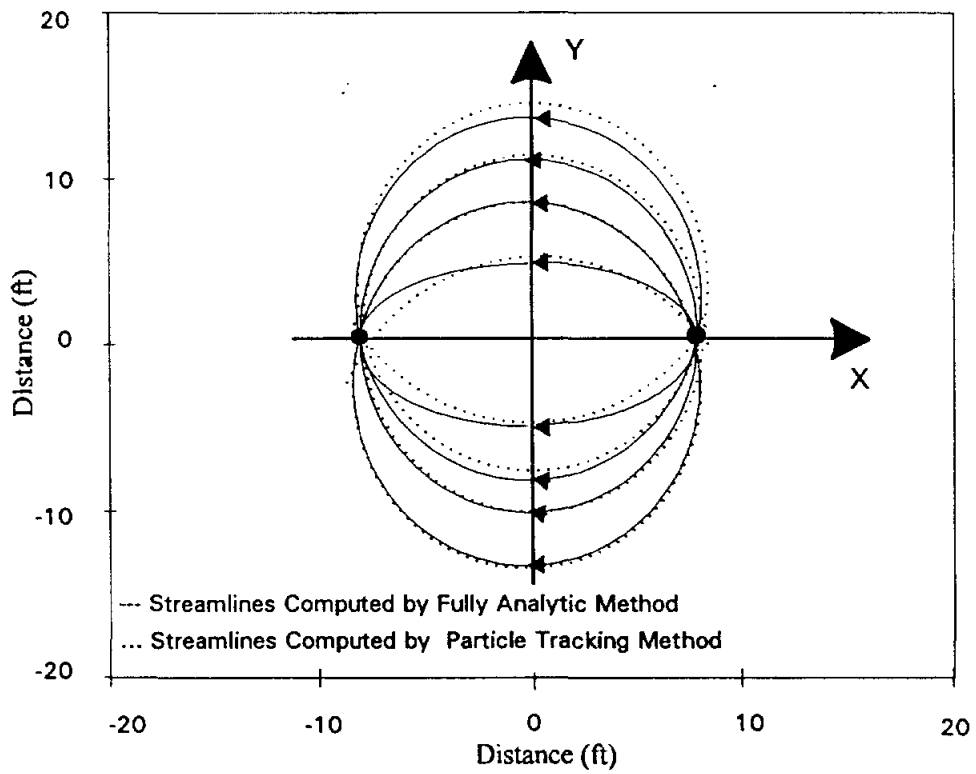
Figure 5. Comparison of streamlines calculated by the computer program with the fully analytic solution for a source and sink problem.
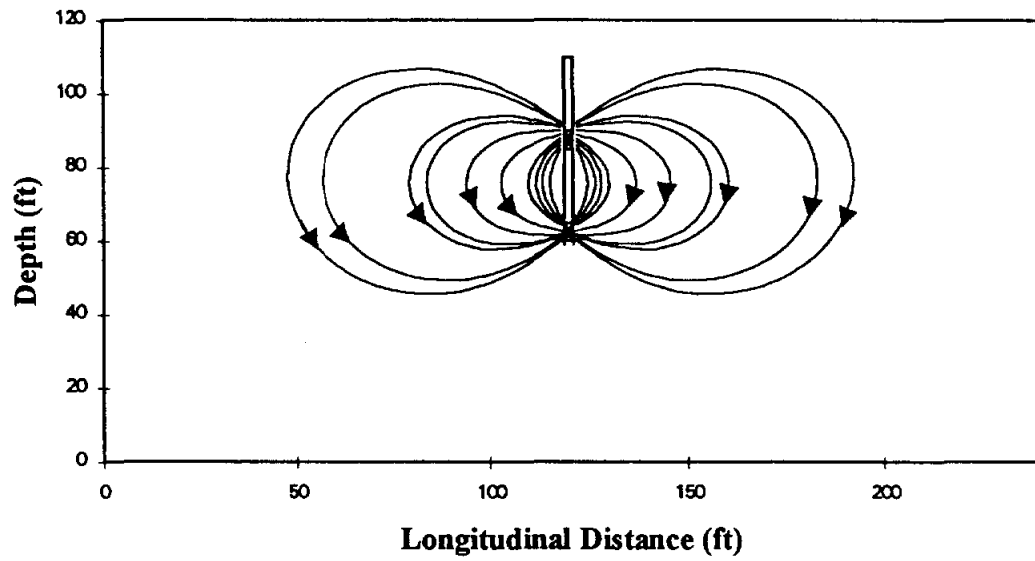
Figure 6. Cross sectional view of the pathlines in the RGRW system with the recirculation pumping rate of 50 ft^3/h, without natural groundwater velocity.

0.44 and the hydraulic conductivity 10 ft/day. The distance between the extracted and the injected screen is 27.5 ft, with two 5 ft screened intervals. The pump rate is 50 ft^3/hour. As might be expected, when there is no ambient horizontal groundwater flow, the velocities are symmetric distribution around the well axis. The magnitude of velocity is greatest in the vicinity of the injection and the extraction interval of the well. In this case, the maximum magnitude of velocity is about $2.5X10^{-3}$ ft/hr. As distance from the well axis increases, the magnitude of velocity decreases.

Figure 6 shows a cross section view of the particle pathlines that start near the top screen section (injection) and end at the bottom screen (extraction) section over a period of 100 days. In three dimensions, these pathlines will form spheres called spheres of influence. Generally, the diameter of influence sphere is defined as the horizontal distance from the well axis to the farthest point at which the circulation flow is still significant (Herrling, 1990).

Flow Pattern with Natural Groundwater Flow

A natural groundwater flow exists at most remediation sites. When a natural groundwater flow is significant, the extent of the capture zone needs to be determined in order to design and operate a remediation system. The optimum number of recirculation wells, the flow rates of the well, and the locations are based on the determined capture zone. Unlike the traditional withdrawal well, where the flow pattern around the well can be considered as two dimensional and the capture zone can be delineated by a plane separating streamline, the flow pattern around the RGRW is three dimensional and the capture zone must be delineated by curved separating streamlines. Those curved separating streamlines form a separating surface. If a water particle is located within the separating surface, the particle will be extracted into the well. If the water particle is located outside the separating surface, the particle will pass out of the well. In practice,

we set many particles at the upstream of the flow field, and track these particle pathlines. The farthest pathline which is extracted into the well is thought as a separating pathline.

Figure 7 depicts a cross sectional view of pathlines with a well recirculation rate of 50 ft^3/hour and the ambient horizontal flow velocity of 4.5 ft/day. In this case, the RGRW can capture the contaminated groundwater above the extraction interval of the well. The captured water is brought into the lower screen section of the well, treated in the well casing, and returned cleaned water to the aquifer at the upper screen section of the well. As noted from the figure, there is some deeper contaminated water not being captured by the well. This means that when designing a RGRW system, the depth of the penetration of the well should be deeper than the location of contaminant in order to avoid deeper contaminant passing through the treatment well.

In the RGRW system, the width of the capture zone depends on the depth of the location in the aquifer. Figures 8, 9 and 10 show the plain view of the width of the capture zone at depth in the vicinity of the extraction screen section , in the middle of the injection and extraction screen, and in the vicinity of the injection screen section, respectively. As see from the figures, the width of the capture zone is largest at the depth in the vicinity extract screen section, and is smallest in the vicinity of the injection screen section.

The pumping rate and the natural groundwater velocity are the most important designing parameters for the RGRW system. Figure 11 shows the width of the upstream capture zone vs. recirculating rate at depth in the vicinity of the extraction interval and in the vicinity of the injection interval. As shown from the figure, with decreasing the pumping rate, the width of the capture zone will decrease. When the recirculation rate decreases to 10 ft^3/h, the width of capture zone near the injection screen section of the well will become zero. It means that there is a minimum required recirculation rate for
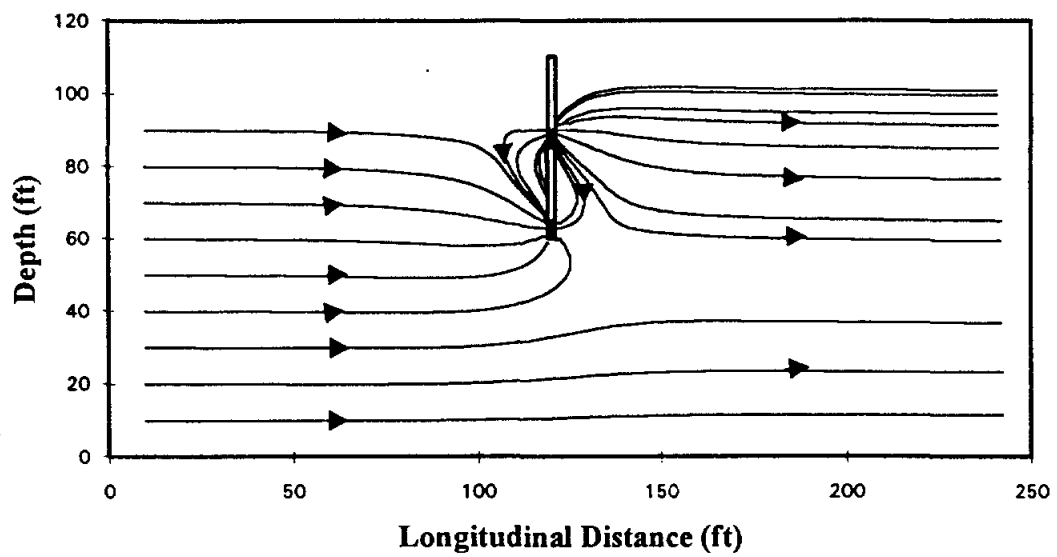
Figure 7. Cross sectional view of the pathlines in the RGRW system with the recirculation pumping rate of 50 ft^3/h and the natural groundwater velocity of 4.5 ft/day.

RGRW to capture a contaminant plume. Generally, the minimum required recirculation pumping rate depends on the natural groundwater velocity and the length of the treatment well.

The width of the capture zone is found to be sensitive to natural groundwater velocity. The higher the natural groundwater velocity, the more difficult it is for contaminant to be captured by the well. Thus, the width of the upstream capture zone decreases as natural groundwater increases. Figure 12 shows the variation of the capture zone with the natural groundwater velocity at the depth of the upper injection screen section and the lower extraction screen section of the recirculation. As seen from the figure, when groundwater velocity is larger than 7 ft/day, the width of capture zone at the depth of injection screen section will approach to zero. This implies that the RGRW is not suitable for a higher groundwater velocity condition for this case. Otherwise, the higher pump rate is required in order to maintain a certain width of capture zone for remediating a plume. Figure 13 shows the case that when pumping rate is too small, the contaminant pass through the treatment well.

The effect of the separation distance between the injection screen section and extraction screen section on the width of capture zone is shown on the Figure 14. The results of the simulation confirmed Philip's (1992) conclusion that increasing the separation distance between the injection and extraction intervals of the well will increase the width of the capture zone at vicinity of extraction screen section because increasing the separation distance may reduce the short circulating between extraction and injection zone. However, we also find that increasing the separation distance between injection and extraction intervals will cause more difficulty for the upper parts of water drawn into the bottom of extraction interval. Thus the width of capture zone at depth of the injection interval will decrease as the separation distance increases. For a
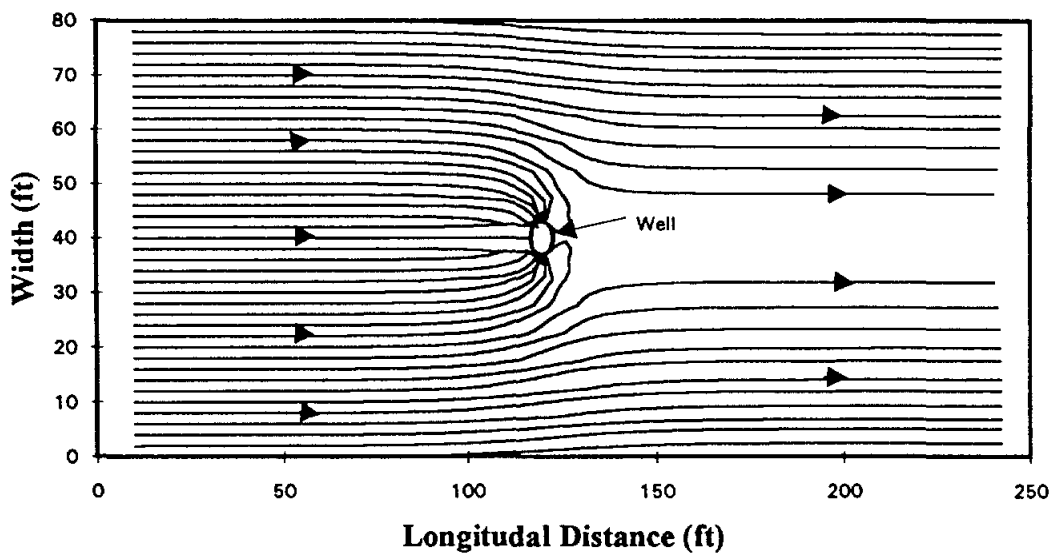
Figure 8. Plan view of the pathlines in the RGRW system for particles started at the depth of the extraction interval with recirculation pumping rate of 50 ft^3/h, natural groundwater velocity of 4.5 ft/day.
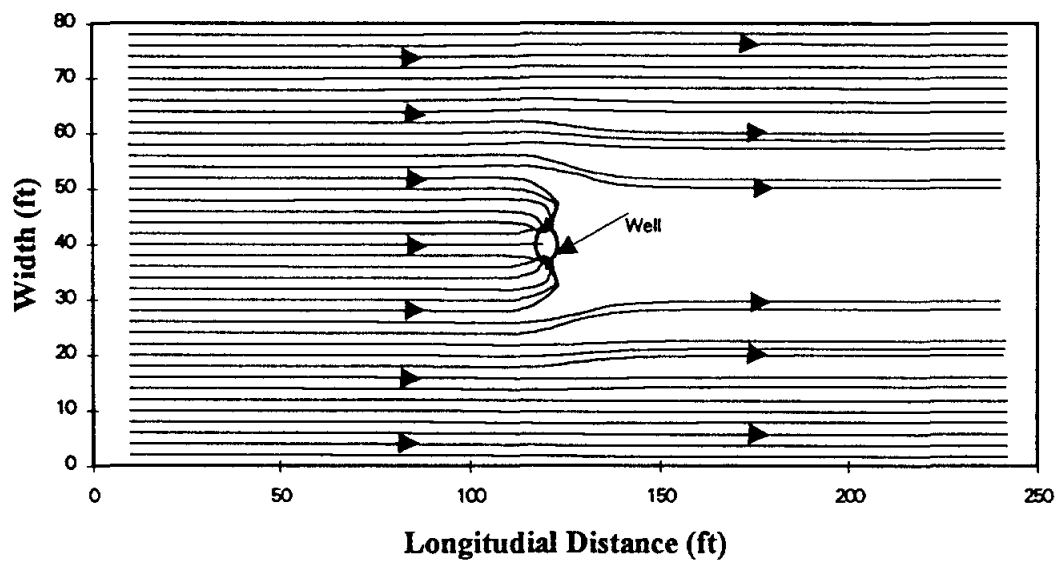
Figure 9. Plan view of the pathlines in the RGRW system for particles started at the depth of the middle of the injection and extraction intervals with recirculation pumping rate of 50 ft^3/h, natural groundwater velocity of 4.5 ft/day.
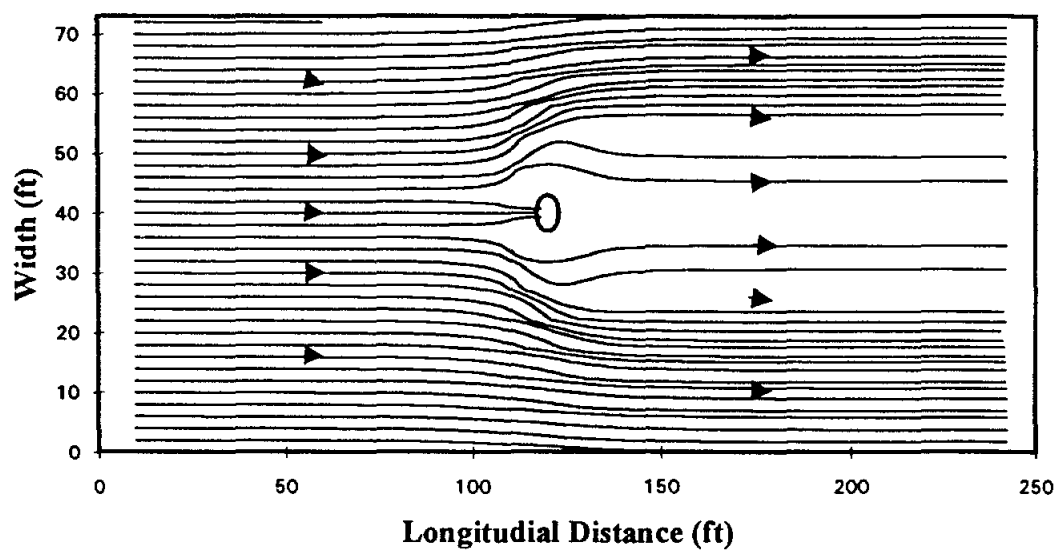
Figure 10. Plan view of the pathlines in the RGRW system for particles started at the depth of the injection interval with recirculation pumping rate of 50 ft^3/h, natural groundwater velocity of 4.5 ft/day.
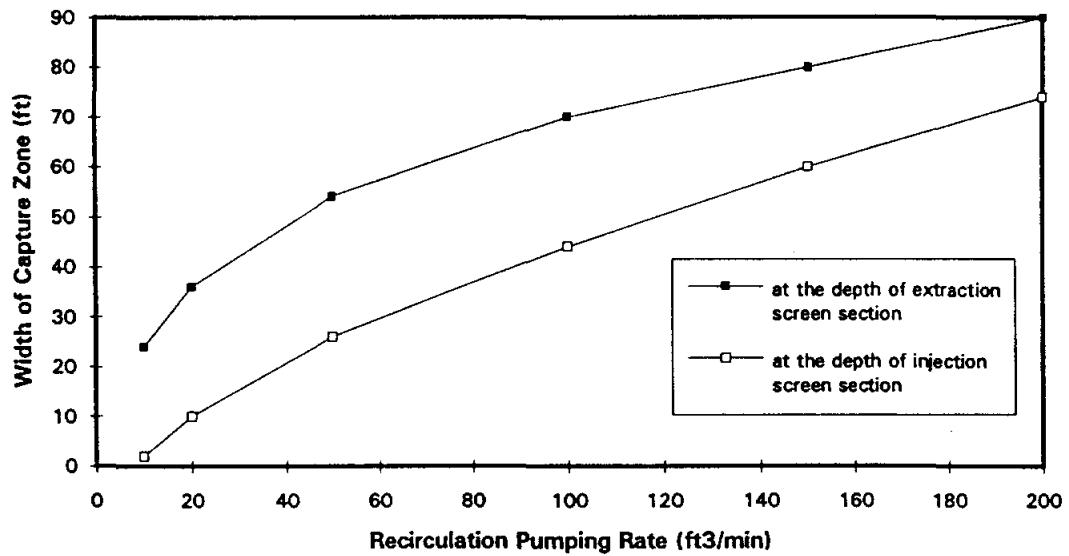
Figure 11. The effect of the recirculation pumping rate on the width of the upstream capture zone with natural groundwater velocity of 1.6 ft/day.
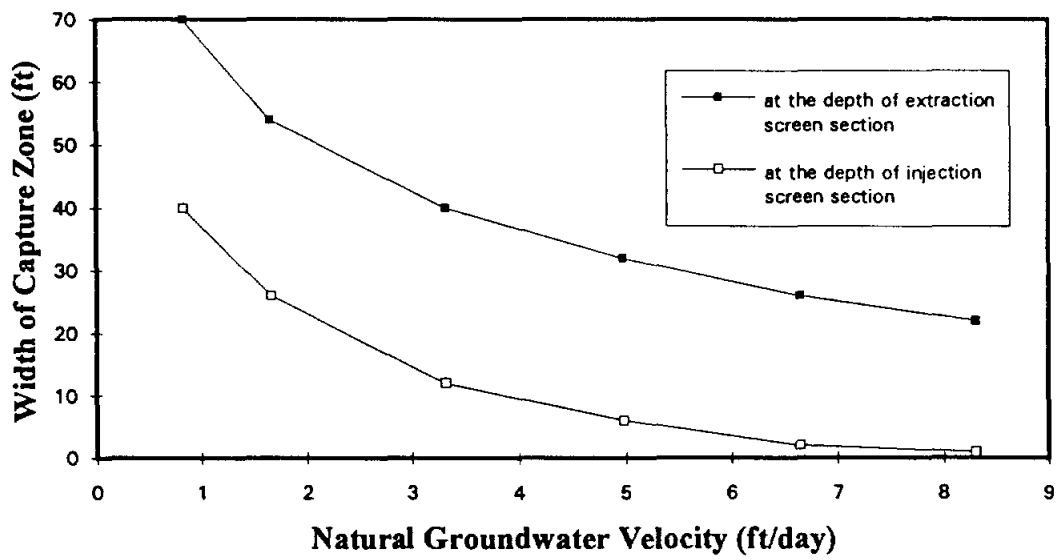
Figure 12. The effect of the natural groundwater velocity on the width of the upstream capture zone with recirculation pumping rate of 50 ft^3/ h.
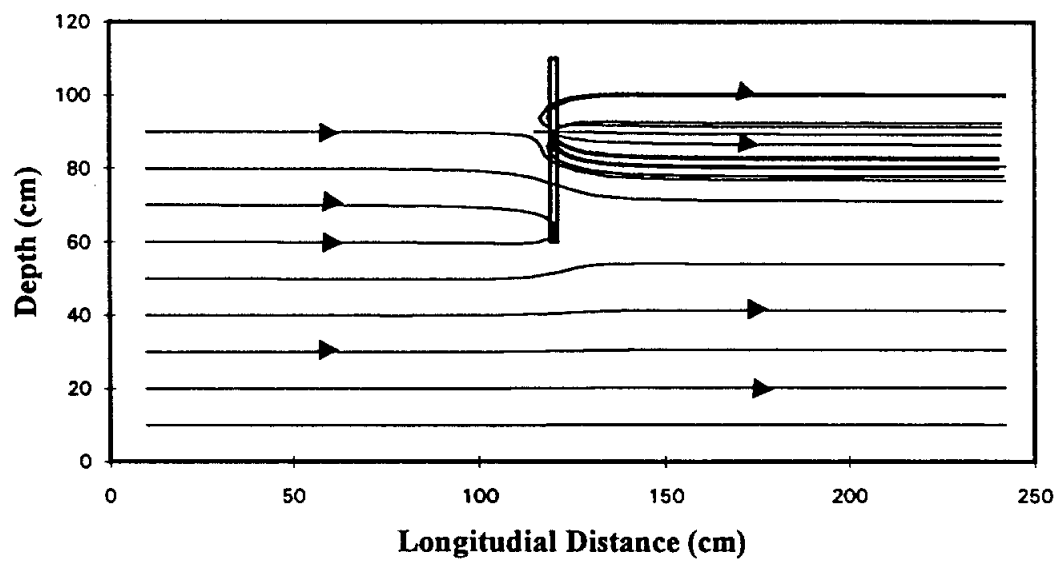
Figure 13. Calculated pathlines for the case that when recirculation pumping rate is too small, the contaminated water passes through the treatment well. (Q = 25 ft^3/h, V = 8.8 ft/day).
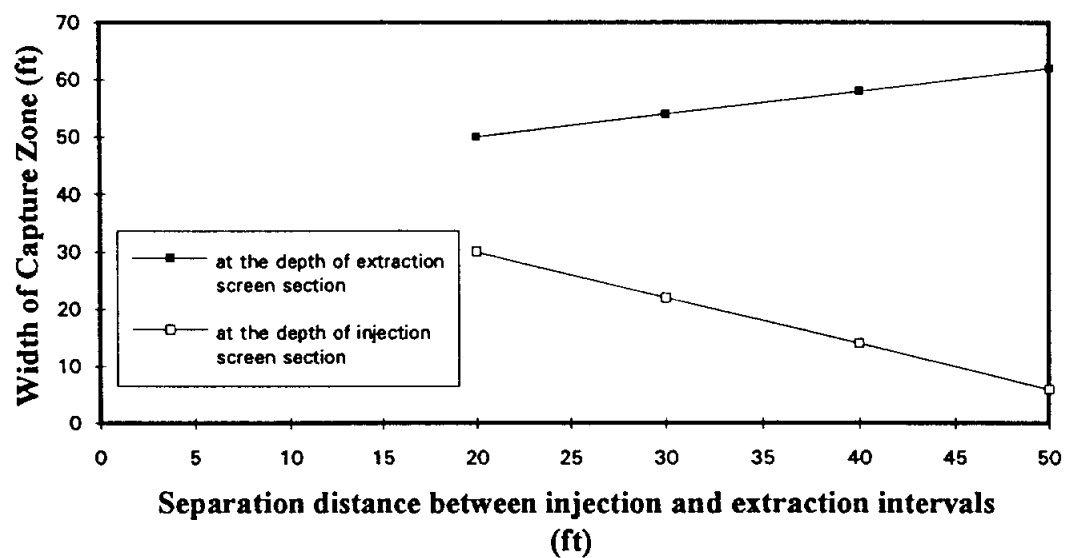
Figure 14. The effect of the separation distance between the injection and extraction intervals on the width of the upstream capture zone with recirculation pumping rate of 20 ft³/ h, natural groundwater velocity of 3.3 ft/day.

longer separation distance, the upper part of contaminant does not reach the extraction screen section, and may pass the treatment well to downstream.

MODEL LIMITATIONS

The solution of the equation 3-8 is based on the small perturbation technique. It is accurate only when the drawdown is much smaller than the thickness of the aquifer. For this reason, the model may not be accurate in the areas of aquifer where the pumping rate is very large or thickness of the aquifer is very small. The solution assumes that pumping rate and porosity are constant. It also assumes that the influence of the specific yield can be negligible. The significance of this assumption decreases as the pumping time increases. Bear and Jacobs (1965) calculated the effects of neglecting storage with an injection well and found that the capture zone of the neglecting storage is only a little larger than the capture zone considering storage and so effects of storage may be neglected for all practical proposes. Like most analytical capture zone models, the influence of the hydrodynamic dispersion is neglected in this model.

SUMMARY AND CONCLUSIONS

The proper design of number of RGRWs, their pumping rates of discharge and locations is very important, both economically and environmentally. The three-dimensional semi-analysis model provides significant insight into the nature of flow patterns and capture zones of the RGRW in a unconfined aquifer. Based on results of the model, we can conclude that recirculating groundwater remediation wells can be effective for intercepting migrating pollutants. The width capture zones is depend on recirculating pumping rate, Natural groundwater velocity, the separation distance between injection and extraction intervals, and the depth of particle location.

CHAPTER V

NUMERICAL MODEL FOR NITRATE TRANSPORT AND DENITRIFICATION IN THE RGRW SYSTEM

Nitrite transport in the RGRW system is a complex process including advective and dispersive transport, sorption, microbial growth, utilization electron donors and acceptors. The solution of the nitrate transport problem requires the simultaneous solution of a set of coupled equations: (1) the equation governing fluid flow, (2) the equation governing the convective-dispersion transport of the nitrate, (3) the equation governing the convective-dispersion transport of the carbon source, (4) the equation governing microbial growth and decay in the aquifer, and (5) the denitrification equation in the treatment reactor. This chapter will present a model of nitrate transport in the RGRW system with denitrification process in both the aquifer and the reactor. The development of the model is based on the law of conservation of mass for water and aqueous species. The next chapter will discuss the numerical implementation of the model. The model simulating results will be discussed in the chapter VII.

FLUID FLOW EQUATION

Contaminant may move in both the saturated and unsaturated zone. Many numerical models have been developed for simulating fluid flow and contaminant transport in the saturated and/or unsaturated zone since the last 20 years (Luthin and Orhun, 1975, Yah et al., 1993). In this study, we treat the flow in both the unsaturated zone and the saturated zone as in a single domain. A single set of equations serves to describe the saturated flow below the water table with the unsaturated flow above the table. The water surface serves as an internal boundary in the computational domain. Above the water table, i.e., unsaturated zone, the water saturation is less than one while below the water table, i.e., saturated zone, the saturation is equal to one.

Properties of Saturated and Unsaturated Zones

In the saturated zone, the fluid pressure, which is measured with respect to atmospheric, is larger than zero. Water saturation S_W, which is defined as the ratio of the water volume to the void volume, is equal to 1. In the unsaturated zone, the void space is only partly filled with water. The water saturation $S_W < 1$ and water pressure is smaller than zero. The negative pressure is defined as the capillary pressure, p_c, i.e., $p_c = -p$ when $p < 0$. As the degree of saturation decreases, the capillary pressure increases and the hydraulic conductivity, K decreases. The relationship among K, S_W, and p_c depends on the solid particles as well as antecedent conditions of drainage or water replenishment. This relationship is typically determined by laboratory experiment. Because measuring unsaturated hydraulic conductivity is time-consuming and expensive, many researchers try to use models for calculating the unsaturated hydraulic conductivity from the more easily measured soil-water retention. Irmay (1954) assumed that the resistance to the flow offered by the solid matrix is proportional to the solid-liquid interfacial area and obtained the relationship between the effective hydraulic conductivity and water saturation

$$K(S_e) = K_o S_e^{3}$$

(5-1)

where $S_e = (S_W - S_0)/(1 - S_0)$ is the dimensionless water saturation, S_0 is the irreducible water saturation, and K_0 is the hydraulic conductivity at saturation.

Gardner (1958) proposed the empirical relationship between the hydraulic conductivity and the capillary pressure head

$$K(\psi) = \frac{a}{\left(b + \psi^m\right)}$$

(5-2)

where a, b and m are constants; and ψ is the capillary pressure head.

We assume that the water content and the permeability are uniquely determined by the capillary pressure. The Van Genuchten's (1980) close-form analytical equation is used for predicting the relationship between the unsaturated hydraulic conductivity, water content, and capillary pressure in the unsaturated zone.

$$K_r = S_e^{1/2}\left[1-\left[1-S_e^{\frac{m}{m-1}}\right]^{\frac{m-1}{m}}\right]^2 \tag{5-3}$$

$$S_w = S_0 + (1-S_0)\left[\frac{1}{1+(\alpha P_c)^m}\right]^{\left(\frac{m-1}{m}\right)} \tag{5-4}$$

Where S_w is a water saturation and S_0 is a residual water saturation below which saturation is not expected to fall (because the fluid becomes immobile), S_e is the dimensionless saturation, Pc is the capillary pressure, K_r is the relative hydraulic conductivity, m is a parameter to the pore size distribution, and α is an empirical constant.

Fluid Mass Balance

If the mass of the fluid is to be conserved, the following fluid mass balance must be satisfied in any element of the system (Bear and Verruijt, 1987).

$$\frac{\partial(\rho\varepsilon S_w)}{\partial t} = -\nabla\cdot\rho(S_w\varepsilon V) + \sum\rho Q_r^{(m)}\delta(X-X^{(m)}) - \sum\rho Q_p^{(m)}\delta(X-X^{(m)}) \tag{5-5}$$

where , V is fluid velocity (L/T); ρ is fluid density (M/L^3); ε is porosity; S_w is the water saturation; t is time (T);δ denotes the Kronecker delta (with $\delta=1$ for $\chi=\chi^{(m)}$ and $\delta=0$ for χ

$\neq\chi(m)$). $Q_r(m)$ is artificial recharge rate at point $\chi(m)$, $(1/T)$; and $Q_p(m)$ is the pump rate at point $\chi^{(r)}$ $(1/T)$.

The term on the left-hand side of equation (5-5) may be recognized as the total change in fluid mass contained in the void space with time. The first term on the right-hand side of equation (5-5) represents the contributions to local mass change due to excess of fluid inflows over outflow at a point. The second and third terms on the right side represent the external additions of fluid.

The amount of the total fluid mass change depends on the fluid pressure. By developing the term on the left-hand side of equation (5-5), we obtain

$$\frac{\partial(\rho\varepsilon S_w)}{\partial t} = \left[\varepsilon\rho\frac{\partial S_w}{\partial p} + S_w\frac{\partial(\varepsilon\rho)}{\partial p}\right]\frac{\partial p}{\partial t} = \rho(C_w + S_s S_w)\frac{\partial p}{\partial t} \tag{5-6}$$

where $S_s = \partial(\varepsilon\rho)/\rho\partial p = \rho\{\varepsilon\beta+(1-\varepsilon)\alpha\}$ is the specific storage. α and β are the porous matrix and fluid compressibility, respectively. Usually, the specific storage is much smaller than the water capacity in the unsaturated zone and can be negligible (Bear and Verruijt, 1987). $C_w = d\theta/dp \approx \varepsilon dS_w/dp$ is the water capacity which is depend on moisture retention. It can be obtained by differentiation of equation (5-4).

$$C_w = \frac{d\theta}{dP} = \frac{\alpha(m-1)(1-S_0)(\alpha P_c)^{m-1}\varepsilon}{\left[1+(\alpha P_c)^m\right]^{\frac{2m-1}{m}}} \tag{5-7}$$

Fluid Flow

The mechanisms of the pressure and the gravity driving forces for the fluid flow may be expressed by a general form of Darcy's law as following

$$q = -\frac{K_r(S_w)K}{\rho g}(\nabla p + \rho g \nabla z) \qquad (5\text{-}8)$$

where q is the specific discharge vector (L/T), $q=S_w \varepsilon V$, K is the saturated hydraulic conductivity tension (L/T) whose principle directions are assumed to be aligned with the coordinate system; $Kr(S_w)$ is the dimensionless relative hydraulic conductivity; p is the fluid (gauge) pressure (M/L/T^2); g is the gravitational acceleration (L/T^2); z is the elevation (L).

By inserting the fluid flow equation (5-8) into equation (5-5) and assuming that fluid is incompressible, we obtain

$$\left(C_w + S_{op}\right)\frac{\partial p}{\partial t} = \nabla\left\{\frac{K_r\left(S_w\right)K}{\rho g}(\nabla p + \rho g \nabla z)\right\} + \Sigma Q_r^{(m)}\delta\left(X - X^{(m)}\right) - \Sigma Q_p^{(m)}\delta\left(X - X^{(m)}\right) \qquad (5\text{-}9)$$

This equation is suitable for both saturated zones and unsaturated zones.

Saturated zone	Unsaturated zone	
$P > 0$, $S_w = 1.0$	$P < 0$, $S_w = S_w(P)$, $S_o \leq S_w < 1$	(5-10)
$K(S_w) = 1.0$, $C_w = 0$	$K_r = K_r(S_w)$, $S_w > S_o$	(5-11)
	$P_c = -P$	(5-12)

NITRATE TRANSPORT AND DENITRIFICATION EQUATIONS IN THE AQUIFER

Based on the mass balance, the partial different equation describing nitrate contaminant transport in the groundwater can be written as follows (Bear and Verruijt, 1987)

$$\frac{\partial(\varepsilon S_w N)}{\partial t} = -\nabla \cdot \varepsilon S_w NV + \nabla \cdot \varepsilon S_w \left(D \cdot \nabla N + D_d^* \nabla N \right) - \rho_b \frac{\partial F}{\partial t}$$

$$+ \sum Q_r^{(m)} \delta\left(X - X^{(m)} \right) N_R^{(m)} - \sum Q_p^{(m)} \delta\left(X - X^{(m)} \right) N - M_f r_n \qquad (5\text{-}13)$$

Where N is the concentration of the dissolved nitrate in the groundwater (M/L^3); V is the water velocity (L/T); D is the mechanical dispersion tensor $(L2/T)$; D_d^* is the diffusion coefficient (L^2/T); F is the quantity of mass sorbed on the surface of porous medium (M/M); ρ_b is the buck density; M_f is the biomass concentration per unit volume of porous media (M/L^3); r_n is the microbial utilization rates per unit of biomass ($M/M/T$); and N_R is concentration of the dissolved nitrate in the source fluid $(M/L3)$. All other terms are as defined previously.

The term on the left-hand side of equation represents the total dissolved nitrate mass changes with time in a unit volume. It can be written as

$$\frac{\partial(\varepsilon S_w N)}{\partial t} = \varepsilon S_w \frac{\partial N}{\partial t} + N \frac{\partial(\varepsilon S_w)}{\partial t} \qquad (5\text{-}14)$$

Substituting equation (5-5) into equation (5-14) and assuming water density ρ is constant, we obtain

$$\frac{\partial(\varepsilon S_w N)}{\partial t} = \varepsilon S_w \frac{\partial N}{\partial t} - N\{ \nabla \cdot (\varepsilon S_w V) - \sum Q_r^{(m)} \delta\left(X - X^{(m)} \right) + \sum Q_p^{(m)} \delta\left(X - X^{(m)} \right) \} \qquad (5\text{-}15)$$

According to the chain rule, the first term on the right side of equation (5-13) can be expressed as

$$\nabla \cdot (\varepsilon S_w V N) = \varepsilon S_w V \nabla \cdot N + N \nabla \cdot (\varepsilon S_w V) \qquad (5\text{-}16)$$

Substituting equations (5-15) and (5-16) into equation (5-13), and rearranging the equation, we obtain

$$\varepsilon S_w \frac{\partial N}{\partial t} = -\varepsilon S_w V \nabla N + \nabla \cdot \varepsilon S_w \left(D \cdot \nabla N + D_d^* \nabla N \right) + \rho_b \frac{\partial F}{\partial t}$$
$$+ \sum Q_r^{(m)} \delta \left(X - X^{(m)} \right) \left(N_R^{(m)} - N \right) - M_f r_n \tag{5-17}$$

Advection

The first term on the right-hand side of equation (5-17) is referred to as the advection term, which describes the transport of the dissolved contaminant at the same velocity as the groundwater. For many practical problems concerning dissolved chemical species transport in groundwater, the advection term dominates. The degree of advection domination can be measured by the dimensionless Peclet number.

$$P_e = \frac{|V| L}{D} \tag{5-18}$$

where P_e is the dimensionless Peclet number; $|V|$ is the magnitude of the linear pore water velocity (L/T); and L is a characteristic length (L). For pure advection problems, the Peclet number becomes infinite.

Dispersion

The second term on the right-hand side of equation (5-17) is the hydrodynamic dispersion which describes the effects of the mechanical dispersion and molecular diffusion in a porous medium. The mechanical dispersion is caused by the variation of the actual velocity on a microscale from the average velocity, both in magnitude and direction along the tortuous paths (Domenico and Schwartz, 1990). The molecular diffusion is a direct result of thermal motion of the individual fluid molecules and carries the solution mass

from areas of high concentration to low concentrations. The molecular diffusion effect is generally secondary and negligible compared to mechanical effects, and only becomes important when groundwater velocity is very low (Bear and Verruijt, 1987).

Several investigators (Nikolaevskii, 1959; Scheidegger, 1961, Bear, 1972) have suggested that the dispersion coefficient in the porous media is described by the following formula

$$D_{ij} = a_{ijkm} \frac{\overline{V_k V_m}}{|V|} f(P_e, \delta) \tag{5-19}$$

where D_{ij} is the dispersion coefficient, a_{ijkl} is the dispersivity of porous mediums, which is a fourth-rank tensor; $|V|$ is the average velocity; Pe is the Peclet number; δ is the ratio of the length characterizing the individual pores of a porous medium to length characterizing their cross-section; $f(P_e, \delta)$ is a function which introduces the effect of tracer transfer by molecular diffusion between adjacent streamlines at the microscopic level (Bear, 1972)

For an isotropic porous medium, the dispersivity tensor can be defined by two constant terms, longitudinal dispersivity (α_L) and transverse dispersivity (α_T) (Scheidegger, 1961). By assuming $f(P_e, \delta) = 1$, we obtain

$$D_{ij} = \alpha_T V \delta_{ij} + (\alpha_L - \alpha_T) V_i V_j / V \tag{5-20}$$

In Cartesian coordinates, the components of the dispersion coefficient may be stated as

$$D_{xx} = \alpha_T V + (\alpha_L - \alpha_T) V_x^2 / V = \left[\alpha_T (V_Y^2 + V_Z^2) + \alpha_L V_X^2 \right] / V \tag{5-21a}$$

$$D_{XY} = (\alpha_L - \alpha_T)V_X V_Y / V = D_{YX} \qquad (5\text{-}21b)$$

$$D_{XZ} = (\alpha_L - \alpha_T)V_X V_Z / V = D_{ZX} \qquad (5\text{-}21c)$$

$$D_{YY} = \alpha_T V + (\alpha_L - \alpha_T)V_Y^2 / V = \left[\alpha_T(V_X^2 + V_Z^2) + \alpha_L V_Y^2\right] / V \qquad (5\text{-}21d)$$

$$D_{YZ} = (\alpha_L - \alpha_T)V_Y V_Z / V = D_{ZY} \qquad (5\text{-}21e)$$

$$D_{ZZ} = \alpha_T V + (\alpha_L - \alpha_T)V_Z^2 / V = \left[\alpha_T(V_X^2 + V_Y^2) + \alpha_L V_Z^2\right] / V \qquad (5\text{-}21f)$$

The longitudinal dispersivity and transverse dispersivity capture the effects of the porous medium's heterogeneity, and can be estimated by interpretation of tracer experiments. Many experiments show that estimates of dispersivity based on the field measurements are two or more order of magnitude larger than those from laboratory data and the values of dispersivity usually increase with increasing scale of observation (Domenico, and Schwartz, 1990).

Sorption

The third term on the right-hand side of equation (5-17) is a sorption term which represents process between chemical species dissolved in groundwater (solution phase) and the chemical species sorbed on the porous medium (solid phase). For the linear equilibrium sorption, the concentration of solute sorbed to the porous medium is directly proportional to the concentration of the solute in the pore fluid, i.e.

$$F = K_d N \qquad (5\text{-}22)$$

where K_d is the distribution coefficient (L^3/M). This reaction is assumed to be instantaneous and reversible.

The temporal change in sorbed concentration can be represented in terms of the concentration of dissolved chemical species using the chain rule of calculus, as follows:

$$\rho_b \frac{\partial F}{\partial t} = (1-\varepsilon)\rho_s K_d \frac{\partial N}{\partial t} \tag{5-23}$$

where ρ_b is the bulk density, ρ_s is the solid's density.

In the unsaturated flow, water occupies only part of the void space and only part of the total area of the solid is exposed to adsorption. The concentration of the solute sorbed to the porous medium depends on the water saturation. Then, the equation (5-23) in unsaturated flow can be written as the equation (Bear and Verruijt, 1987)

$$\rho_b \frac{\partial F}{\partial t} = (1-\varepsilon)\rho_s K_d f(S_w)\frac{\partial N}{\partial t} \tag{5-24}$$

Substituted equation (5-23) and (5-24) into equation (5-17); and rearranging them, we can obtain as

$$\frac{\partial N}{\partial t} = -V_R \nabla N + \frac{1}{\varepsilon S_w R_d(S_w)}\left\{ \nabla \cdot \varepsilon S_w \left(D \cdot \nabla N + D_d^* \nabla N\right) - M_f r_n \right.$$
$$\left. + \sum Q_r^{(m)} \delta\left(X - X^{(m)}\right)\left(N_R^{(m)} - N\right)\right\} \tag{5-25}$$

where $R_d(S_w) = 1 + \dfrac{(1-\varepsilon)\rho_s f(S_w)}{\varepsilon S_w} K_d$ is called the retardation factor which depends on the water saturated degree in the unsaturated flow and $_R = V/R_d(S_w)$, represents the "retarded" velocity of a contaminant particle.

Source and Sink Term

The fourth term is the source and sink term which represents the mass of solute injected into or pumped out from the porous medium domain. When solute is injected into the aquifer, the concentration of solute is necessary to be specified. When solute is pumped out from the aquifer, the concentration of solute is generally equal to the concentration of the groundwater in the aquifer and should not be specified.

Biodegradation

The last term on the left hand side of equation is the mass lost due to the biodegradation. In this study, biofilm conception has been applied to simulate the microbiological processes. According to study of Charachlis et al. (1982), in the porous medium, most of bacteria (95%) are found to be attached to the solid phase of medium by means of the matrix of polysaccharides. Only small parts of bacteria may suspend in the water. Those suspend bacteria may play a role in the degradation of pollutants in the subsurface. However, compared with the attached bacteria, the effects of such a population is smaller. Also if we include such effects, the equations will be much more complicated. Therefore, potential microbial transport mechanisms such as deposition, chemotaxis motion, random (tumbling) motion, and decolgging have not been incorporated into the present model.

The attached bacteria grow and reproduce at the interface of water and solid phases and form a separate, relatively impermeable phase called a biofilm. Generally, the concentration of the substrate within the biofilm is smaller than the concentration in the water phase because of the substrate consumption at the biofilm by microbe. In order for this consumption to continue, the substrate must be transported from the water phase to the liquid-solid interface through diffusive transfer processes(Taylor et al., 1990). In the

steady state, there is no accumulation of substrate at the surface of the biofilm. Hence the rate of substrate supply across the water-biofilm phase boundary from the water phase must be equal to the rate of substrate consumption by reaction within the biofilm.

In the denitrification process, the microbial metabolism can be limited by the lack of either carbon sources (electron donor), nitrate (electron accept) or both simultaneously. Under anaerobic conditions, the rates of carbon and nitrate utilization can be expressed by a double-Monod-type as (Semprini and McCart, 1991)

$$M_f r_{nf} = M_f \left(\eta Y_{cf} + \alpha_n k_d \frac{N_s}{K_n' + N_s} \varepsilon_f I(o) \right)$$
$$= M_f \left(\eta \frac{\mu_{max}}{Y_c} \frac{C_s}{K_c + C_s} \frac{N_s}{K_n + N_s} + \alpha_n k_d \frac{N_s}{K_n' + N_s} \right) \beta_f I(o) \qquad (5\text{-}26a)$$

$$M_f r_{cf} = M_f \frac{\mu_{max}}{Y_c} \frac{C_s}{K_c + C_s} \frac{N_s}{K_n + N_s} \beta_f I(o) \qquad (5\text{-}26b)$$

where r_{cf} and r_{nf} are the rate of carbon and nitrate utilization, respectively, $1/T$; C_s and N_s are the concentration of carbon and nitrate at the water/biofilm interface; β_f is the effectiveness factor, which accounts for the reduction of the overall reaction rate caused by diffusional resistance inside the biofilm (Rittmann, 1993). μ_{max} is the maximum specific growth rate of bacteria; Y_c is carbon yield coefficient (defined as the ratio of the mass of cells formed to the mass of carbon consumed), K_c, K_n is the saturation constant for carbon and nitrate, respectively; η is the stoichiometric ratio of nitrate to carbon utilization for biomass synthesis; α_n is the nitrate use coefficient for energy of maintenance; k_d is the microbial decay coefficient; k'_n is the nitrate saturation constant for decay; and $I(o)$ is the hyperbolic oxygen inhibition function (Stryer, 1988). It can be expressed as

$$I(o) = \frac{K_o}{K_o + o} \qquad (5\text{-}27)$$

where o is the oxygen concentration within the biofilm (inhibitor), and K_O is the inhibition coefficient (M/L3).

We assume that the biofilm is fully penetrated with substrate with no mass-transfer limitations, i.e. C_S =C, N_S = N, and β_f=1. Many studies (Suidan et al., 1987, Semprini and McCart, 1991) indicate that the assumption of a fully penetrated biofilm without external or internal mass transfer limitations is appropriate for the conditions of the field experiments.

Substituting equation (5-26a) into (5-25), we can obtain nitrate transport equations in the aquifer as

$$\frac{\partial N}{\partial t} = -V_R \nabla N + \frac{1}{\varepsilon S_w R_d(S_w)} \nabla \cdot \varepsilon S_w (D_k \cdot \nabla N) + \frac{1}{\varepsilon S_w R_d(S_w)} \sum Q_r^{(n)} \delta(x - x^{(n)})(N_R^{(n)} - N)$$
$$- \frac{1}{\varepsilon S_w R_d(S_w)} \left(\eta \frac{\mu_{max}}{Y_c} \frac{C}{K_c + C} \frac{N}{K_n + N} + \alpha_n k_d \frac{N}{K_n + N} \right) \beta_f I(o) M_f \qquad (5-28)$$

With the same principle, we can obtain carbon transport equation in the aquifer as:

$$\frac{\partial C}{\partial t} = -V_R \nabla C + \frac{1}{\varepsilon S_w R_d(S_w)} \nabla \cdot \varepsilon S_w (D_k \cdot \nabla C) + \frac{1}{\varepsilon S_w R_d(S_w)} \sum Q_r^{(n)} \delta(x - x^{(n)})(C_R^{(n)} - C)$$
$$- \frac{1}{\varepsilon S_w R_d(S_w)} \frac{\mu_{max}}{Y_c} \frac{C}{K_c + C} \frac{N}{K_n + N} \beta_f I(o) M_f \qquad (5-29)$$

The rate of change in the biomass concentration is equal to the difference between the specific rate of biomass growth and the specific rate of mass decay multiplied by the biomass concentration.

$$\frac{\partial M_f}{\partial t} = Y_c r_{cf} M_f - k_d M_f = \left(\mu_{max} \frac{C}{K_c + C} \frac{N}{K_n + N} \beta_f I(o) - K_d \right) M_f \qquad (5-30)$$

The thickness of the biofilm increases with the bacterial growth. In this biofilm model, we use Taylor's sphere assumption (Taylor, 1990) that porous medium is comprised of spheres of equal diameter packed and a biofilm develops in such a way that all spheres are coated with an impermeable biofilm with uniform thickness L_f. The biomass concentration is approximated as $M_f = X_f \, a_f \, L_f$, where a_f is the biofilm affected specific surface (the biofilm surface area per unit of porous medium volume) and X_f is bacterial density.

Assuming that X_f is constant (Rittmann, 1993), the growth of biofilm thickness can be derived from equation (5-30) as

$$\frac{\partial L_f}{\partial t} + \frac{L_f}{a_f} \frac{\partial a_f}{\partial t} = \left(\mu_{max} \frac{C}{K_c + C} \frac{N}{K_n + N} \beta_f I(o) - K_d \right) L_f \tag{5-31}$$

The biofilm affected specific surface can be expressed as a function of biofilm (Taylor, 1990)

$$a_f = \frac{\pi}{\alpha_m d} \left[\frac{(2-m)}{2} \left(\frac{2L_f}{d} \right)^2 + \frac{(4-m)}{2} \left(\frac{2L_f}{d} \right) + 1 \right] \tag{5-32}$$

where α_m is a packing arrangement factor, m is the number of contact points of sand, and d is the diameter of sand particles.

If we assume that the L_f is much smaller than d, the second order of $(2L_f/d)$ can be negligible. We have

$$\frac{\partial a_f}{\partial t} = \frac{\pi}{\alpha_m} \frac{(4-m)}{d^2} \frac{\partial L_f}{\partial t} \tag{5-33}$$

Substituting equation (5-33) into equation (5-31) and rearranging yield

$$\frac{\partial L_f}{\partial t} = \frac{\left(\mu_{max} \dfrac{C}{K_c + C} \dfrac{N}{K_n + N} \beta_f I(o) - K_d \right)}{\left(1 + \dfrac{L_f}{a_f} \dfrac{\pi}{\alpha_m} \dfrac{(4-m)}{d^2} \right)} L_f \qquad (5-34)$$

The biofilm growth causes the permeability and porosity decrease. Based on in-site experiments, Taylor (1990) indicated that if the porous medium has a homogeneous grain size distribution, the porosity and permeability, as a function of biofilm thickness, can be expressed as

$$\varepsilon_f = 1 - \frac{\pi}{\alpha_m} \left[\frac{(2-m)}{12} \left(\frac{2L_f}{d} \right)^3 + \frac{(4-m)}{8} \left(\frac{2L_f}{d} \right)^2 + \frac{1}{2} \left(\frac{2L_f}{d} \right) + \frac{1}{6} \right] \qquad (5-35)$$

$$k_f = c_f \frac{\varepsilon_f}{a_f} = c_f \frac{\left\{ 1 - \dfrac{\pi}{\alpha_m} \left[\dfrac{(2-m)}{12} \left(\dfrac{2L_f}{d} \right)^3 + \dfrac{(4-m)}{8} \left(\dfrac{2L_f}{d} \right)^2 + \dfrac{1}{2} \left(\dfrac{2L_f}{d} \right) + \dfrac{1}{6} \right] \right\}^3}{\left\{ \dfrac{\pi}{\alpha_m d} \left[\dfrac{(2-m)}{2} \left(\dfrac{2L_f}{d} \right)^2 + \dfrac{(4-m)}{2} \left(\dfrac{2L_f}{d} \right) + 1 \right] \right\}^2} \qquad (5-36)$$

Where ε_f is the biofilm-affected porosity, α_f is specific surface, k_f is the biofilm-affected permeability. c_f is Kozeny's constant.

It is assumed that flow varies instantaneously in response to the changes in the biofilm thickness. The iteration technique has been used to solve the equations of flow, substrate transport , nitrate transport and biofilm growth.

BIOLOGICAL DENITRIFICATION IN THE REACTOR

Using biological reactor for denitrification is one of the most promising methods to remove nitrate from water. In this study, the completed-mix, suspended-growth reactor, which is also known as the Continuous-flow Stirred Tank Reactor (CSTR), was selected for removal of nitrate from groundwater. This method has successfully been applied in waste water treatment.

A schematic diagram of a CSTR is shown in Figure 15. A reactor with volume $\forall$ receives a flow called influent at rate Q containing soluble nitrate at concentration N_0, soluble carbon component at concentration C_0 and the suspended microorganism at concentration X_0. Within the reactor, microorganisms utilize the nitrate and substrate growing while reducing the concentration of nitrate and carbon concentration. The influent is mixed completely by a powerful mixer in the reactor, so that any reactant carried into the reactor is dispersed evenly throughout the reactor without any time delay. Thus, the samples taken from all parts of the reactor have the same composition.

Assumption

The main simplifications and assumptions are made during the development of the model of the complex CSTR system as following:

1. The system operates at constant temperature and pH;

2. The system works under anaerobic condition$S$;

3. The influent contains sufficient nutrients to allow microorganism growth.

4. The heterotrophic biomass is homogenous and does not undergo changes in the species diversity with time.

5. The concentration of the bacteria in the influent is zero.

Stirrer

Q, Xo, No, Co

X, Vr, N*, C*

Q, X, N*, C*

A complete-mix reactor
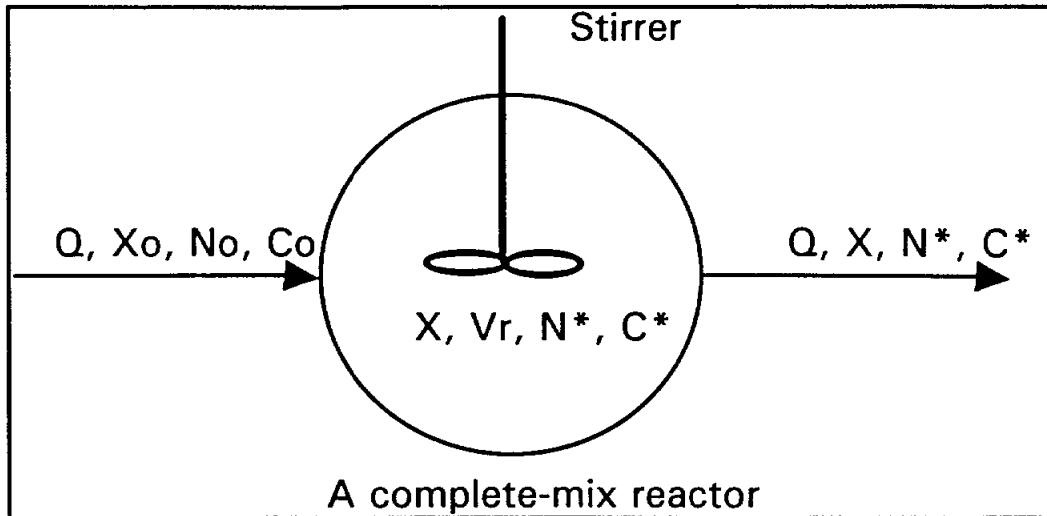
Notations:

Q: Flow rate

Vr: Reactor Volume

Xo: Concentration of Microorganisms in Influent

No: Concentration of Nitrate in Influent

Co: Concentration of Organic Carbon in Influent

X: Concentration of Microorganism in the Reactor

N*: Concentration of Nitrate in the Reactor

C*: Concentration of Carbon in the Reactor

Figure 15. Schematic of a suspended-growth, complete-mix treatment reactor.

Rate of Microorganisms Growth

In the denitrification process, in order to enhance the biotransform, the organic carbon matter needs to add the denitrification reactor as energy sources and electronic acceptors. The amount of carbon matter added must balance the amount of nitrate to be removed. If the amount of carbon source is added in excess, it will pass to the effluent and reduce the quality of the effluent. If insufficient amount of carbon source is added, some nitrate will remain in the effluent and the treatment objective will not be attained.

The net rate of the growth of microorganisms in a continuous culture system can be defined as follows:

$$r_g = \mu X - K_d X \qquad (5\text{-}37)$$

where r_g is the rate of bacterial growth, $M/(L^3 T)$, μ is the specific growth rate, $1/T$, X is the concentration of microorganism, (M/L^3); k_d is the microorganism decay coefficient.

The rate of nitrate and carbon utilization can be written as

$$r_N = \frac{\mu}{Y_{N*}} X \qquad (5\text{-}38)$$

$$r_C = \frac{\mu}{Y_{C*}} X \qquad (5\text{-}39)$$

where r_n, r_c are the rates of nitrate and carbon utilization, respectively, $(M/L3)$; Y_{N*}, Y_{C*} are the maximum yield coefficients of nitrate and carbon (defined as the ratio of the mass of cells formed to the mass of nitrate and carbon removed, mg/mg), respectively.

In general conditions the specific growth rate of the microorganism is dependent on the concentrations of the carbon source and nitrate. A double Monod-type form of the specific growth can be used to model the dual limitation substrates. The specific growth rate can be expressed as

$$\mu = \mu_{max} \frac{C^*}{\left(K_{C^*} + C^*\right)} \frac{N^*}{\left(K_{N^*} + N^*\right)} f_1(T) f_2(pH) \qquad (5\text{-}40)$$

where μ_{max} is the maximum specific growth rate, N^* is the concentration of nitrate in the reactor, C^* is the concentration of carbon in the reactor, K_{s^*}, K_{c^*} are the half-velocity constants for nitrate and carbon in the reactor, respectively. $f_1(T)$ and $f_2(pH)$ are the functions of temperature and pH which can be expressed as (Timmermans and Haute, 1983):

$$f_1(T) = K_t^{(T-20)} \qquad (5\text{-}41)$$

$$f_2(pH) = \frac{1}{1 + k_p\left(10^{|8.3-pH|} - 1\right)} \qquad (5\text{-}42)$$

where K_p, K_t are coefficients of pH and temperature, respectively.

Equation (5-40) indicates the general relationship between specific growth and concentration of substrate and nitrate. There are four extreme cases:

(1) when C^* is very high ($C^* \gg K_{c^*}$), equation (5-40) can be approximated as

$$\mu = \mu_{max} \frac{N^*}{\left(K_{N^*} + N^*\right)} f(pH) f(T) \qquad (5\text{-}43a)$$

In this condition, the concentration of nitrate is a rate limiting.

(2) When N^* is very high ($N^* \gg K_{n^*}$), equation (5-40) can be approximated as

$$\mu = \mu_{max} \frac{C^*}{\left(K_{c^*} + C^*\right)} f(pH) f(T) \qquad (5\text{-}43b)$$

In this condition, the concentration of carbon matter is a growth rate limiting substrate.

(3) When both N* and C* are very high, equation (5-40) can be approximated as

$$\mu = \mu_{max} f(pH) f(T)$$ (5-43c)

In this condition, the growth rate approaches a maximum rate (μmax) that is independent of substrate concentration.

(4) When both N* and C* are very low (N*<<Kn*; C*<<Kc*), Equation (5-40) can be approximated as

$$\mu = k' C^* N^* f(pH) f(T)$$ (5-43d)

where $k' = \mu_{max} / (K_C \cdot K_N)$

In this condition, the growth rate is depend on concentrations of nitrate and carbon.

Mass Balance of Microorganisms, Carbon and Nitrate

A mass balance for the mass of microorganisms in the complete-mix reactor can be written as following:

Rate of accumulation of microorganism in the reactor	=	Rate of flow of microorganism into the reactor	-	Rate of flow of microorganism out of the reactor	+	Net growth of microorganism within the rector
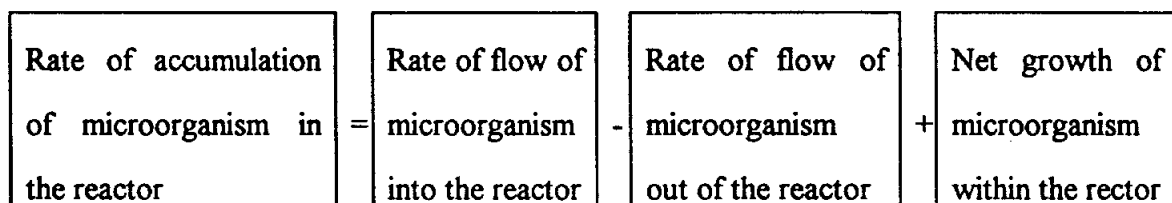
Using symbolic representation

$$V_r \frac{dX}{dt} = QX_0 - QX + V_r \gamma_g$$ (5-44)

where V_r is the reactor volume, X_0 is the concentration of microorganisms in influent, X is the concentration of microorganisms in the reactor, Q is the flow rate, γ_g is the net rate of microorganism growth.

The net rate of the microorganism growth can be written as

$$\gamma_g = \mu_{max}\left(\frac{N^*}{K_{N^*} + N^*}\right)\left(\frac{C^*}{K_{C^*} + C^*}\right)X - K_d^* X \tag{5-45}$$

Substituting equation (5-45) into equation (5-44) yields

$$V_r \frac{dX}{dt} = QX_0 - QX + V_r\left(\mu_{max}\left(\frac{N^*}{K_{N^*} + N^*}\right)\left(\frac{C^*}{K_{C^*} + C^*}\right)X\right) \tag{5-46}$$

A mass balance for nitrate in the reactor can be written as

Rate of accumulation of nitrate in the reactor	=	Rate of flow of nitrate into the reactor	-	Rate of flow of nitrate out of the reactor	-	Rate of nitrate utilization within the reactor

$$V_r \frac{dN^*}{dt} = QN_o - QN^* - V_r \frac{\mu_{max}}{Y_{N^*}}\left(\frac{N^*}{K_{N^*} + N^*}\right)\left(\frac{C^*}{K_{C^*} + C^*}\right)X \tag{5-47}$$

where N_0 is the concentration of nitrate in influent, Y_{N^*} is the yield coefficient of (defined as the ratio of the mass of cells formed to the mass of nitrate removed, mg/mg).

A mass balance for carbon in the reactor can be expressed as

Rate of accumulation of substrate in the reactor	=	Rate of flow of substrate into the reactor	-	Rate of flow of substrate out of the reactor	-	Rate of substrate utilization within the reactor

$$V_r \frac{dC^*}{dt} = QC_o - QC^* - V_r \frac{\mu_{max}}{Y_{C^*}} \left(\frac{N^*}{K_{N^*} + N^*} \right) \left(\frac{C^*}{K_{C^*} + C^*} \right) X \qquad (5\text{-}48)$$

where C_0 is the concentration of carbon added into the reactor, Y_{C^*} is the maximum yield coefficient of carbon(defined as the ratio of the mass of cells formed to the mass of carbon removed, mg/mg).

If it is assumed that the concentration of microorganisms in the influent can be neglected and that the steady state prevails, (i.e. $dX/dt = dS/dt = dC/dt = 0$), equation (5-46) can be simplified to yield:

$$\mu_{max} \left(\frac{C^*}{K_{C^*} + C^*} \right) \left(\frac{N^*}{K_{N^*} + N^*} \right) = \frac{1}{\theta} + K_d^* = \frac{1 + K_d^* \theta}{\theta} \qquad (5\text{-}49)$$

where $\theta = V_r / Q$ is the hydraulic detention time.

Equation (5-49) suggests that when K_d^* is fixed for a given microbial population, the specific growth rate may only be controlled by the hydraulic detention time, θ. This can be done by manipulating either the flow rate with a given volume of reactor, or the volume of reactor for a given flow rate.

Effluent Nitrate and Carbon Concentrations in the Reactor

The effluent microorganism concentration can be obtained by substituting equation (5-49) into equations (5-47) and (5-48)

$$X = \frac{(C_0 - C^*)Y_C}{1 + K_d^* \theta} = \frac{(N_0 - N^*)Y_N}{1 + K_d^* \theta}$$

(5-50)

From equation (5-50), we can get the relationship between the concentration of nitrate and substrate

$$C^* = \frac{Y_{N^*}}{Y_{C^*}} N^* - \frac{Y_{N^*}}{Y_{C^*}} N_0 + C_0$$

(5-51)

Substituting equation (5-51) into equation (5-49), and rearranging it, we obtain

$$\left(\frac{\theta \mu_{max}}{1 + K_d^* \theta} - 1\right) Y_{C^*} C^{*2} + \frac{\theta \mu_{max}}{1 + K_d^* \theta} [(Y_{N^*} N^* - Y_{C^*} C_0)$$
$$+ (Y_{C^*} C_0 - K_{N^*} Y_{N^*} - K_{N^*} N_0 - K_{C^*} Y_{C^*})] C^* + (Y_{C^*} C_0 - K_{N^*} Y_{N^*} - K_{N^*} N_0) K_{C^*} = 0$$

(5-52)

Solving quadratic equation (5-52), we obtain

$$C^* = \frac{1}{2\left(\frac{\theta \mu_{max}}{1 + k_d^* \theta} - 1\right) Y_{C^*}} \left\{ \frac{\theta \mu_{max}}{1 + k_d^* \theta} (Y_{C^*} C_0 - Y_{N^*} N_0) \right.$$

$$+ (Y_{N^*} K_{N^*} + Y_{N^*} N_0 + Y_{C^*} K_{C^*} - Y_{C^*} C_0)$$

(5-53)

$$+ \left[\left[\frac{\theta \mu_{max}}{1 + k_d^* \theta} (Y_{N^*} N_0 - Y_{C^*} C_0) + (Y_{C^*} C_0 - Y_{N^*} K_{N^*} - Y_{N^*} N_0 - Y_{C^*} K_{C^*}) \right]^2 \right.$$

$$\left. \left. + 4\left(\frac{\theta \mu_{max}}{1 + k_d^* \theta} - 1\right) (Y_{N^*} K_{N^*} + Y_{N^*} N_0 - Y_{C^*} C_0) K_{C^*} Y_{C^*} \right]^{1/2} \right\}$$

Similarly, we can obtain the effluent of nitrate concentration as follows

$$N^* = \frac{1}{2\left(\frac{\theta\mu_{max}}{1+k_d^*\theta}-1\right)Y_s}\left\{\frac{\theta\mu_{max}}{1+k_d^*\theta}\left(Y_{N*}N_0-Y_{C*}C_0\right)\right.$$

$$+\left(Y_cK_c+Y_cC_0+Y_{N*}K_{N*}-Y_{N*}N_0\right)$$

$$+\left[\left[\frac{\theta\mu_{max}}{1+k_d^*\theta}\left(Y_{C*}C_0-Y_{N*}N_0\right)+\left(Y_{N*}N_0-Y_{C*}K_{C*}-Y_{C*}C_0-Y_{N*}K_{N*}\right)\right]^2\right.$$

$$\left.\left.+4\left(\frac{\theta\mu_{max}}{1+k_d^*\theta}-1\right)\left(Y_{C*}K_{C*}+Y_{C*}C_0-Y_{N*}N_0\right)K_{N*}Y_{N*}\right\}^{1/2}\right\}$$

(5-54)

From equations (5-53) and (5-54) we can see that for a given biological community, and a particular set of environmental conditions, the effluent concentrations of nitrate and carbons are $\overset{a}{\cancel{\text{the}}}$ function of both the hydraulic detention time and the influent concentrations of nitrate and carbon. The influent concentrations of nitrate and carbon may be determined by the transport equations that were described $\overset{in}{}$ previous sections. Meanwhile, the effluent concentration of nitrate and carbon will affect the nitrate transport. Thus, nitrate transport equations must be solved simultaneously with denitrification equations in the reactor. The effluent concentrations of nitrate and carbon will be used as source$\overset{s}{}$ term$\overset{s}{}$ in the transport equations

INITIAL AND BOUNDARY CONDITIONS OF NITRATE TRANSPORT EQUATION

The initial conditions include information of the concentration distribution at time t=0 at all points of simulated domain. It is written as

$$C(X,Y,Z,t=0)=C^*(X,Y,Z) \quad on\,\mathfrak{R}$$

(5-55)

where $C^*(X, Y, Z)$ is a known concentration distribution and $\Re$ denotes the simulated domain.

In this model we assume that the indigenous microbial population and the species concentration are uniformly distributed at time zero.

Generally, there are three kinds of boundary conditions used in the transport equations: (1) Dirichlet boundary condition (first boundary condition); (2) Neumann boundary condition (second boundary condition); and (3) Cauchy boundary condition (third boundary condition).

For the Dirichlet boundary condition, the concentration is specified around a given boundary. We can write the boundary condition in the form of

$$C(x,y,z,t) = g_1(x,y,z,t) \quad on\ \Gamma_1 \quad t \ge 0 \tag{5-56}$$

where Γ_1 refers to the specified-concentration boundary, and $g_1(x, y, z, t)$ is the specified concentration along Γ_1.

For the Neumann boundary condition, the concentration gradient is specified $\overset{\alpha}{\text{cross}}$ the boundary. It can be written as

$$D_h \frac{\partial C(x,y,z,t)}{\partial t} = g_2(x,y,z,t) \quad on\ \Gamma_2 \quad t \ge 0 \tag{5-57}$$

where $g_2(x, y, z, t)$ is a known flux at all point of a boundary segment, Γ_2. For the impervious boundary, $g_2(x, y, z, t) = 0$, The equation (5-57) reduces to

$$\frac{\partial C(x,y,z,t)}{\partial t} = 0 \tag{5-58}$$

For the Cauchy boundary condition, which is a combination of the first and second boundary condition, both the concentration and the concentration gradient are specified. It can be written in the form of

$$D_h \frac{\partial C}{\partial x} - vC = g_3(x,y,z,t) \quad on\ \Gamma_3 \quad t \geq 0 \tag{5-59}$$

where $g_3(x, y, z, t)$ is a known function representing the total flux (dispersive and advective)normal to the boundary Γ_3.

CHAPTER VI

NUMERICAL APPROXIMATION METHOD

EULERIAN-LAGRANGIAN METHOD

Numerical methods used to solve the advection-dispersion equation may be classified as three perspectives: the Eulerian method, the Lagrangian method and a combination of the two that will be referred to as the Eulerian-Lagrangian method (Neuman, 1984). In the Eulerian method, the discretization of the advection-dispersion equation is performed to a fixed grid in space by methods such as the finite-different or finite-element method. Many investigators have presented that the Eulerian method performs quite well when problems are the dispersion dominated problems. For the advection dominated problems, in which the physical dispersion is small and or negligible, this method causes a large numerical dispersion, leading to the smearing of the concentration fronts which should have a sharp appearance (Cheng et al., 1984). This phenomenon is caused by the approximation of the first-order derivatives of advective term, which involves errors of the order of magnitude of the second-order derives (Bear and Verruijt, 1987). If using high-order schemes to eliminate numerical dispersion, the artificial oscillation may become a serious problem (Neuman, 1984). In the Lagrangian method, the advection-dispersion equation is solved by a moving grid. This method is often suited to solve simple advection dominated problems. McBride and Rutherford (1984) use this method successfully to solve the one-dimensional pollutant transport in the river. However, Lagrangian methods are often not strictly conservative and the technique that involves a moving reference may lead to numerical instability and computational difficulties under a complex subsurface environment (Neuman, 1981). The Eulerian-Lagrangian method attempts to combine the advantages of the Eulerian method and the Lagrangian

method by solving the advection term with a set of moving particles, and the dispersion and other terms with a finite difference or finite element method. Garder et al. (1964) first introduced this concept to the groundwater problems. They stated that the technique does not introduce numerical dispersion. The development and application of this technique have been presented by Pinder and Cooper (1970), Reddell and Sunada (1970), and Bredehoeft and Pinder (1973), Konikow and Bredehoeft (1978), Neuman (1981), Cheng (1984), Corapcioglu and Haridas (1985) and Zheng (1992).

Depending on the tracking movement of the particles, the Eulerian-Lagrangian method is divided into: the forward particle tracking method of characteristics (MOC) (e.g., Garder et al. 1964; Konikow and Bredhoeft, 1978; Goode, 1990); the backward particle tracking modified method of characteristics (MMOC) (e.g., Cheng et. al., 1984, Yeh et al., 1993) and a hybrid of these two methods (HMOC) (e.g., Neuman, 1984, Zhang, 1993). These three techniques are similar except in the treatment of the advection term. The advantages of the MMOC technique are that this technique uses only one particle for each finite-difference cell, whereas, the MOC method generally requires several particles (such as 9 particles) per cell. Therefore, the MMOC method is more time efficiency and requires less computer memory than the MOC method. However, when dealing with the sharp front problems, the MMOC technique introduces some unwanted numerical dispersion (Zheng, 1993). In this study, we use the MOC technique to simulate the nitrate transport equations in order to get more accuracy of nitrate plume.

According to the chain rule, the dissolved concentration of chemical species can be derived as

$$\frac{dC}{dt} = \frac{\partial C}{\partial t} + \frac{\partial C}{\partial X_i}\frac{\partial X_i}{\partial t} = \frac{\partial C}{\partial t} + V_R \nabla C \qquad (6\text{-}1)$$

Substituting equation (6-1) into equations (5-28) , (5-29) and (5-30), nitrate and carbon transport equations can be expressed in the Lagrangian forms as

$$\frac{DN}{Dt} = \frac{1}{\varepsilon S_w R_d(S_w)} \nabla \cdot \varepsilon S_w (D_h \cdot \nabla N) + \frac{1}{\varepsilon S_w R_d(S_w)} \sum Q_r^{(m)} \delta(X - X^{(m)})(N_R^{(m)} - N)$$
$$- \frac{1}{\varepsilon S_w R_d(S_w)} \left(\eta \frac{\mu_{max}}{Y_c} \frac{C}{K_c + C} \frac{N}{K_n + N} + \alpha_n k_d \frac{N}{K_n' + N} \right) \beta_f I(o) M_f \qquad (6\text{-}2)$$

$$\frac{DC}{Dt} = \frac{1}{\varepsilon S_w R_d(S_w)} \nabla \cdot \varepsilon S_w (D_h \cdot \nabla C) + \frac{1}{\varepsilon S_w R_d(S_w)} \sum Q_r^{(m)} \delta(X - X^{(m)})(C_R^{(m)} - C)$$
$$- \frac{1}{\varepsilon S_w R_d(S_w)} \frac{\mu_{max}}{Y_c} \frac{C}{K_c + C} \frac{N}{K_n + N} \beta_f I(o) M_f \qquad (6\text{-}3)$$

$$\frac{\partial M_f}{\partial t} = \left(\mu_{max} \frac{C}{K_c + C} \frac{N}{K_n + N} \beta_f I(o) - K_d \right) M_f \qquad (6\text{-}4)$$

$$\frac{\partial L_f}{\partial t} = \frac{\left(\mu_{max} \frac{C}{K_c + C} \frac{N}{K_n + N} \beta_f I(o) - K_d \right)}{\left(1 + \frac{L_f}{a_f} \frac{\pi}{\alpha_m} \frac{(4 - m)}{d^2} \right)} L_f \qquad (6\text{-}5)$$

The solution of equations (6-1), (6-2), (6-3) (6-4), and (6-5) may be obtained as X=X(t); Y=Y(t), Z=Z(t), and C=C(t); N=N(t); M_f=M_f(t); L_f=L_f(t). These solutions are referred to the characteristics curves of the governing equations (5-28), (5-29) (5-30) and (5-31).

NUMERICAL IMPLEMENTATION

The method of characteristics uses a forward particle tracking technique for solving the advection term. Initially, the particles with a given initial concentration are uniformly distributed throughout the cells. At each time interval, the moving particles are relocated by using the following finite-difference forms of equations (6-6a) and (6-6b):

$$X^{t+1} = X^t + \frac{\Delta t}{R_d(S_w)} V_x(X^t, Z^t) \qquad (6\text{-}6a)$$

$$Z^{t+1} = Z^t + \frac{\Delta t}{R_d(S_w)} V_z(X^t, Z^t) \qquad (6\text{-}6b)$$

where X^{n+1} and Z^{n+1} are the particle coordinates at the new time level (n+1); X^n and Z^n are the particle coordinates at the old time level (n); V_x and V_z are the linear velocity at position (X^n, Z^n); Δt is the time increment and $R_d(S_w)$ is retardation factor.

When all the moving particles have been relocated, each cell is temporarily assigned a concentration, $C_{i,j}^{t+\Delta}$, which is the average concentration of all the particles lying inside the cell (i,j,k) due to advection, i.e.,

$$C_{i,j}^{t+\Delta} = \frac{\sum_{m}^{M_p} C_m^*}{M_p} \qquad (6\text{-}7)$$

where $C_{i,j}^{t+\Delta}$ is the concentration at cell (i, j); C_m^* is the concentration of the mth particle in cell (i, j), Mp is the total number of particles at cell (i, j).

The changes of concentration results from the dispersion and other terms can be written as:

$$\Delta C_{i,j}^{t+1} = \left(\Delta C_{i,j}^{t+1}\right)_{dis} + \left(\Delta C_{i,j}^{t+1}\right)_{sou} + \left(\Delta C_{i,j}^{t+1}\right)_{bio} \qquad (6\text{-}8)$$

where $\left(\Delta C_{i,j}^{t+1}\right)_{dis}$ is the concentration change due to dispersion; $\left(\Delta C_{i,j}^{t+1}\right)_{sou}$ is the concentration change due to the source and sink mixing; $\left(\Delta C_{i,j}^{t+1}\right)_{bio}$ is the concentration change due to the biologic reaction.

According to the summation convection of the tensor notation, the concentration change of the dispersion term of equation (6-8) may be written as

$$\left(\Delta C_{i,j}^{t+1}\right)_{dis} = \frac{\Delta t}{\varepsilon S_w}\left[\frac{\partial}{\partial X}\left(\varepsilon S_w D_{xx}\frac{\partial C}{\partial X} + \varepsilon S_w D_{xz}\frac{\partial C}{\partial Z}\right)\right.$$
$$\left. + \frac{\partial}{\partial Z}\left(\varepsilon S_w D_{zx}\frac{\partial C}{\partial X} + \varepsilon S_w D_{zz}\frac{\partial C}{\partial Z}\right)\right]$$

(6-9)

To develop a finite difference form of equation (6-9), consider the spatial derivatives of concentration at i+½

$$\left(\frac{\partial C}{\partial X}\right)_{i+\frac{1}{2},j} = \frac{C_{i+1,j} - C_{i,j}}{\Delta X}$$

(6-10a)

$$\left(\frac{\partial C}{\partial Z}\right)_{i+\frac{1}{2},j} = \frac{C_{i+\frac{1}{2},j+1} - C_{i+\frac{1}{2},j-1}}{2\Delta Z}$$

(6-10b)

Using a linear interpolation scheme, it has

$$C_{i+\frac{1}{2},j+1} = \frac{C_{i,j+1} + C_{i+1,j+1}}{2}$$

(6-11a)

$$C_{i+\frac{1}{2},j-1} = \frac{C_{i,j-1} + C_{i+1,j-1}}{2}$$

(6-11b)

Substituting equation (6-11) into equation (6-10) gives:

$$\left(\frac{\partial C}{\partial X}\right)_{i+\frac{1}{2},j} = \frac{C_{i+1,j} - C_{i,j}}{\Delta X}$$

(6-12a)

$$\left(\frac{\partial C}{\partial Z}\right)_{i+\frac{1}{2},j} = \frac{C_{i,j+1} + C_{i+1,j+1} - C_{i,j-1} - C_{i+1,j-1}}{4\Delta Z} \tag{6-12b}$$

Similarly, for a point (i-$\frac{1}{2}$, j, k), spatial derivatives are

$$\left(\frac{\partial C}{\partial X}\right)_{i-\frac{1}{2},j,k} = \frac{C_{i,j,k} - C_{i-1,j,k}}{\Delta X} \tag{6-13a}$$

$$\left(\frac{\partial C}{\partial Z}\right)_{i-\frac{1}{2},j} = \frac{C_{i,j+1} + C_{i-1,j+1} - C_{i,j-1} - C_{i-1,j-1}}{4\Delta Z} \tag{6-13b}$$

The spatial derivatives at points (i, j+$\frac{1}{2}$), (i, j-$\frac{1}{2}$) may be obtained by using the same manner.

Assuming that the grad space is the same along any direction, the finite difference form of equation (6-9) may be obtained by using the fully explicit central finite-difference scheme as:

$$\left(\Delta C_{i,j}^{t+1}\right)_{dis} = \frac{\Delta t}{\varepsilon S_w}\left[\frac{\varepsilon S_w D_{xx(i+\frac{1}{2},j)}\left(C_{i+1,j}-C_{i,j}\right)}{(\Delta X)^2} - \frac{\varepsilon S_w D_{xx(i-\frac{1}{2},j)}\left(C_{i,j}-C_{i-1,j}\right)}{(\Delta X)^2}\right.$$

$$+\frac{\varepsilon S_w D_{xx(i+\frac{1}{2},j)}\left(C_{i,j+1}+C_{i+1,j+1}-C_{i,j-1}-C_{i+1,j-1}\right)}{4\Delta X\Delta Z}$$

$$-+\frac{\varepsilon S_w D_{xx(i-\frac{1}{2},j)}\left(C_{i,j+1}+C_{i-1,j+1}-C_{i,j-1}-C_{i-1,j-1}\right)}{4\Delta X\Delta Z}$$

$$+\frac{\varepsilon S_w D_{zz(i,j+\frac{1}{2})}\left(C_{i,j+1}-C_{i,j}\right)}{(\Delta Z)^2} - \frac{\varepsilon S_w D_{zz(i,j-\frac{1}{2})}\left(C_{i,j}-C_{i,j-1}\right)}{(\Delta Z)^2}$$

$$+\frac{\varepsilon S_w D_{zx(i,j+\frac{1}{2})}\left(C_{i+1,j}+C_{i+1,j+1}-C_{i-1,j}-C_{i-1,j+1}\right)}{4\Delta X\Delta Z}$$

$$\left.-\frac{\varepsilon S_w D_{zx(i,j-\frac{1}{2})}\left(C_{i+1,j}+C_{i+1,j-1}-C_{i-1,j}-C_{i-1,j-1}\right)}{4\Delta X\Delta Z}\right]$$

(6-14)

The finite difference form of concentration change due to the source and sink mixing from old time level (n) to new time level (n+1) at cell ((i, j) can be written as:

$$\left(\Delta C_{i,j}^{t+1}\right)_{sou} = \frac{\Delta t}{\varepsilon S_w R_d(S_w)} Q_{sou(i,j)}\left(C_{sou(i,j)}^{n} - C_{i,j}^{n}\right)$$

(6-15)

where $Q_{sou(i,j)}$ is the volumetric flux of water per unit volume of source at cell (i, j); $C_{sou(i,j)}^{n}$ and $C_{i,j}^{n}$ are the concentrations of source and aquifer at cell (i, j).

The finite difference form of carbon and nitrate concentration change due to biological reaction may be written as

$$\left(\Delta C_{i,j}^{t+1}\right)_{bio} = \frac{\Delta t r_{d(i,j)}^{n} M_{f_{i,j}}^{n}}{\varepsilon S_w R_d(S_w)}$$

$$= \frac{\Delta t M_{f_{i,j}}^{n}}{\varepsilon S_w R_d(S_w)}\left(\frac{\mu_{max}}{Y_c}\frac{C_{i,j}^{n}}{K_c+C_{i,j}^{n}}\frac{N_{i,j}^{n}}{K_n+N_{i,j}^{n}}\beta_f I(o)\right)$$

(6-16)

$$\left(\Delta N_{i,j}^{l+1}\right)_{bio} = \frac{\Delta t r_{n(i,j)}^{n} M_{f_{i,j}}^{n}}{\varepsilon S_{w} R_{d}(S_{w})}$$

$$= \frac{\Delta t M_{f_{i,j}}^{n}}{\varepsilon S_{w} R_{d}(S_{w})}\left(\eta \frac{\mu_{max}}{Y_{c}} \frac{C_{i,j}^{n}}{K_{c}+C_{i,j}^{n}} \frac{N_{i,j}^{n}}{K_{n}+N_{i,j}^{n}} + \alpha_{n} k_{d} \frac{N_{i,j}^{n}}{K_{n}^{'}+N_{i,j}^{n}}\right)\beta_{f}I(O) \qquad (6\text{-}17)$$

The microbial growth can be calculated by integrating the equation (6-4) over the time interval (tn, tn+1) as

$$M_{f_{i,j}}^{n+1} = M_{f_{i,j}}^{n} \exp\left[\int_{n}^{n+1}\left(\mu_{max}\frac{C}{K_{c}+C}\frac{N}{K_{n}+N}\beta_{f}I(o)-K_{d}\right)d\tau\right] \qquad (6\text{-}18)$$

Using the forward Euler time integrator in equation (6-18), we obtained

$$M_{f_{i,j}}^{n+1} = M_{f_{i,j}}^{n} \exp\left[\left(\mu_{max}\frac{C_{i,j}^{n}}{K_{c}+C_{i,j}^{n}}\frac{N_{i,j}^{n}}{K_{n}+N_{i,j}^{n}}\beta_{f}I(o)-K_{d}\right)\Delta t\right] \qquad (6\text{-}19)$$

The finite difference form of the growth of the biofilm thickness from old time level (n) to new time level (n+1) at cell ((i,j) can be written as:

$$L_{i,j}^{n+1} = \frac{\left(\mu_{max}\frac{C_{i,j}^{n}}{K_{c}+C_{i,j}^{n}}\frac{N_{i,j}^{n}}{K_{n}+N_{i,j}^{n}}\beta_{f}I(o)-K_{d}\right)L_{f_{i,j}}^{n}\Delta t}{\left(1+\frac{L_{f_{i,j}}^{n}}{a_{f_{i,j}}^{n}}\frac{\pi}{\alpha_{m}}\frac{(4-m)}{d^{2}}\right)} \qquad (6\text{-}20)$$

Note the explicit numerical method is used in solving the equations (6-2), (6-3), (6-4) and (6-5). This may require that the step size can not exceed an upper limit in one transport step. According to Konikow and Bredehoeft (1978), the time step criterion for

the advection part of equations (6-2) and (6-3) may be determined from the "Courant condition" as:

$$\Delta t \leq \gamma R_d(S_w) MIN\left(\frac{\Delta X}{(V_x)_{max}}, \frac{\Delta Y}{(V_y)_{max}}\right) \tag{6-21}$$

where γ is the fraction of the grid dimension that will be allowed to move $(0 < \gamma \leq 1)$.

The time step criterion for the dispersion and the source term may be written as follows:

$$\Delta t \leq \frac{0.5}{\frac{D_{xx}}{\Delta X^2} + \frac{D_{yy}}{\Delta Z^2}} \qquad \text{and} \tag{6-22}$$

$$\Delta t \leq \left|\frac{\varepsilon S_w R_d(S_w)}{Q_{sou(i,j)}}\right| \tag{6-23}$$

CODE STRUCTURE

Using the algorithm described above, the computer code, which is called TAMRGRWS, was developed in a FORTRAN 77 running on the VAX/VAM mainframe computer at Texas A&M University. A simplified flow chart of the code is shown in Figure 16. The simulated results have been discussed in the next chapter.
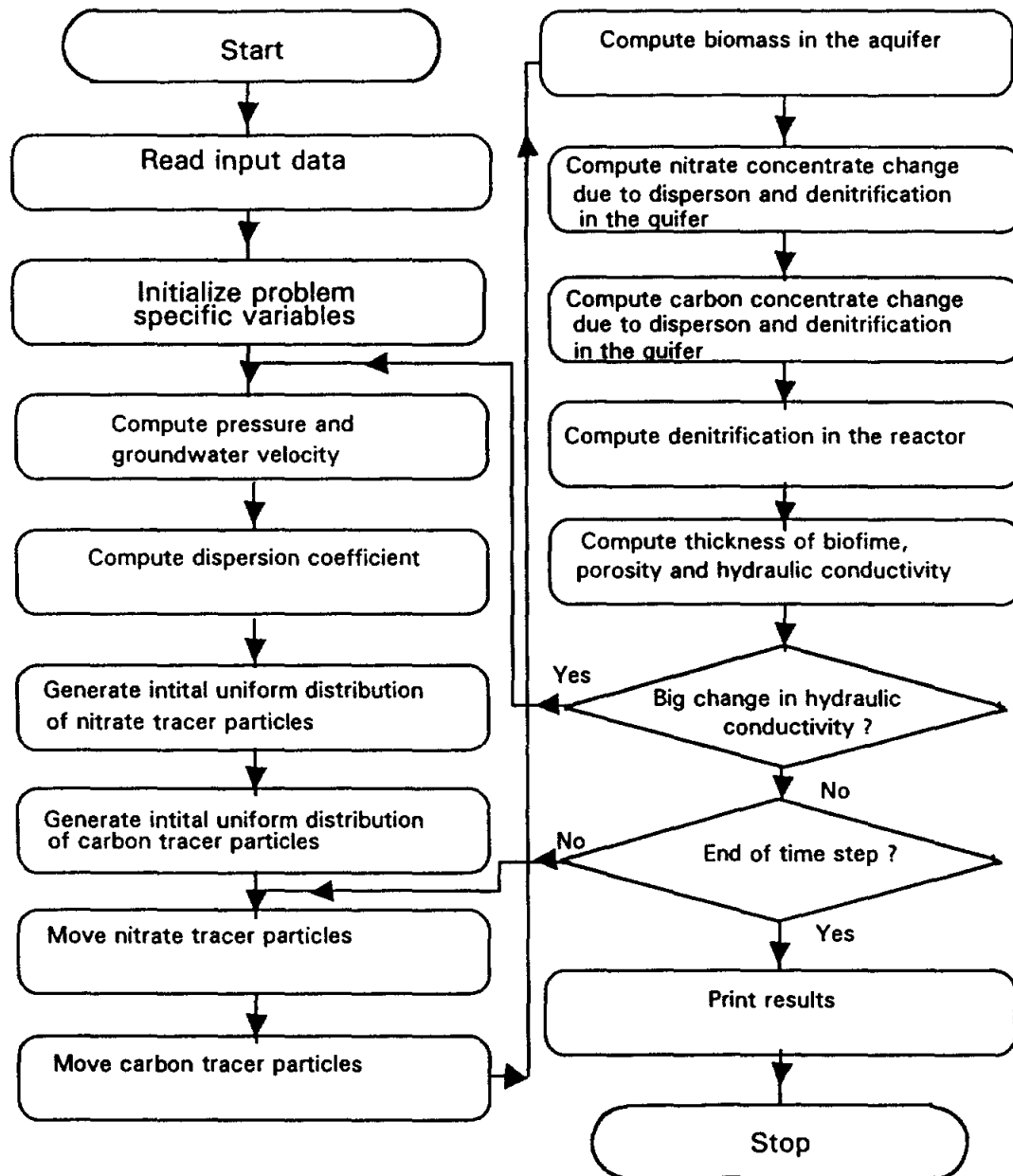
Figure 16. Simplified Flow Chart for TAMRGRWS Module

CHAPTER VII

NUMERICAL RESULTS AND DISCUSSIONS

NUMERICAL MODEL VALIDATION

To assess the accuracy of the nitrate transport model and to determine the effectiveness of the Eulerian-Lagrangian technique, the numerical model has been verified through comparison of the numerical results with the analytical and experimental data.

Test 1. Comparison of Numerical Solutions with One-Dimensional Analytic Solutions of Nitrate Transport

Generally, the one-dimensional movement of nitrate in soil and groundwater with the first-order decay can be expressed as an advection-dispersion equation (Rolston and Marino, 1976)

$$\frac{\partial(\theta N)}{\partial t} = \frac{\partial}{\partial X}\left(D\theta\frac{\partial N}{\partial X}\right) - \frac{\partial(qN)}{\partial X} - \lambda\theta N \tag{7-1}$$

where N is the solute nitrate concentration (M/L^3), θ is the volumetric water content; q is the Darcy velocity(L/T), $V=q/\theta$ is the average pore water velocity (L/T); $D=\alpha_x V$ is the hydrodynamic dispersion coefficient (L^2/T); α_x is the longitudinal dispersivity and λ is the reaction rate coefficient of biodegradation ($1/T$). For steady uniform water movement the variables q, θ, V, and D are constant.

Assuming the problem involves the following initial and boundary conditions:

$N = N_0 \quad at \quad X = 0 \quad for \ all \ t$

$\dfrac{\partial N}{\partial X} \to 0 \quad as \quad X \to \infty$

$N = 0 \quad at \quad t = 0 \quad for \ all \ X$ (7-2)

The analytic solution of equation (7-1) is obtained with the following equation presented by (Domenico and Schwartz, 1990)

$$\frac{N}{N_0} = \frac{1}{2}\exp\left\{\left(\frac{X}{2\alpha_x}\right)\left[1-\left(1+\frac{4\lambda\alpha_x}{V}\right)\right]^{\frac{1}{2}}\right\}erfc\left[\frac{X-Vt\left(1+4\lambda\alpha_x/V\right)^{\frac{1}{2}}}{2(\alpha_x Vt)^{\frac{1}{2}}}\right]$$ (7-3)

The nitrate transport computer program was modified for application to this case. The parameters used in the simulation are as following: the boundary concentration of nitrate is 100 mg/l; the initial concentration of nitrate throughout the column is zero; the total length of column is 100 cm; time is 100 hour; the longitudinal dispersivity is 0.4 cm; the reaction rate coefficient of biodegradation is 0.005 hr^{-1}; and the average pore water velocity is 0.25 cm/hr. The following cases have been simulated:

Case (a). $\alpha_x = 0, \quad \lambda = 0$

Case (b). $\alpha_x = 0.4cm, \quad \lambda = 0$

Case (c). $\alpha_x = 0.4cm, \quad \lambda = 0.005hr^{-1}$

Figure 17 shows a comparison of the numerical approximation with the analytical solution. It can be observed that the excellent agreement between the numerical approximation and the analytical solution in all cases. No apparent numerical dispersion exists.

Test 2. Comparison of Denitrification Model Simulations with Experimental Data in a Completed-mix, Suspended -growth Reactor

The denitrification model equations (5-53) and (5-54) presented in Chapter V is used to predict the effluent of nitrate and carbon concentration in a suspended-growth
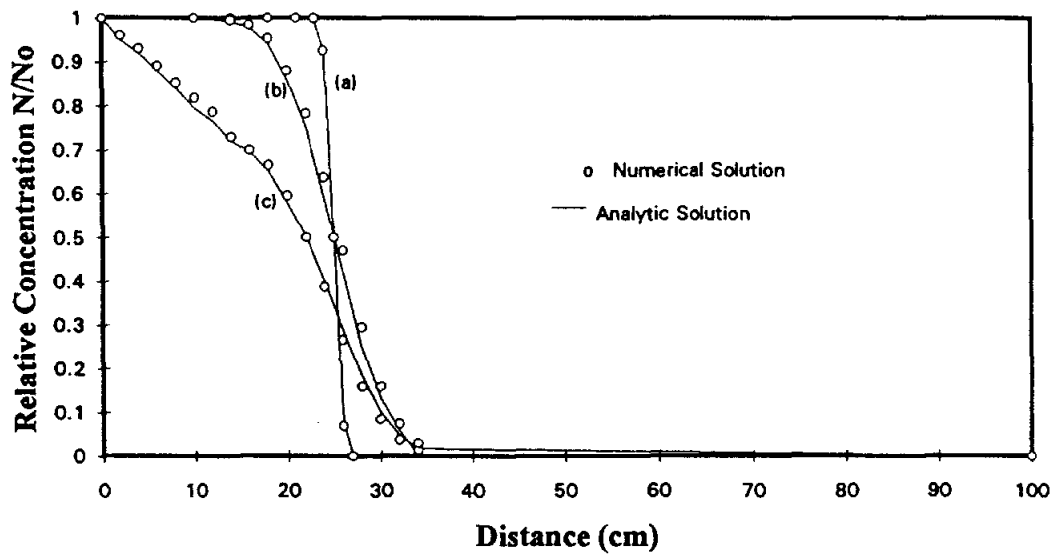
Figure 17. Comparison of the numerical solutions with the analytic solutions of the one - dimensional advection-dispersion equation with and without decay. (a) $\alpha x=0$, $\lambda=0$; (b) $\alpha x=0.4$ cm, $\lambda=0$; and (c) $\alpha x=0.4$ cm, $\lambda=0.005$ hr^{-1}.
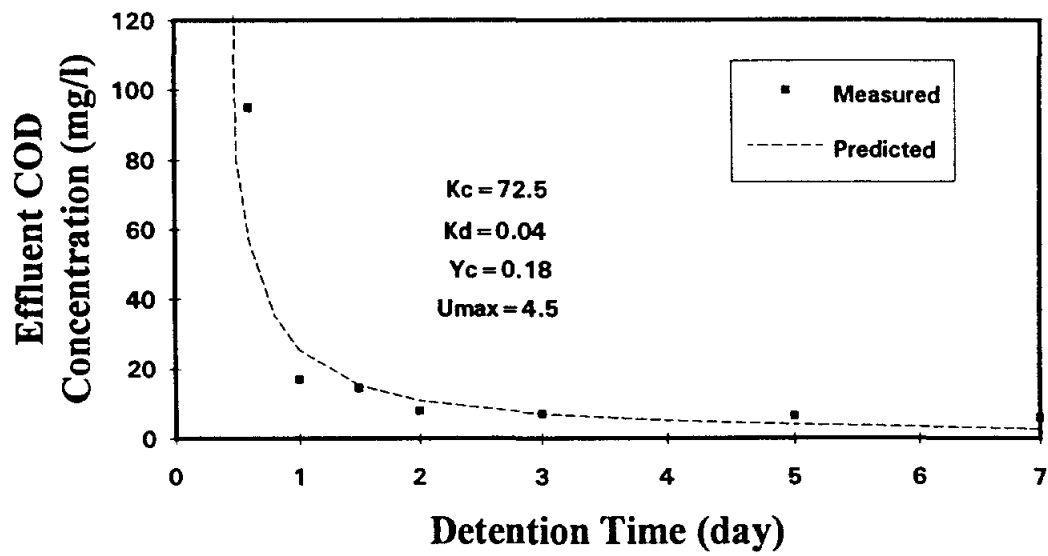
Figure 18. Comparison of the model predicted effluent concentration of a completed -mix, suspended-growth reactor with experimental data (from Stensel et al., 1973).

reactor. The Model results have been compared with the denitrification experimental data in a suspended-growth reactor described by Stensel et al. (1973). In the experiment, the concentration of organic added into the reactor is a growth-rate-limiting substrate for denitrification. The biological kinetic parameters which are directly obtained from the experiment are as following: The maximum specific substrate utilization rate K is 25.0 (1/day); the yield coefficient of organic carbon Y_c is 0.18 (mg cell /mg COD); the microbial solid decay coefficient K_d is 0.04 (1/day); the organic carbon half-velocity constant Kc is 72.5 (mg/l); and the maximum specific growth rate μ_{max}=K·Yc=4.5 (1/day). The comparison of the prediction of a steady-state effluent organic carbon concentration (mg/l as COD) by equation (5-53) with experimental data at different detention time is shown in Figure 18. The excellent agreement between the predicted and the measured effluent concentration is observed. The denitrification equations (5-53) and (5-54) can successfully predict the effluent of nitrate and carbon concentrations in the reactor at any given detention time.

SIMULATIONS OF A RGRW SYSTEM

In order to calibrate and validate the proposed model, the numerical model has also been compared with the experiment data of a two-dimensional recirculation groundwater well (Stallard et al., 1993, Wu, 1994). The experimental apparatus consists of a ground water tank, a scaled remediation well, and a contaminant monitoring and treatment control system. The design and dimensions of the groundwater simulation tank are shown in Figure 19. The comparison can be divided into two parts: contaminant transport and biological treatment.

Contaminant Transport

The three cases have been simulated by the nitrate transport model to compare with experimental data.

Case I: Surface contaminant leakage

In the case I, a condition of a surface contaminant leakage was simulated. The distribution of pollutant would be typical of a solute that had been applied to the groundwater from the surface, such as agricultural source nitrate. In the experiment, sodium hydroxide (NaOH) has been used as a tracer to demonstrate contaminant transport in the recirculating groundwater remediation well system. The concentration of sodium hydroxide, which was fixed at pH12, was added on the surface of the groundwater as a point contaminant source. The hydrochloric acid (HCl), which can neutralize the sodium hydroxide to pH=8, was added into the reactor well to represent the treatment effect during the experiment. The concentration of sodium hydroxide at pH 9 contour is plotted as the boundary of the contaminant plume. For the numerical simulation, the general computer program was modified. The biological transform part of program was temporally removed for application on this case. The simulation domain was divided into 48 X 24 uniform grad blocks, each 5 cm in length. The parameters used in the model are shown in Table 1. The comparison of the calculated and the measured plume with 1 m/d ambient horizontal flow velocity and 100 ml/min well recirculation rate are shown in Figure 19. One finds agreement between the plume predicted by the model and the plume observed experimentally. From the numerical simulation and experimental observation, we can note that a surface contaminant source can be totally intercepted by the recirculation well. There is always a clean zone downstream of the recirculation treatment well.

Table 1: The Physicochemical Parameters Employed in the Model Simulations.

Property	Value	Units
Longitudinal Dispersivity (α_l)	1.2	cm
Transversal Dispersivity (α_t)	0.12	cm
Dynamic Viscosity (μ)	0.01	g/ cm·s
Gravitational Acceleration (g)	9.8	m / s^2
Density of Water (ρ)	1.0	g / cm^3
Residual Water Content (θ_r)	0.1	-
Retardation Coefficient (R_d)	1.0	-
Initial porosity (ε)	0.34	-
Mean grain diameter (d)	0.15	cm
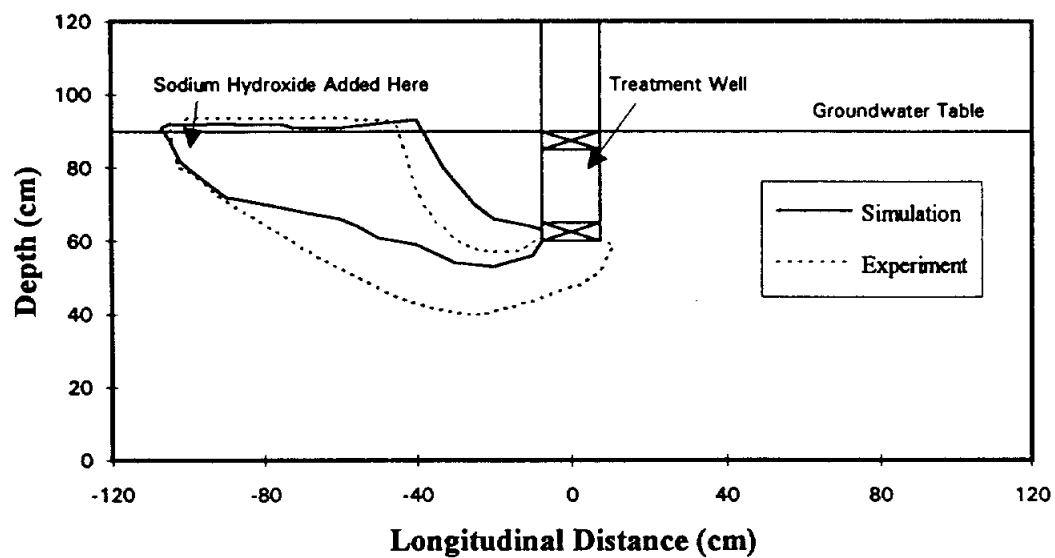
Figure 19. Model predicted and measured plumes (from Wu, 1994) with NaHO applied at the surface of the ground water table, with ambient groundwater velocity of 1 m/d and recirculating pumping rate of 100 ml/min.

Case II. A uniform distribution of contaminant source through the depth upstream of the RGRW

The Case 2 condition is the same as case 1 condition except that the sodium hydroxide was uniformly added to the water entering at the upstream side of the tank. The model simulated results are plotted in Figure 20, and shows reasonable agreement with the measured plumes except at the lower downstream end. We can see from Figure 20 that the recirculating groundwater remediation well system can form a protection zone near the treatment well. The depth of the formed protection zone depends on the depth of the well penetration and the recirculation rate of the well. For a deeper contaminate source, the recirculation well must penetrate deep enough to prevent the passing of the contaminant from the treatment well into downstream. This conclusion is the same as the conclusion reached from the use of the pathline method in chapter IV.

Case III. The influence zone of the RGRW

In order to demonstrate the influence zones of the RGRW, sodium nitrate as a tracer is added into the treatment well in the experiment as shown in Figure 21. The development of a plume was monitored visually over time. The plume shape predicted by numerical model is compared with the measured plumes in Figure 21. Again, there is excellent agreement between the predicted and measured plumes.

Biological Treatment of Nitrate Contaminant

The results of biological treatment simulated by the model have also been compared with the experimental data conducted by Wu (1994). The simulated conditions are shown in Figure 22. It is similar to case 1 condition of contaminant transport except that nitrate is added at surface of groundwater and bacteria and carbon material are added the treatment reactor for denitrification. The treatment reactor size and measured points are also shown in the Figure 22. The biological parameters for the model are taken from Grady and Lim
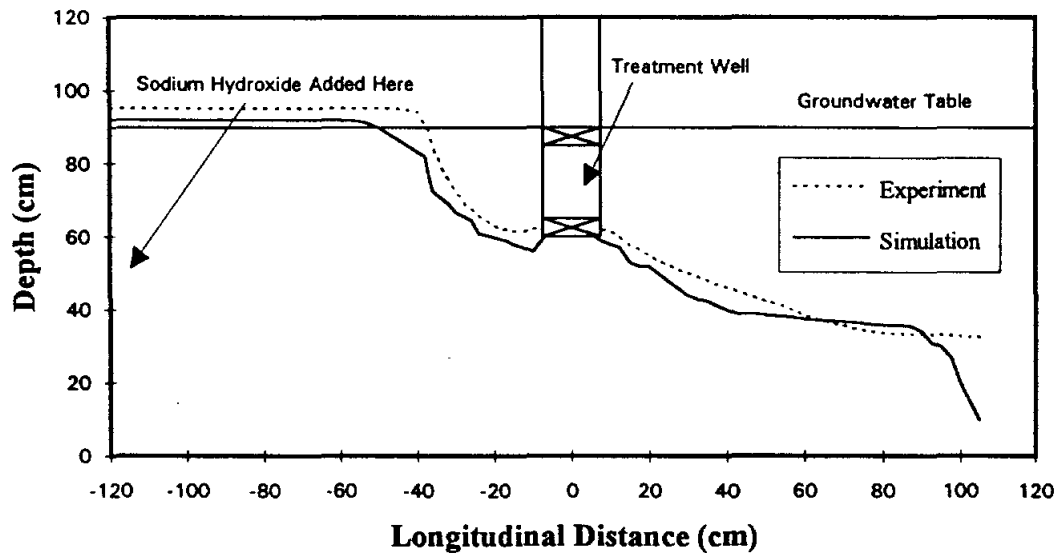
Figure 20. Model predicted and measured plumes (from Wu, 1994) with NaHO uniformly distributed through the depth of the upstream tank, with ambient groundwater velocity of 1 m/d and recirculating pumping rate of 100 ml/min.
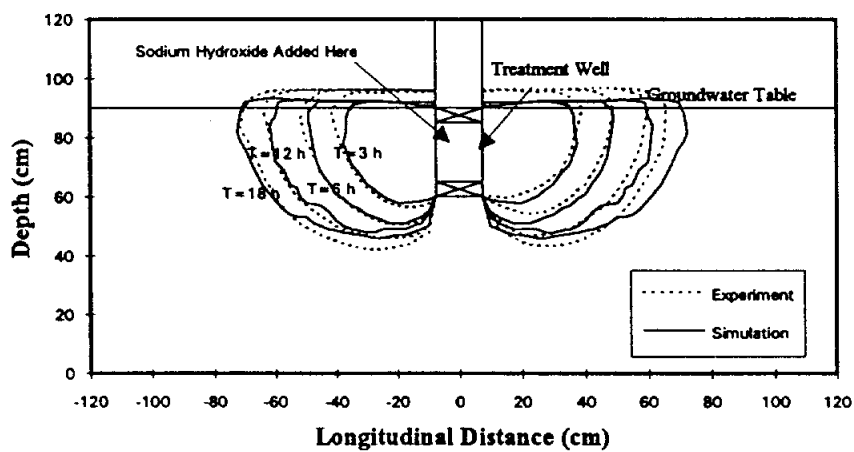
Figure 21. Model predicted and measured influent zones of the RGRW (from Wu, 1994) without ambient flow velocity, recirculating pumping rate of 100 mg/min, and NaOH added into the RGRW.

(1980), Stensel et al. (1973), Wu (1994), and Widdowson et al (1988), and are summarized in Table 2.

Figure 22 shows the predicted concentration contour of nitrate in the RGRW system. Figure 23 shows the comparison of predicted nitrate profiles with experimental results at depths of the extraction interval and injection interval of the well. The simulated condition is as following: the ambient horizontal groundwater velocity is 1m / day; the well recirculation rate is 50 ml/min; the nitrate concentration injected at upstream is 1000 mg/l and the rate is 2.5 ml/min (total nitrate loading is 2.5 mg/min); and the carbon added into the reactor is 2.0 mg/min as TOC. It is assumed that the initial nitrate and carbon concentration are zero and initial hydraulic conductivity at the tank is homogenous. Reasonable agreement between experimental results and model prediction can be seen. According to the flow pattern of recirculation well we know that treated water reinjected into the aquifer will form a protection zone at both the upstream and downstream sides. When the measured points, such as points A and point H, are not covered by the protection zone, the concentration of nitrate will be higher. When the measured points locate within the protection zone, the concentration of nitrate is lower.

Figure 24 shows the comparison of the predicted results by model with experiment in same condition as in Figure 23 except that well recirculation rate is 25 ml/min. Again, there is good agreement between the predicted and measured nitrate concentration distribution. As expected, when the well recirculation rate decreases, the ambient groundwater will push the contaminant plume downward and the protection zone at upstream side will decrease. Thus, the profile of the nitrate concentration will move downward.

TABLE 2. The Microbial Kinetic Parameters Used in the Model Simulations.

Property	Value
In the reactor	
K_n*	0.15 mg/L, NO^3-N
K_c*	12.5 mg/L, TOD
K_d*	0.0016 h^{-1}
U_{max}*	0.29 h^{-1}
Y_n*	0.61mg Cell/ mg NO^3-N
Y_c*	0.72 mg Cell / mg TOD
K_p*	0.03
K_t*	1.15
$\forall$	16500 cm^3
In the aquifer	
X_f	2500 mg/l
K_n	0.5 mg/l
K_c	6 mg/l
K_d	0.002 h^{-1}
U_{max}	0.13 h^{-1}
Y_c	0.625 mg Cell/mg TOC
α_n	0.1
K_n'	0.002 mg/l
K_o	0.01 mg/l
η	1.25
β_f	1.0
M_{fo}	1mg/l
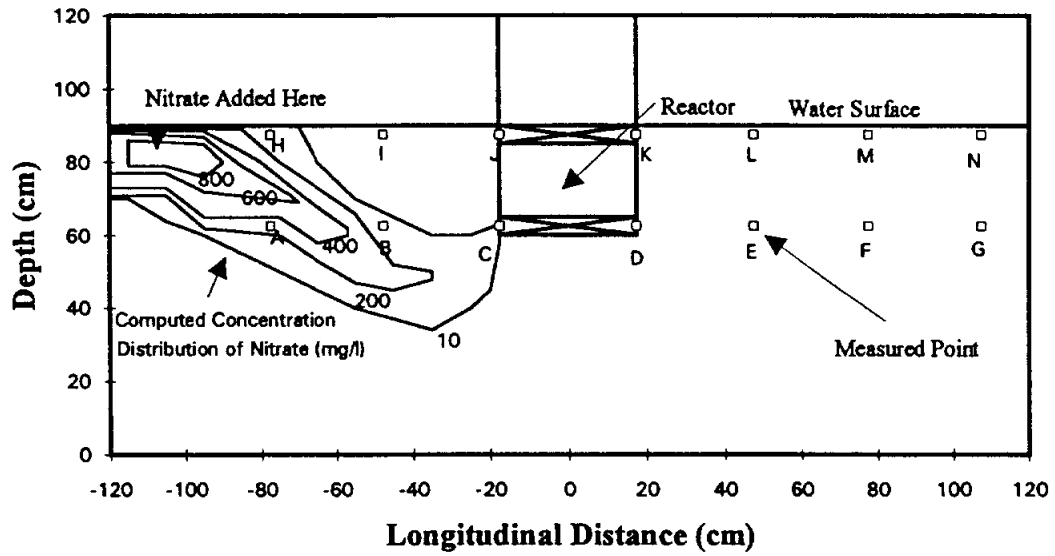
Figure 22. Predicted concentration contours of nitrate in the RGRW system.
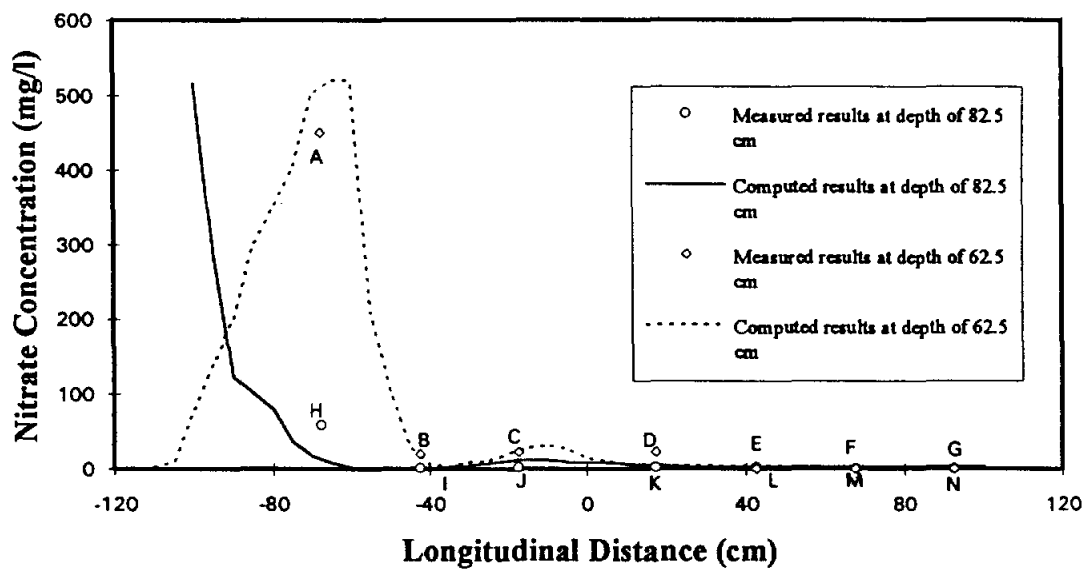
Figure 23. Comparison of computed nitrate distribution profiles with measured data (from Wu, 1994) at depths of the extraction and injection intervals of the well with ambient groundwater velocity of 1 m/d, recirculating pumping rate of 50 ml/min, and carbon feed of 2.0 mg/min as TOC.
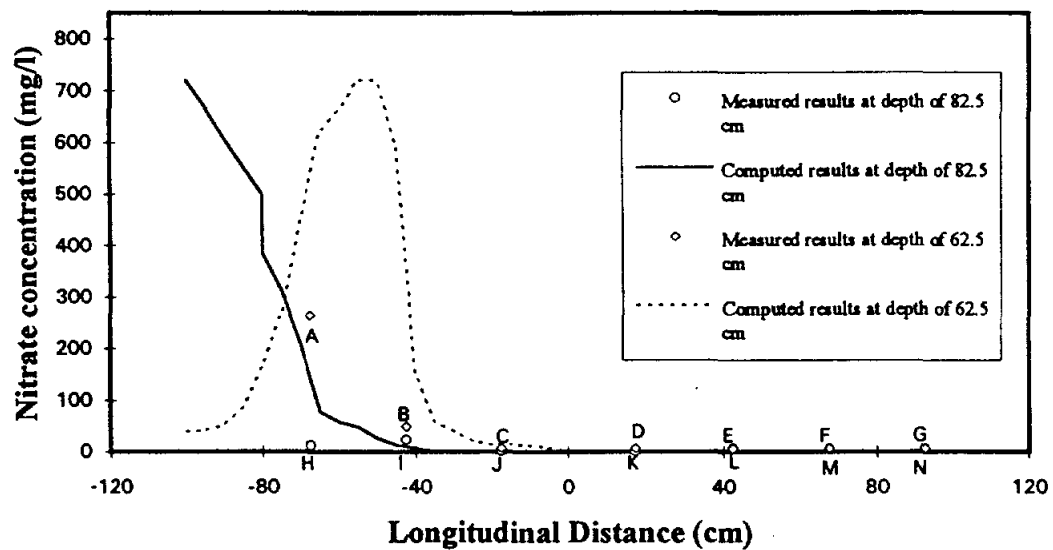
Figure 24. Comparison of computed nitrate distribution profiles and measured data (from Wu, 1994) at depths of the extraction interval and injection intervals of the well with ambient groundwater velocity of 1 m/d, recirculating pumping rate of 25 ml/min, and carbon feed of 2.0 mg/min as TOC.

SENSITIVITY ANALYSIS

Multiple simulations were run to test the sensitivity of the model at variation of parameters. Since the effects of various hydraulic parameters on the capture zone of the recirculating groundwater remediation well have been analyzed in chapter IV, the sensitivity analysis here was focused on the biological parameters.

Effects of Hydraulic Detention Time

Hydraulic detention time is defined as the volume of the reactor divided by the recirculating flow rate. In the continuous stirred tank reactor without cell recycle, hydraulic detention time is equal to the mean cell residence time, which is defined as the mass of organisms in the reactor divided by the mass of organisms removed from the reactor each day (Tchobanoglous and Burton, 1991). Generally, the hydraulic detention time must be larger than the critical value minimum detention time τ_{min}, otherwise the organisms are washed from the reactor faster than they can be produced and process fails. The minimum detention timeτ_{min} is also called the washout point. Figure 25 shows the typical effect of detention time on the effluent of nitrate and carbon concentration of reactor. As seen from Figure 25, the washout point is 3.8 hours; when detention time is less than 3.8 hours, no cell growth occurs and no nitrate and carbon are removed. As the detention time increases, nitrate and carbon remove rapidly. For the kinetic parameter employed, effluent of the nitrate concentration in the reactor reduces from 100 mg/l to 7 mg/l with detention time from 3.8 hours to 10 hours. When detention time is beyond 10 hours, there are only smaller changes in effluent of nitrate and carbon concentration.

Figure 26 (a), (b) and (c) show the concentration profiles of nitrate, carbon and biomass at the depth of 62.5 cm of aquifer near the extraction interval of the well at
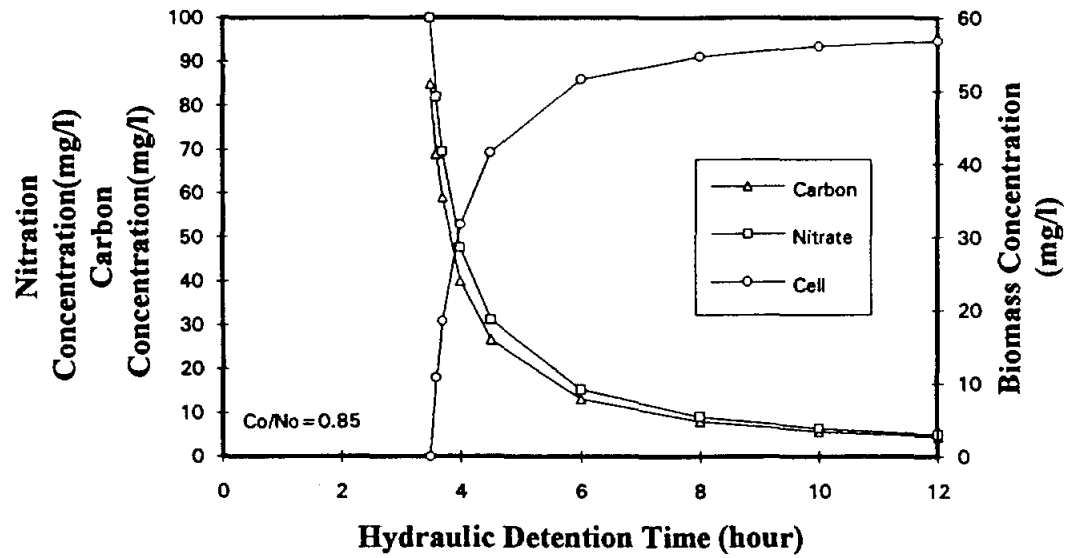
Figure 25. Effect of the detention time on effluent of nitrate, carbon and cell concentrations in the reactor.

different detention times. As seen from the figures, during small detention times, much residual nitrate and carbon flow out of the reactor and causes higher concentrations of nitrate and carbon in both upstream and downstream sides of reactor. As the detention time increases, the concentrations of nitrate and carbon apparently decrease. One notes from Figure 26 (c) that the biomass concentration in the aquifer is changed from the initial concentration of 1 mg/l to 40 mg/l at the detention time of 4 hours and changed from the initial concentration of 1 mg/l to 18 mg/l at detention time of 6 hours. It means that denitrification occurs in the aquifer. When the detention time increases to 10 hours, carbon concentration in the aquifer reduces to approximate zero. In this condition, no denitrification will occur at aquifer, thus no biomass grows in the aquifer.

Effects of Ratio of Carbon to Nitrate

The ratio of the added carbon to the influent nitrate nitrogen is an important parameter to control denitrification process in the reactor. For ethanol as a carbon source, the stoichiometric ratio of carbon to nitrate nitrogen for complete denitrification is approximately 0.81 TOC/NO_3^--N. If the ratio is less than stoichiometric ratio, the carbon matter will be the growth rate limiting substrate. Figure 27 (a) shows that when the input carbon concentration to nitrate ratios is 0.50 TOC/NO_3^--N, the ratio less than stoichiometric will allow carbon to be depleted very quickly but leave considerable residual nitrate concentration in the effluent. In contrast, Figure 27(b) shows that when the input carbon concentration to nitrate ratios is 1.25 TOC/NO_3^--N, the excess carbon matter will allow complete removal of nitrate but leave a considerable amount of carbon matter in the reactor and the effluent. One may also note from the figures that the rate of carbon to nitrate will not affect on the washout point of the reactor.
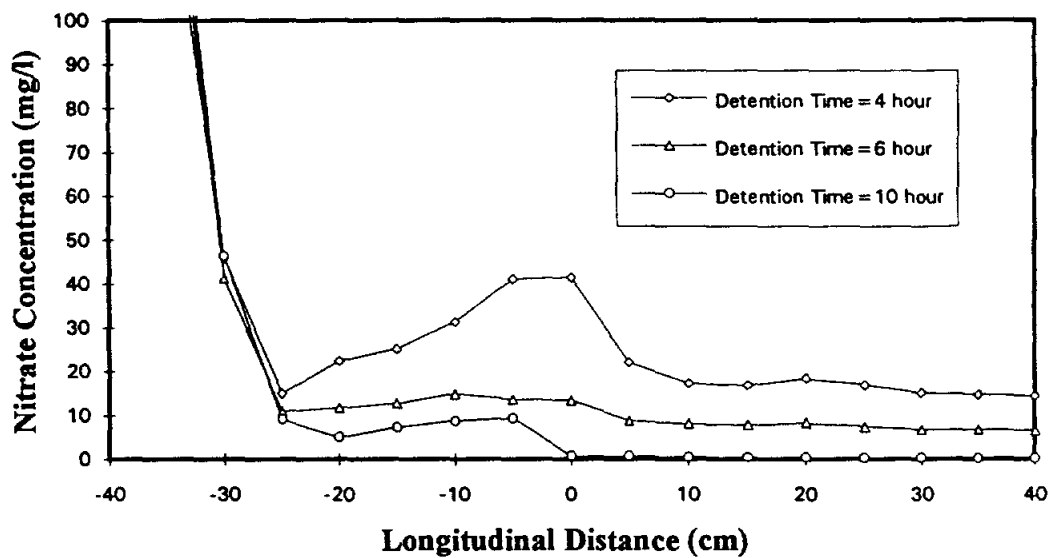
Figure 26 (a). Simulated nitrate concentration profiles in the aquifer near the extraction interval of the well at different detention time.
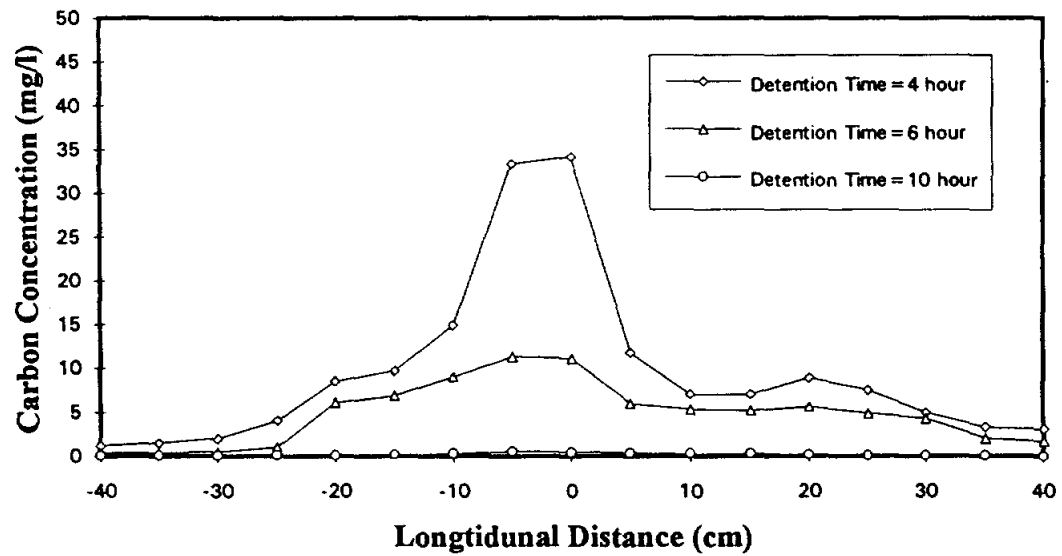
Figure 26 (b). Simulated carbon concentration profiles in the aquifer near the extraction interval of the well at different detention time.
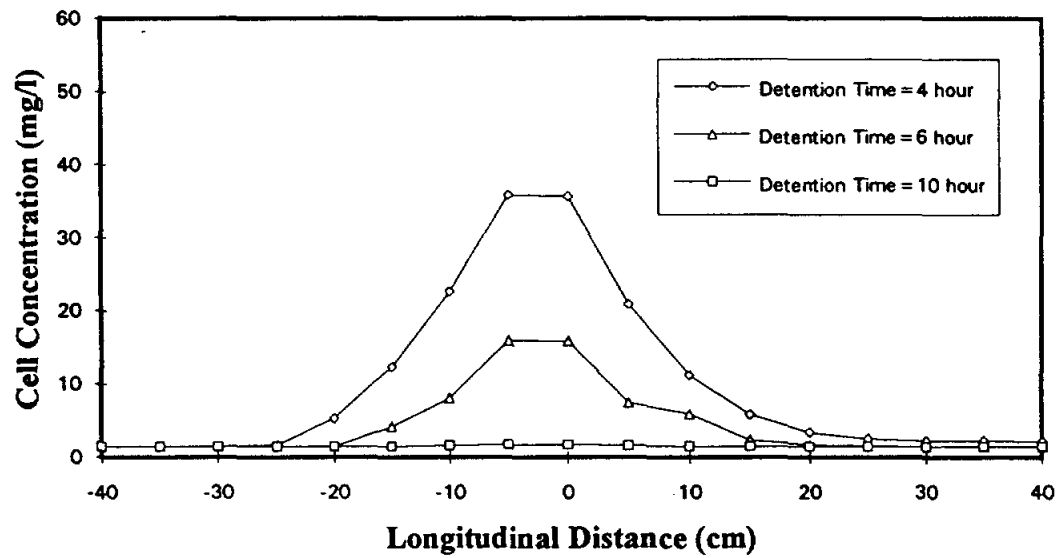
Figure 26 (c). Simulated biomass concentration profiles in the aquifer near the extraction interval of the well at different detention time.

Figures 28(a), 28(b) and 28(c) show the simulated concentration profiles of nitrate, carbon and biomass in the aquifer near the extraction interval of the well at different Co/No ratios. The simulated condition is the same as in the Figure 26 with the exception of the Co/No ratio. From these figures, one may note that when the ratio of Co/No is 0.5, which is less than stoichiometric, not enough carbon would leave a relatively large residual nitrate concentration in the effluent and cause nitrate concentration at downstream side of reactor to be higher than the drinking water standard. In contrast, when the Co/No ratio is 1.25, nitrate becomes the limiting substrate which allows complete removal of nitrate but causes large carbon concentrations in the aquifer. Concentration profiles of the biomass, plotted in Figure 28(c), indicate that the denitrification in the aquifer is obviously affected by Co/No ratio. When the Co/No ratio is less than stoichiometric, concentration of the biomass in the aquifer is very low. It suggests that no denitrification occur in the aquifer since no carbon in the aquifer in this case. When the Co/No ratio increases to 1.25, the concentration of the biomass in the upstream side of the reactor is much higher than its initial concentration. This suggests that the carbon being fed in excess of the stoichiometric amount will allow a large carbon concentration to flow into the aquifer and to simulate denitrification in the aquifer, especially at the upstream side of reactor because both the nitrate and carbon concentrations are larger in this area. The growth of biomass at outside of the treatment well will cause the biofilm thickness to increase and the permeability to decrease. It agrees the experimental observation that flows with over carbon supplied into reactor tended to be blocked by the decreased permeability of the aquifer around the exit of the upstream side of treatment reactor (Wu, 1994).
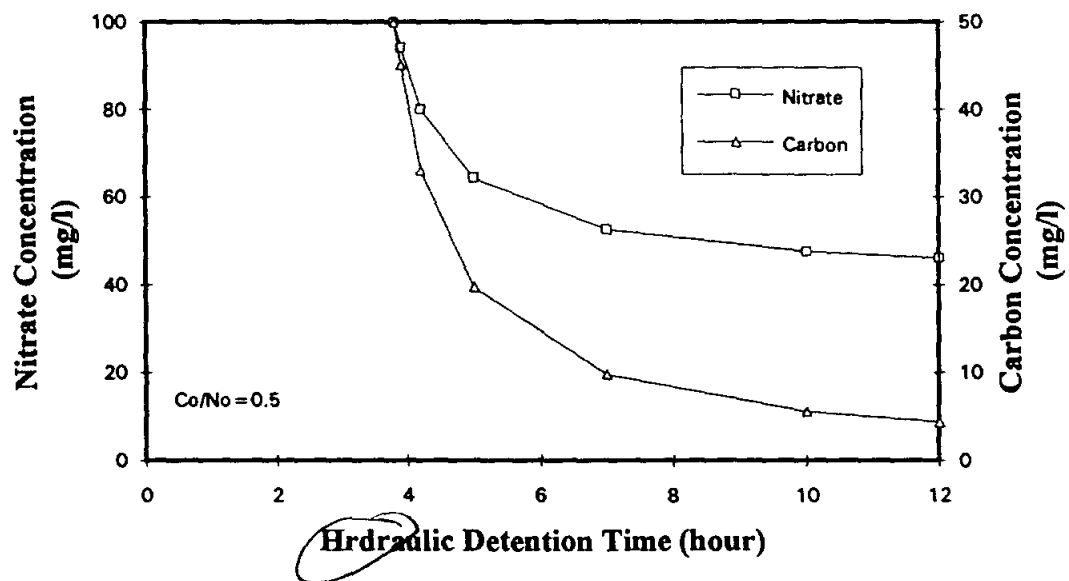
Figure 27(a). Effect of ratios of carbon to nitrate on effluent of nitrate and carbon concentrations (Co/No=0.5).
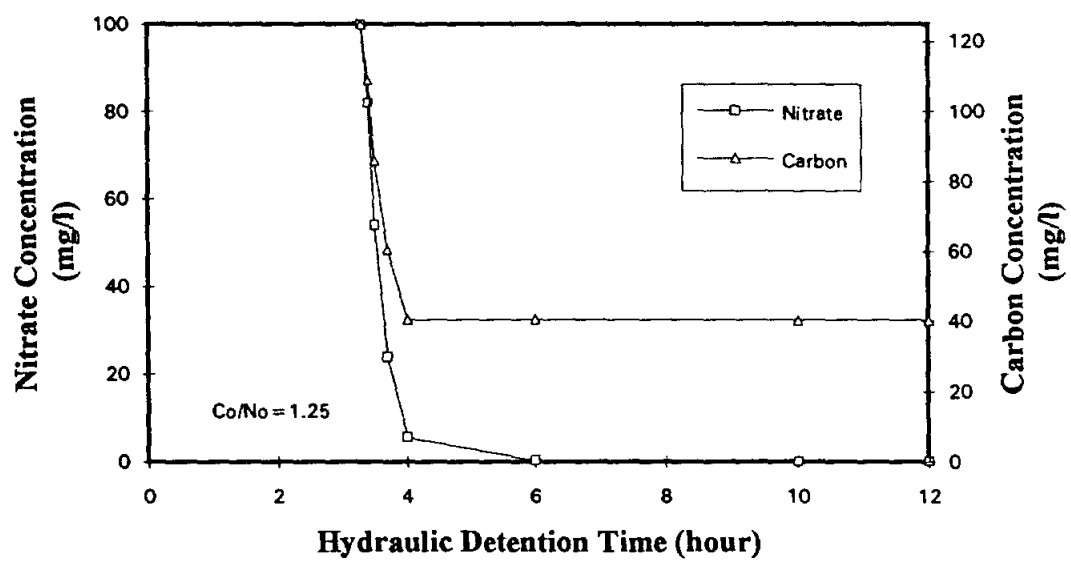
Figure 27(b). Effect of ratios of carbon to nitrate on effluent of nitrate and carbon concentrations (Co/No=1.25).
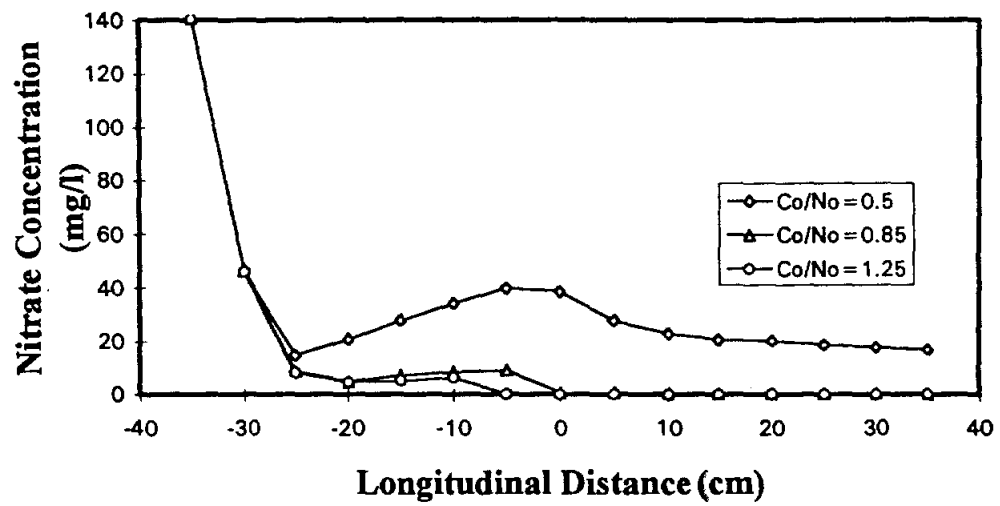
Figure 28 (a). Simulated nitrate concentration profiles in the aquifer near the extraction interval of the well at different C_O/N_O rate.
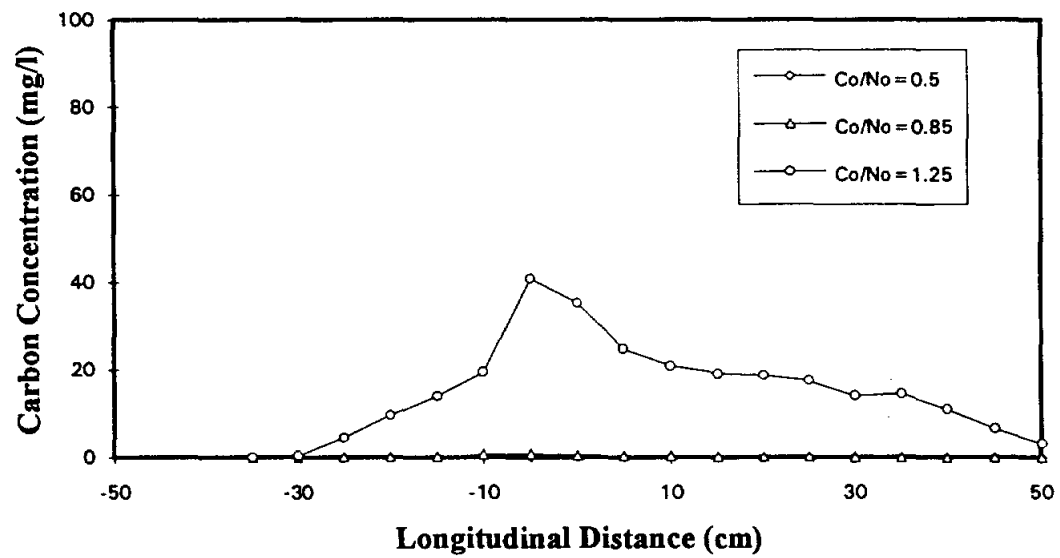
Figure 28 (b). Simulated carbon concentration profiles in the aquifer near the extraction interval of the well at different C_0/N_0 rate.
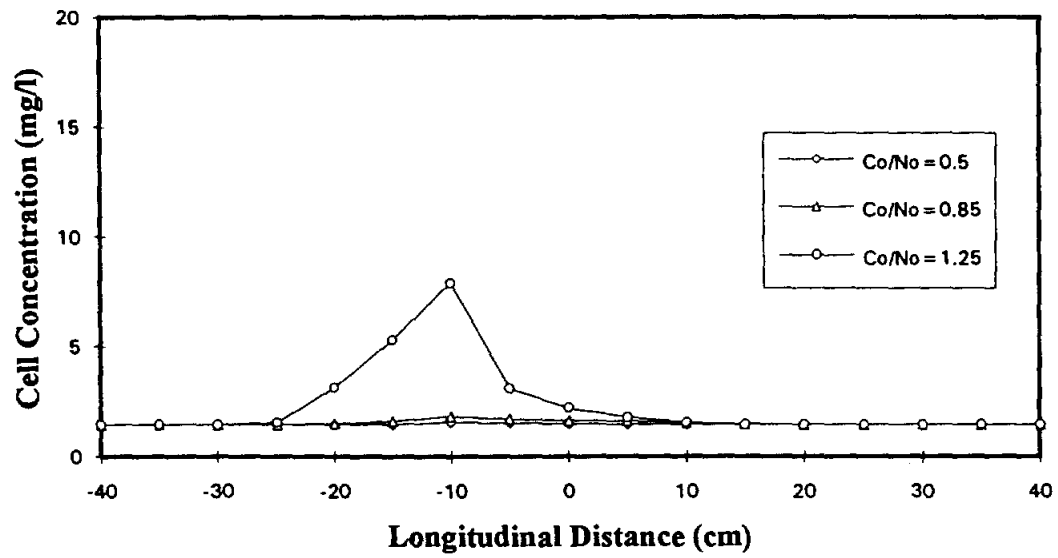
Figure 28 (c). Simulated biomass concentration profiles in the aquifer near the extraction interval of the well at different C_0/N_0 rate.
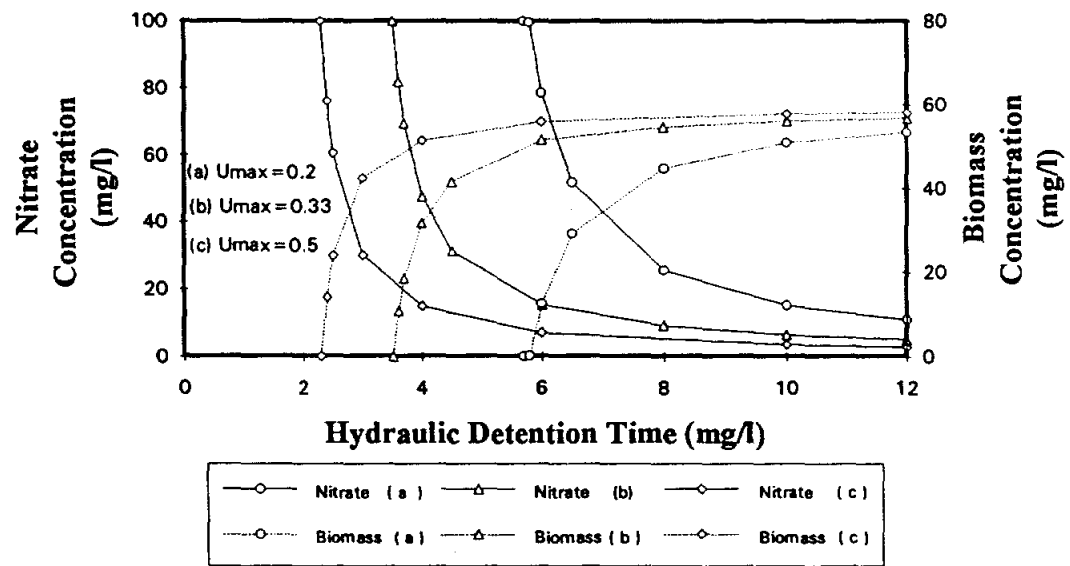
Figure 29. Effect of maximum specific growth on effluent of nitrate and cell concentration in the reactor.

Effects of Maximum Specific Growth

Figure 29 shows that the effect of the maximum specific growth rate μ_{max} on the effluent of the nitrate nitrogen concentration and the cell concentration at μ_{max}=0.50 (1/hour), μ_{max}=0.33 (1/hour), μ_{max}=0.20 (1/hour). One can note from the figure that a higher value of maximum specific growth rate allows the organism to grow faster so that the less operation detention time is needed for the required effluent of nitrate concentration. The maximum specific growth rate also will influent on the minimum detention time τ_{min} (washout point). If μ_{max} was increased from 0.2 (1/hour) to 0.5 (1/hour), the minimum detention time τ_{min} would decrease from 5.7 hours to 2.3 hours. There is almost no effect when the detention time is larger than 10 hours.

Effects of Temperature

The value of the kinetic parameters discussed in the previous paragraphs are average for typical conditions, i.e., neutral pH , temperatures around 20 °C, etc. Generally, the rate of the microbial growth increases as temperature is increased until a maximum value is reached. Figure 30 shows the effect of temperature on the effluent of nitrate at different detention times. It is apparent from the figure that temperature has a significant effect on the washout point. An minimum operation detention time of 3.5 hours would be required if process is operated at 20 °C and 6 hour if process was operated at 15 °C which would prevent washout.

Effects of pH

The effect of pH on the effluent of nitrate concentration is shown in Figure 31. There is almost no effect when the pH is within the range 7 and 9.5. Beyond that range the effect is significant, especially when pH is below 6.5 or above 10.
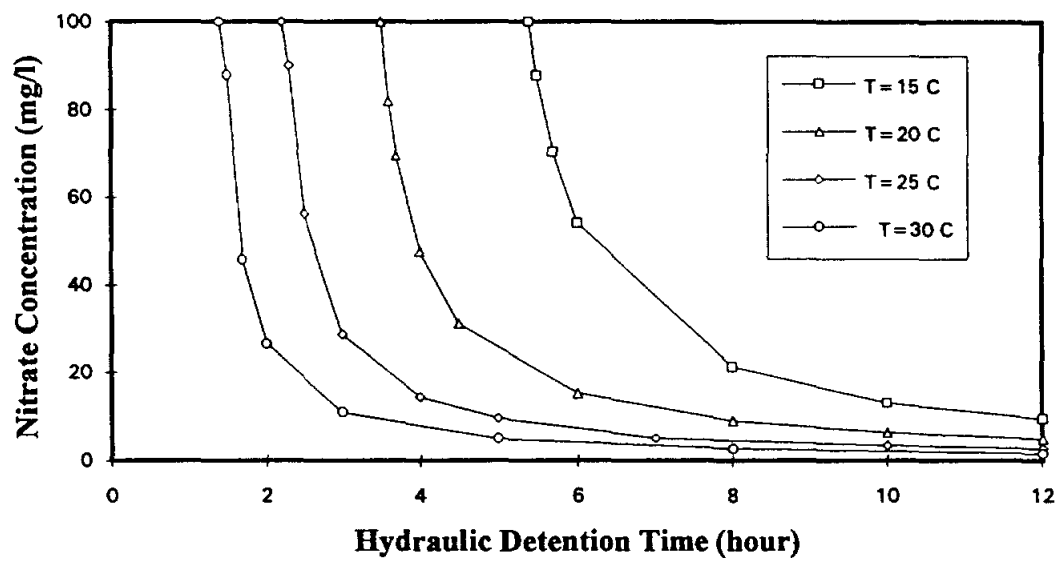
Figure 30. Effect of temperature on effluent of nitrate concentration in the reactor.
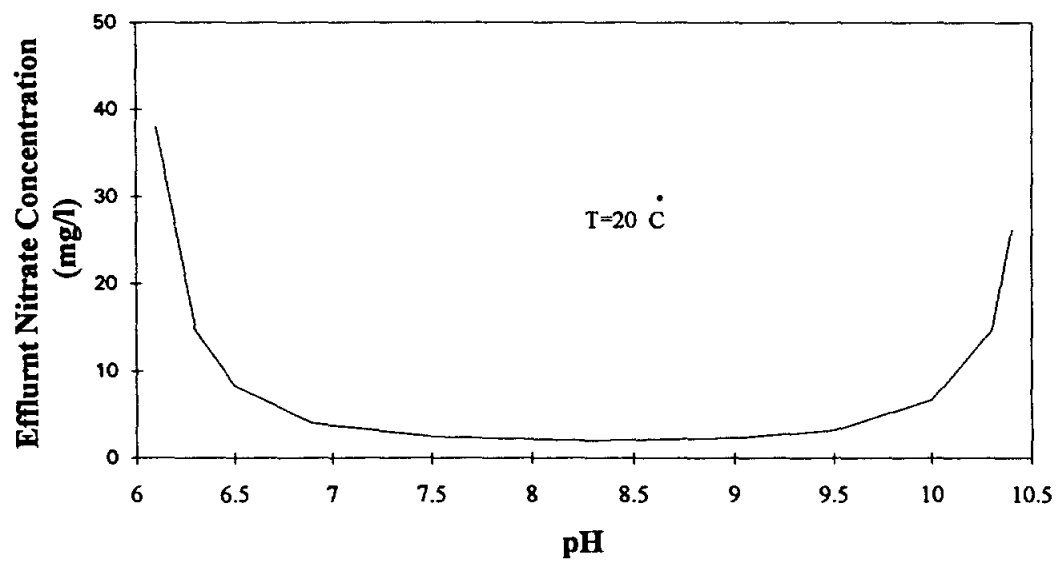
Figure 31. Effect of pH on effluent of nitrate concentration in the reactor.

CONCLUSIONS

In this study, we present a model to describe nitrate transport with biodegration in the RGRW system. The model includes denitrification process both in the aquifer and treatment reactor, nitrate and carbon advective transport, dispersion, and sorption in the porous media. Eulerian-Lagrangian numerical method is employed to solve a set of nonlinear governing equations. Simulated results are compared with the analytic solutions and experiment data. The agreement found between simulated results and experiment data. Sensitivity analyses conducted the performance of RGRW system indicated that the hydraulic detention time, the well recirculting rate, the ratio of carbon added into the reactor to the influent nitrate nitrogen, and temperature are the most important parameters of design and operation of the RGRW system.

CHAPTER VIII

SUMMARY AND CONCLUSIONS

CONCLUSIONS

In this study, two computer models were developed to help design and operate the RGRW system. The first model employed a semi-analytical technique for predicting three dimensional flow patterns and capture zones of the RGRW in the unconfined aquifer. This model can assist in determining the optimum number of RGRWs, their rate of discharge and their locations. The second model was developed for simulating the nitrate transport and denitrification in the RGRW system. The model couples the nitrate transport equation, carbon transport equation, the microbial growth and decay equation, as well as the denitrification equation in both of the treatment well (reactor) and the aquifer. The nonlinear coupled equations were solved by an Eulerian-Lagrangian method which is highly resistant to numerical dispersion in the presence of small dispersivities. The model is calibrated and verified again analytical solutions and laboratory experimental data.

Based on the results of the model simulations, the following conclusions are obtained:

- The recirculating groundwater remediation well system is a promising method for treating contaminated groundwater in the aquifer. Numerical results have demonstrated that the recirculating groundwater remediation well system can be an effective interception of migrating contaminants and can form a hydraulic barrier to protect downstream drinking water well.

- Comparing with a traditional pump-and-treat technique, the recirculating groundwater treatment system offers many advantages. For example: there are no lowering of the groundwater level, no groundwater extraction, and no seasonal temperature effect.

- The recirculation pumping rate is the most important factor affecting performance of the treatment well system. Increasing the recirculation rate can increase the width of capture zones. But increase of the recirculation rate will reduce the retention time. In order to maintain the required hydraulic detention time, the large treatment chamber is required. Thus, balance must be considered between the recirculation rate and treatment well diameter when designing a RGRW system.

- The model simulated results show that in order to prevent the clogging of the aquifer space with biomass and gaseous products, the carbon added into the treatment well should be equal or less than the amount determined by the stochiometric ratio of carbon to nitrate nitrogen. However, the limitation of the carbon supply in the treatment chamber may leave some amount of nitrate in the reactor and aquifer.

- The width of the capture zone of the recirculation remediation well changes with the depth. The largest width of the capture zone is at its depth near the extraction screen section and the smallest is near the injection screen section.

FURTHER RESEARCH

Although this work has illustrated the utility of a comprehensive modeling approach for the enhancement of our understanding of recirculating groundwater remediation well, more accurate predictions of the efficiency of the denitrification both in the remediation well system and in the aquifer are required for further studies. Multiple possibilities for additional research are presented here:

- The extension of the two dimensional nitrate transport model into three dimensions will facilitate the application of the insight gained from those laboratory studies to the exploration of alternative field remediation schemes. Three dimensional model requires new numerical techniques for more efficient computation and less computer memory.

- The addition of the phenomena such as mass exchange between different phases (solid, liquid, gas, and biomass) in the biofilm coupled in the model would improve model to predict denitrification in the aquifer.

- More field tests are required to verify the model.

- Current understanding of clogging in the aquifer by bubbles produced from the denitrification process is inadequate. More studies are needed in this area.

REFERENCES

Alexander, M., *Introduction to Soil Microbiology*, 2nd Ed., John Wiley & Sons, New York, 1977.

Anderson, J. H., Agriculture and natural resources, in *Rural Groundwater Contamination*, Edited by F. M. D'Itri and L. G. Wolfson, Lewis Publishers, Inc., Chelsea, Michigan, 1987.

Bailey, L. D., and E. G. Beauchamp, Effects of temperature on NO_3 and NO_2 reduction, nitrogenous gas production, and redox potential in a saturated soil, *Can. J. Soil Sci.* 53, 213-218. 1973.

Bear, J., *Dynamics of Fluids in Porous Media*, American Elsevier Publishing Company, Inc., New York, 1972.

Bear, J., and M. Jacobs, On the movement of water bodies injected into aquifers, *Journal of Hydrology*, 3, 37-57, 1965.

Bear, J., and A. Verruijt, *Modeling Groundwater Flow and Pollution*, D. Reidel Publishing Company, Boston, 1987.

Betlach, M. R., and J. M. Tiedje, Kinetic explanation for accumulation of nitrate, nitric oxide, and nitrous oxide during bacterial denitrification, *Appl. Environ. Microbiol.*, 42, 1074-1084, 1981.

Bitton G., and Gerba, C. P. , *Groundwater Pollution Microbiology: The Emerging Issue*, John Wiley and Sons Inc., New York, 1984.

Bouchard, D. C., M. K. Williams, and R. Y. Surampalli, Nitrate contamination of groundwater: sources and potential health effects, *J. AWWA*, 84(9), 85-90, 1992.

Bouldin, D. R., R. L. Johnson, C. Burda, and C. W. Kao., Losses of inorganic nitrogen from aquatic systems. *J. Environ. Qual.*, 3, 107-114, 1974.

Bredehoeft, J. D., and G. F. Pinder, Mass transport in flowing groundwater, *Water Resour. Res.*, 9(1), 194-210, 1973.

Broadbent, F. E., and F. Clark, Denitrification, in *Soil Nitrogen*, edited by W. V. Bretholomew and F. E. Clark, Madison, Wisconsin, 1965.

Burford, J. R., and J. M. Bremner, Relationship between the denitrification capacities of soil and total, water-soluble, and readily decomposable soil organic matter. *Soil Biol. Biochem*, 7, 389-394, 1975.

Burns, W. A., Jr., New single-well test for determining vertical permeability. *J. Pet. Tech.*, 6, 743-752, 1969

Champ D. R., J. Gulns, and R. E. Jackson, Oxidation-reduction sequences in groundwater flow system. *Can. J. Earth Sci.*, 16, 12-23, 1979.

Characklis, W. G., M. G. Trulear, J. D. Bryers, and N. Zelver, Dynamics of biofilm processes, *Water Res.*, 16, 1207-1216, 1982.

Cheng, R. T., V. Casulli, and S. N. Milford, Eulerian-Lagrangian solution of the convection-dispersion equation in natural coordination, *Water Resour. Res.*, 20(2), 944-952, 1984.

Cho, C. M., Convective transport of ammonium with nitrification in soil., *Can. J. Soil Sci.*, 51, 339-350, 1971.

Cho, C. M., and J. G. Mills, Kinetic formulation of the denitrification process in soil, Can. J. Soil Sci., 59, 249-257, 1979.

Corapcioglu, M. Y., Deposition of solids in drilling fluids on borehole walls, *Water Resour. Res.*, 24, 1893-1900, 1988.

Corapcioglu, M. Y., N. M. Abboud, and A. Haridas, Governing equations for particle transport in porous media, in *Advances in Transport Phenomena in Porous Media*, edited by J. Bear and M. Y. Corapcioglu, Martinus Nijhoff, Dordrecht, 209-342, 1987.

Corapcioglu, M. Y. and A. Haridas, Microbial transport in soils and groundwater: A numerical model, *Adv. Water Resources*, 8, 188-200, 1985.

Corapcioglu, M. Y., and M. A. Hossain, Methanogenic biotransformation of chlorinated hydrocarbons in groundwater, *J. Environ. Eng.*, 117, 47-65, 1991.

Corapcioglu, M. Y., and M. A. Hossain, Groundwater contamination by high-density immiscible hydrocarbon slugs in gravity-driven gravel aquifer. *Groundwater*, 31, 774-780, 1993

Cunningham, A. B., W. G. Characklis, F. Abedeen, and D. Crawford, Influence of biofilm accumulation on porous media hydrodynamics, *Environ. Sci. Technol.*, 25, 1305-1311, 1991.

Dagan, G., The solution of the linearized equation of free-surface flow in porous media, *J. Mecanique*, 5(2), 207-215, 1966

Dahab, M, F. and Y. M. Lee, Nitrate removal from water supplied using biological denitrification, *J. WPCF*, 60(9), 1670-1674, 1988

De Renzo, D. J., *Nitrogen Control and Phosphorus Removal in Sewage Treatment*, Noyes Data Corporation, Park Ridge, New Jersey, 1978

Domenico , P. A. and F. W. Schwartz, *Physical and Chemical Hydrogeology*, John Wiley & Sons, New York, 1990.

Dorsch, M. M., R. K. Scragg, A. J. McMichael, P. A. Baghurst and K. F. Dyer, Congenital malfunctions and maternal drinking water supply in rural South Australia: A case control study, *Am. J. Epidemiol.* 119, 473-486, 1984.

Firestone, M., K., Biological denitrification, in *Nitrogen in Agriculture Soils*, Edited by F. J. Stevenson, American Society of Agronomy, Madison, Wisconsin, 1982.

Foster, S. D, D. P. Kelly, and R. James, The evidence for zones of biodenitrification in British aquifers, in *Planetary Ecology*, edited by D. E. Caldwell, J. A. Brierley, and C. L. Brierley, Van Nostrand Reinhold, New York, 1985.

Fotch, D. D., The effect of temperature, pH, and aeration on the production of nitrous oxide and gaseous nitrogen- a zero-order kinetic model, *Soil Sci.*, 118, 173-179, 1974.

Fotch, D. D., and W. Verstraete, Biochemical ecology of nitrification and denitrification, In *Advances in Microbial Ecology*, Edited by Martin Alexander, Plenum Press, New York, 135-214, 1977.

Fraser, P. A. and C. Chilvers, Health aspects of nitrate in drinking water. *The Science of the Total Environment*, 18, 103-116, 1981.

Goode, D. J., Particle velocity interpolation in black-centered finite difference groundwater flow models, *Water Resour. Res.*, 26(5), 925-940, 1990.

Grader, A. O., D. W., Peaceman, and A. L. Pozzi, Jr., Numerical calculation of multidimensional miscible displacement by the method of characteristics, *Society of Petroleum Engineers Journal*, 4(1), 641-651, 1984.

Gradner, W. R., Some steady state solutions of the unsaturated moisture flow equations with application to evaporation from a water table, *Soil Sci.* 85(4), 228-232, 1958.

Grady, C. P., and H. C. Lim, *Biological Wastewater Treatment -Theory and Applications*, Marcel Dekker, Inc., New York, 1980.

Gray, T. R. G., and S. T. Williams, *Soil Microorganisms*, Hafner Publishing Co, New York, 1971

Hall, T., Biological denitrification for potable water treatment, *J. Chem. Tech. Biotechnol.*, 54, 185-186, 1992

Hamon, M., and E. Fustec., Laboratory and field study of an in situ groundwater denitrification reactor, *J. WPCF*, 63(7), 942-946, 1991

Herbert, D., Some principles of continuous culture, in *Recent Progress in Microbiology*, Edited by G. Tunevall, Blackwell Scientific, Boston, 1958.

Herrling, B., W. Buermann, A new method for in-situ remediation of volatile contaminates in groundwater - Numerical simulation of the flow regime, *Computational Methods in Subsurface Hydrology*, Edited by G. Gambolati, A. Rinaldo, G. A. Brebbia, and W.G. Gray, Computation Mechanics Publications, Boston, 1990.

Herrling, B., W. Buermann and J. Stamm, In-situ remediation of volatile contaminants in groundwater by a new system of "Vacuum-Vaporizer-Wells", in *Subsurface Contamination by Immiscible Fluids*, Edited by K. U. Weyer, Rotterdam, 1991.

Hill, M. J., G. Hawksworth, and G. Tattersall, Bacteria, nitrosamines and cancer of the stomach, *Br. J. Cancer*, 28, 562-567, 1973.

Hiscock, K. M., J. W. Lloyd, and D. N. Lerner, Review of natural and artificial denitrification of groundwater, *Wat. Res.* 25(9), 1099-1111,1991.

Hmon, M., and E. Fustec, Laboratory and field study of an in situ groundwater denitrification reactor, *J. WPCF*, 63 (7), 942-949, 1991.

Hoek J. P., P. J. Van Der Ven, and A. Klapwijk, Combined into exchange/biological denitrification for nitrate removal from ground water under different process conditions, *Wat. Res.*, 22(6), 679-684, 1988.

Irmay, S., On the hydraulic conductivity of unsaturated soils, *Eoc, Transations, American Geophysical Union*, 35, 463-468, 1954.

Javandel, I., C. Doughty, and C.F. Tsang, *Groundwater Transport: Handbook of Mathematical Models*, American Geophysical Union, Washington, D. C., 1984.

Javandel, I., and C. F. Tsang, Capture-zone type curves: A tool for aquifer cleanup, *Ground Water*, 24(5), 616-625, 1986.

Kanwar, R. S., J. L. Baker, H. P. Johnson, and D. Kirkham, Nitrate movement with zero-order denitrification in a soil profiles, *Soil Sci, Soc. Am. J.*, 44, 898-902, 1980.

Kelmedtsson, L. B., H. Svensson, T. Lindberg, and T. Rosswall, The use of acetylene inhibition of nitrous oxide reductase in quantifying denitrification in soils. *Swedish J. Agric. Res.*, 7, 179-185, 1977.

Kinzelbach W., W. Schafer, and J. Herzer, Numerical modeling of natural and enhanced denitrification processes in aquifers, *Water Resour. Res.*, 27(6), 1123-1135, 1991.

Konikow, L. F., and J. D. Bredehoeft, Computer model of two-dimensional solute transport and dispersion in ground water, *U.S. Geol. Surv. Water Resour. Invest.*, Book 7, chapter C2, 1978.

Kruithof, J. C., C. A. Van Bennek, and H. A. Dierx, Nitrate removal from groundwater by sulphur/limestone filtration, *Wat. Supply*, 6, 207-217, 1985.

Lee, K L., and J. L. Wilson, Pollution-zones for pumping wells in aquifers with ambient flow, *Eos, Transations, American Geophysical Union*, 67, 966-967, 1986.

Lee, Y. W., and M. f. Dahab, Kinetics of low solid bio-denitrification of water supplies, *J. WPCF.* 60(10), 1857-1861, 1988.

Lindstrom, F. T., A mathematical Model for the one-dimensional transport and fate of oxygen and substrate in a water- saturated sorbing homogeneous porous medium, *Wat. Resour. Res.*, 28(9), 2499-251, 1992.

MacDonald, T. R., and P. K. Kitanidis, Modeling the free surface of an unconfined aquifer near a recirculation well, *Ground Water*, 31(5), 774-780, 1993

MacQuarrie, K. T., E. A. Sudicky, and E. O. Frind, Simulation of biodegradable organic contaminants in groundwater, 1. Numerical formulation in principal directions, *Wat. Resour. Res.*, 26(2), 207-222, 1990.

McBride, G. B., and J. C., Rutherford, Accurate modeling of river pollution transport, *Journal of Environmental engineering*, ASCE, 110(4), 808-827, 1984.

McCarty. P. L., L. Brck, and P. Amant, Biological denitrification of wastewater by addition of organic materials, *Proceeding of the 24th Purdue Industrial Waste Conference*, Lafayette, Indiana, 1969.

McConnaughey, P. K., Transport microsite models of denitrification: theory and experiment, *Dissertation*, Cornell University, 1983.

Mercado, A., M. Libhaber, and M. I. Soares, In situ biological groundwater denitrification: concepts and preliminary field tests, *Wat. Sci. Tech.*, 20(3), 197-209, 1988.

Misra, C., D. R. Nielson, and J. W. Biggar, Nitrogen transformations in soil during leaching: III. nitrate reduction in soil columns. *Soil Sci. Soc. Am. Proc.*, 38, 300-304, 1974.

Molz, F. J., M. A. Widdowson, and J. F. Benefield, Simulation of microbial growth dynamics coupled to nutrient and oxygen transport in porous media, *Water Resour. Res.*, 22 (8), 1207-1216, 1986.

Neuman, S. P., A Eulerian-Lagrangian numerical scheme for the dispersion-convection equation using conjugate space-time grids, *Journal of computational physics*, 41(2), 270-294, 1981

Neuman S. P., Adaptive Eulerian-Lagrangian finite element method for advection-dispersion. *Int. J. Numer. Methods Eng.*, 20, 321-337, 1984.

Nikolaevskii, V. N., Convective diffusion in porous media, J. *Appl. Math. Meth.*, 23(6), 1042-1050, 1959.

Novak, J. T., Temperature-substrate interactions in biological treatment, *J. WPCF*, 46, 1984-1994, 1974.

Parker, D. S., Biological denitrification, in *Process Design Manual for Nitrogen Control*, U.S. Environmental Protection Agency, 1975.

Payne, W. J., *Denitrification*, John Wiley, New York, 1973.

Payne, W. J., Jr., Reduction of nitrogenous oxides by microorganism, *Bacteriol. Rev.*, 37, 409-452, 1973.

Philip R. D., and G. R. Walter, Prediction of flow and hydraulic head fields for vertical circulation wells, *Ground Water*, 30(5), 765-773, 1992.

Pinder, G. F., and H. H. Cooper, Jr., A numerical technique for calculating the transient position of the saltwater front, *Water Resour. Res.*, 6(3), 875-882, 1970.

Polprasert, C, and H. S. Park, Effluent denitrification with anaerobic filters, *Wat. Res.*, 20(8), 1015-1021, 1986.

Reddell, D. L., and D. K. Sunada, Numerical simulation of dispersion in groundwater aquifers, *Hydrology Paper*, Colorado State Univ., 41, 1970

Reddy, K. R., W. H. Patrick, Jr., and R. E. Phillips, The role of nitrate diffusion in determining the order and rate of denitrification in flooded soil: I. Experimental results. *Soil Sci. Soc. Am. J.*, 42, 268-272, 1978.

Rittmann, B. E., The significance of biofilms in porous media, *Water Resour. Res.*, 29, 2195-2202, 1993.

Roels, J. A., *Energetic and Kinetics in Biotechnology*, Elsevier Science, New York, 1983.

Rolston, D. E., and M. A. Marino, Simultaneous transport of nitrate and gaseous denitrification products in soil, *Soil Sci. Soc. Am. J.*, 40, 860-865, 1976.

Scheidegger, A., E., General theory of dispersion in porous media., *J. Geophys. Res.*, 66, 3273-3278, 1961.

Semprini, L., and P. L. McCarty, Comparison between model simulations and field results for in-suit biorestoration of chlorinated aliphatics: Part 1., Biostimulation of methanotrophic bacteria, *Ground Water*, 29(3), 365-374, 1991.

Smith, R. L. and J. H. Duff, Denitrification in a sand and gravel aquifer, *Applied and Environmental Microbiology*, 54 (5), 1071-1078, 1988.

Spalding, R. F., and M. E. Exner, Occurrence of nitrate in groundwater -a review, *J. Enviro. Qual.*, 22, 392-402, 1993.

Spector W. S. *Handbook of Biological Data*, Saunders, Philadelphia, PA, 1956.

Stallard, W. M., K. C. Wu, N. Shi, and M. Y. Corapcioglu, Recirculating nitrate treatment well hydraulics, *Eos, Transaction, American Geophysical Union.* 74, 258, 1993.

Stallard, W. M., K. C. Wu, N. Shi, and M. Y. Corapcioglu, Hydraulics of recirculating groundwater remediation wells in unconfined aquifers, *ASCE, J. Enviro. Eng.*, (in press).

Stanford, G., R. A. VanderPol, and S. Dzienia, Denitrification rates in relation to total and extractable soil carbon, *Soil Sci. Soc. Am. Proc.*, 39, 284-289, 1975.

Starr, J. L., and J. Y. Parlange, Relation between the kinetics of nitrogen transformation and biomass distribution in a soil column during continuous leaching, *Soil Sci. Sco. Am. J.*, 40, 458-460, 1976.

Stensel, H. D., R. C. Loehr, and A. W. Lawrence, Biological kinetic of suspended-growth denitrification, *Jour. Water Poll. Control Fed.*, 45(2), 249-261, 1973.

Suidan, M. T., B. E. Rittmann, and U. K. Traegner, Criteria establishing biofilm kinetic types, *Water Resour. Res.* 21(4), 491-498, 1987.

Super, M., H. Heese, D. MacKenzie, W. S. Dempster, J. DuPless, and J. J. Ferreira. An epidemiological study of well-water nitrates in a group of Southwest African Namibian infants, *Water Res.*, 15, 1265-1270, 1981.

Taylor, S. W., and P. R. Jaffe, Substrate and biomass transport in a porous medium, *Water Resour. Res.*, 26(9), 2181-2104, 1990(a).

Taylor, S. W., and P. R. Jaffe, Biofilm growth and the related changes in the physical properties of a porous medium, 2, Permeability, *Water Resour. Res.*, 26, 2161-2169, 1990(b).

Tchobanoglous, G., and F. L. Burton, *Wastewater Engineering—Treatment, Disposal, and Reuse*, McGraw-Hill, Inc., New York, 1991.

Thruman, E. M., *Organic Geochemistry of Natural Water*, Nijhoff-Junk, Dordrecht, Netherland, 1985.

Timmermans, P., and A. Van Haute, Denitrification with methanol, *Water Res.*, 17(10), 1249-1255, 1983.

US Environmental Protection Agency, National survey of pesticides in drinking water wells, phase I report, *EPA Rep.*, *570/0-90-015*, Office of Water, Washington, D. C., 1990.

Van Genuchten, M., A closed-form Equation for predicting the hydraulic conductivity of unsaturated soils, *Soil Sci. Am. J.*, 44, 892-898, 1980.

Widdowson, M. A., and F. J. Molz, and L. D. Benefield, A numerical transport model for oxygen- and nitrate- based respiration linked to substrate and nutrient availability in porous media, *Wat. Resour. Res.*, 24(9), 1553-1565, 1988.

Wu, K. C, Protection of a drinking water well from nitrate contamination by recirculating nitrate treatment well system, Ph.D *Dissertation*, Texas A&M University, 1994.

Yeh T. J., R. Srivastava, A. Guzman, and T. Harter, A numerical model for water flow and chemical transport in variable saturated porous media, *Ground Water*, 31(4), 634-644, 1993.

Zheng C., Extension of the method of characteristics for simulation of solution transport in three dimensions, *Ground Water*, 31(3), 456-465, 1992.

APPENDIX G

Results of EPIC Sensitivity Analysis

EPIC Variable DRT, Days Required for Drainage to Reduce Plant Stress

DRT days	PRCP mm	Q mm	SSF mm	PRK mm	QDRN mm	IRGA mm	ET mm	YON kg/ha	YNO3 kg/ha	SSFN kg/ha	PRKN kg/ha	DRNN kg/ha	FNO3 kg/ha	FNH3 kg/ha	YP kg/ha	YAP kg/ha	PRKP kg/ha	MUSS t/ha	YW t/ha	UNO3 kg/ha	UPP kg/ha	DN kg/ha	GRSG t/ha	COTP t/ha
0.2	762.80	193.85	227.11	1.10	223.39	320.04	740.33	13.96	3.88	27.25	0.12	25.61	28.32	84.00	3.38	0.03	0.00	15.50	5.52	381.93	62.31	16.90	5.51	2.33
0.5	762.80	193.86	225.28	2.72	222.04	320.04	740.47	13.96	3.88	27.03	0.30	25.47	28.32	84.00	3.38	0.03	0.01	15.51	5.52	381.87	62.29	16.91	5.51	2.33
1	762.80	193.90	222.21	5.39	219.83	320.04	740.79	13.95	3.88	26.66	0.59	25.25	28.32	84.00	3.38	0.03	0.01	15.51	5.50	381.74	62.25	16.92	5.51	2.33
1.5	762.80	193.92	219.27	8.00	217.44	320.04	741.05	13.97	3.88	26.31	0.96	25.01	28.32	84.00	3.38	0.03	0.02	15.52	5.52	381.62	62.22	16.94	5.50	2.33
2	762.80	193.94	216.53	10.55	215.04	320.04	741.18	14.00	3.88	25.98	1.27	24.77	28.32	84.00	3.39	0.03	0.03	15.52	5.58	381.47	62.17	16.95	5.50	2.33
2.5	762.80	193.96	213.91	13.05	212.67	320.04	741.22	14.09	3.88	25.67	1.57	24.54	28.32	84.00	3.41	0.03	0.03	15.52	5.72	381.28	62.13	16.96	5.50	2.33
3	762.80	193.97	211.40	15.48	210.33	320.04	741.22	14.20	3.88	25.37	1.86	24.31	28.32	84.00	3.44	0.03	0.04	15.53	5.89	381.10	62.08	16.97	5.49	2.32
3.5	762.80	193.99	208.97	17.87	208.03	320.04	741.17	14.27	3.88	25.08	2.14	24.09	28.32	84.00	3.46	0.03	0.05	15.53	5.99	380.90	62.04	16.98	5.49	2.32
4	762.80	194.00	206.61	20.20	205.78	320.04	741.11	14.32	3.88	24.79	2.42	23.87	28.32	84.00	3.47	0.03	0.05	15.53	6.07	380.69	61.99	16.99	5.49	2.32
4.5	762.80	194.01	204.32	22.48	203.57	320.04	741.02	14.31	3.88	24.52	2.70	23.65	28.32	84.00	3.47	0.03	0.06	15.54	6.05	380.48	61.94	17.01	5.48	2.32
5	762.80	194.02	202.08	24.71	201.40	320.04	740.91	14.30	3.88	24.25	2.97	23.43	28.32	84.00	3.46	0.03	0.06	15.54	6.04	380.25	61.89	17.02	5.48	2.32
5.5	762.80	194.04	199.90	26.89	199.27	320.04	740.80	14.30	3.88	23.99	3.23	23.22	28.32	84.00	3.46	0.03	0.07	15.54	6.03	380.03	61.84	17.03	5.48	2.32
6	762.80	194.05	197.77	29.03	197.19	320.04	740.68	14.29	3.88	23.73	3.48	23.01	28.32	84.00	3.46	0.03	0.08	15.55	6.02	379.80	61.79	17.05	5.47	2.31
6.5	762.80	194.06	195.69	31.13	195.15	320.04	740.56	14.29	3.88	23.48	3.74	22.81	28.32	84.00	3.46	0.03	0.08	15.55	6.01	379.58	61.74	17.06	5.47	2.31
7	762.80	194.07	193.66	33.18	193.15	320.04	740.43	14.29	3.88	23.24	3.98	22.61	28.32	84.00	3.46	0.03	0.09	15.55	6.01	379.35	61.69	17.07	5.47	2.31
7.5	762.80	194.08	191.67	35.19	191.19	320.04	740.29	14.29	3.88	23.00	4.22	22.41	28.32	84.00	3.46	0.03	0.09	15.55	6.01	379.14	61.64	17.09	5.46	2.31
8	762.80	194.09	189.72	37.16	189.28	320.04	740.16	14.29	3.88	22.77	4.46	22.21	28.32	84.00	3.46	0.03	0.10	15.56	6.00	378.91	61.60	17.10	5.46	2.31
8.5	762.80	194.10	187.81	39.09	187.39	320.04	740.02	14.29	3.88	22.54	4.69	22.02	28.32	84.00	3.46	0.03	0.10	15.56	6.00	378.70	61.55	17.11	5.46	2.30
9	762.80	194.11	185.94	40.98	185.55	320.04	739.89	14.30	3.88	22.31	4.92	21.83	28.32	84.00	3.46	0.03	0.11	15.56	6.00	378.47	61.50	17.12	5.45	2.30

Description of Variables:
CN2   Runoff curve number, antecedent moisture condition 2
COTP   Crop yield for picker cotton (t/ha)
DN   N loss by denitrification (kg/ha)
DRNN   Mineral N loss in subsurface drain flow (kg/ha)
DRT   Drain time, days required for drainage to reduce plant stress (days)
ET   Evapotranspiration (mm)
FNH3   Fertilizer N applied in the form NH₃-N (kg/ha)
FNO3   Fertilizer N applied in the form NO₃-N (kg/ha)
GRSG   Crop yield for grain sorghum (t/ha)
IRGA   Irrigation water applied (mm)
MUSS   Soil loss from water erosion using a modified MUSLE option for small watersheds
PRCP   Precipitation (mm)
PRK   Percolation below the root zone (mm)
PRKN   Mineral N loss in percolate (kg/ha)
PRKP   Percolation of P below the root zone (kg/ha)
Q   Runoff (mm)
QDRN   Subsurface drain flow (mm)
SSF   Lateral subsurface flow (mm)
SSFN   Mineral N loss in subsurface flow (kg/ha)
UNO3   N uptake by the crop (kg/ha)
UPP   P uptake by the crop (kg/ha)
WNO3   Initial nitrate concentration in the soil (ppm)
YAP   Soluble P loss in runoff (kg/ha)
YNO3   NO₃ loss in surface runoff (kg/ha)
YON   Organic N loss with sediment (kg/ha)
YP   P loss with sediment (kg/ha)
YW   Soil loss from wind erosion (t/ha)

EPIC Variable DRT, Days Required for Drainage to Reduce Plant Stress
% Change

DRT	PRCP	Q	SSF	PRK	QDRN	IRGA	ET	YON	YNO3	SSFN	PRKN	DRNN	FNO3	FNH3	YP	YAP	PRKP	MUSS	YW	UNO3	UPP	DN	GRSG	COTP
-94%	0.0%	-0.1%	8.7%	-93.9%	7.4%	0.0%	-0.1%	-2.2%	-0.1%	8.7%	-94.4%	6.3%	0.0%	0.0%	-2.2%	-0.1%	-93.8%	-0.2%	-7.9%	0.3%	0.4%	-0.5%	0.4%	0.3%
-86%	0.0%	-0.1%	7.8%	-84.8%	6.7%	0.0%	-0.1%	-2.2%	-0.1%	7.8%	-85.0%	5.7%	0.0%	0.0%	-2.2%	-0.1%	-84.8%	-0.1%	-7.9%	0.3%	0.4%	-0.4%	0.4%	0.3%
-71%	0.0%	0.0%	6.3%	-69.8%	5.7%	0.0%	-0.1%	-2.1%	0.0%	6.3%	-72.3%	4.8%	0.0%	0.0%	-2.1%	0.0%	-69.9%	-0.1%	-8.2%	0.2%	0.4%	-0.3%	0.3%	0.2%
-57%	0.0%	0.0%	4.9%	-55.2%	4.5%	0.0%	0.0%	-1.8%	0.0%	4.9%	-55.2%	3.6%	0.0%	0.0%	-1.9%	0.0%	-55.1%	-0.1%	-7.9%	0.2%	0.3%	-0.2%	0.2%	0.2%
-43%	0.0%	0.0%	3.6%	-40.9%	3.4%	0.0%	0.0%	-1.2%	0.0%	3.6%	-40.9%	2.8%	0.0%	0.0%	-1.2%	0.0%	-41.0%	-0.1%	-6.9%	0.1%	0.2%	-0.2%	0.2%	0.2%
-29%	0.0%	0.0%	2.4%	-27.0%	2.2%	0.0%	0.0%	-1.2%	0.0%	2.4%	-27.0%	1.9%	0.0%	0.0%	-1.2%	0.0%	-26.9%	0.0%	-4.6%	0.1%	0.1%	-0.2%	0.1%	0.1%
-14%	0.0%	0.0%	1.2%	-13.3%	1.1%	0.0%	0.0%	-0.4%	0.0%	1.2%	-13.3%	0.9%	0.0%	0.0%	-0.5%	0.0%	-13.5%	0.0%	-1.7%	0.1%	0.1%	-0.1%	0.1%	0.1%
0%	0.0%	0.0%	0.0%	0.0%	0.0%	0.0%	0.0%	0.0%	0.0%	0.0%	0.0%	0.0%	0.0%	0.0%	0.0%	0.0%	0.0%	0.0%	0.0%	0.0%	0.0%	0.0%	0.0%	0.0%
14%	0.0%	0.0%	-1.1%	13.0%	-1.1%	0.0%	0.0%	0.4%	0.0%	-1.1%	13.0%	-0.9%	0.0%	0.0%	0.4%	0.0%	13.0%	0.0%	1.4%	-0.1%	-0.1%	0.1%	-0.1%	-0.1%
29%	0.0%	0.0%	-2.2%	25.8%	-2.1%	0.0%	0.0%	0.3%	0.0%	-2.2%	25.8%	-1.8%	0.0%	0.0%	0.3%	0.0%	25.6%	0.0%	1.0%	-0.1%	-0.2%	0.2%	-0.1%	-0.2%
43%	0.0%	0.0%	-3.3%	38.3%	-3.2%	0.0%	-0.1%	0.2%	0.0%	-3.3%	38.3%	-2.7%	0.0%	0.0%	0.2%	0.0%	38.2%	0.1%	0.8%	-0.2%	-0.2%	0.3%	-0.2%	-0.2%
57%	0.0%	0.0%	-4.3%	50.5%	-4.2%	0.0%	-0.1%	0.2%	0.0%	-4.3%	50.5%	-3.6%	0.0%	0.0%	0.2%	0.0%	50.4%	0.1%	0.6%	-0.2%	-0.3%	0.3%	-0.2%	-0.3%
71%	0.0%	0.0%	-5.4%	62.5%	-5.2%	0.0%	-0.1%	0.2%	0.0%	-5.4%	62.5%	-4.5%	0.0%	0.0%	0.2%	0.0%	62.4%	0.1%	0.5%	-0.3%	-0.4%	0.4%	-0.3%	-0.4%
86%	0.0%	0.0%	-6.4%	74.2%	-6.2%	0.0%	-0.1%	0.2%	0.0%	-6.4%	74.2%	-5.3%	0.0%	0.0%	0.1%	0.0%	74.1%	0.1%	0.4%	-0.3%	-0.5%	0.5%	-0.4%	-0.4%
100%	0.0%	0.0%	-7.3%	85.7%	-7.2%	0.0%	-0.1%	0.2%	0.0%	-7.3%	85.7%	-6.2%	0.0%	0.0%	0.1%	0.0%	85.5%	0.1%	0.3%	-0.4%	-0.6%	0.6%	-0.4%	-0.5%
114%	0.0%	0.0%	-8.3%	96.9%	-8.1%	0.0%	-0.1%	0.2%	0.0%	-8.3%	96.9%	-7.0%	0.0%	0.0%	0.1%	0.0%	96.8%	0.2%	0.2%	-0.5%	-0.6%	0.6%	-0.5%	-0.6%
129%	0.0%	0.1%	-9.2%	106.0%	-9.0%	0.0%	-0.1%	0.2%	0.1%	-9.2%	108.0%	-7.8%	0.0%	0.0%	0.1%	0.1%	107.7%	0.2%	0.2%	-0.5%	-0.7%	0.7%	-0.5%	-0.7%
143%	0.0%	0.1%	-10.1%	118.8%	-9.9%	0.0%	-0.2%	0.2%	0.1%	-10.1%	118.8%	-8.6%	0.0%	0.0%	0.1%	0.1%	118.6%	0.2%	0.2%	-0.6%	-0.8%	0.8%	-0.6%	-0.8%
157%	0.0%	0.1%	-11.0%	129.3%	-10.8%	0.0%	-0.2%	0.2%	0.1%	-11.0%	129.3%	-9.4%	0.0%	0.0%	0.1%	0.1%	129.1%	0.2%	0.2%	-0.6%	-0.9%	0.8%	-0.6%	-0.8%

EPIC Variable WNO3, Initial Nitrate Concentration (ppm) in Soil Layers 1 - 3

WNO3 ppm	PRCP mm	Q mm	SSF mm	PRK mm	QDRN mm	IRGA mm	ET mm	YON kg/ha	YNO3 kg/ha	SSFN kg/ha	PRKN kg/ha	DRNN kg/ha	FNO3 kg/ha	FNH3 kg/ha	YP kg/ha	YAP kg/ha	PRKP kg/ha	MUSS t/ha	YW t/ha	UNO3 kg/ha	UPP kg/ha	DN kg/ha	GRSG t/ha	COTP t/ha
1	762.80	193.98	208.96	17.87	208.02	320.04	741.13	12.98	3.88	14.63	1.25	14.65	28.32	84.00	3.14	0.03	0.05	14.06	5.69	321.83	60.41	10.61	5.08	2.32
2	762.80	193.98	208.96	17.87	208.02	320.04	741.15	13.37	3.88	16.72	1.43	16.85	28.32	84.00	3.24	0.03	0.05	14.53	5.79	336.12	61.23	12.06	5.27	2.32
3	762.80	193.98	208.96	17.87	208.02	320.04	741.16	13.68	3.88	18.81	1.61	19.12	28.32	84.00	3.32	0.03	0.05	14.88	5.87	350.60	61.69	13.57	5.39	2.32
4	762.80	193.99	208.97	17.87	208.03	320.04	741.17	14.05	3.88	20.90	1.79	21.52	28.32	84.00	3.41	0.03	0.05	15.30	5.95	365.61	61.91	15.21	5.45	2.32
5	762.80	193.99	208.97	17.87	208.03	320.04	741.17	14.27	3.88	25.08	2.14	24.09	28.32	84.00	3.46	0.03	0.05	15.53	5.99	380.90	62.04	16.98	5.49	2.32
6	762.80	193.99	208.94	17.86	208.01	320.04	741.21	14.38	3.88	27.16	2.32	26.65	28.32	84.00	3.48	0.03	0.05	15.61	6.01	391.65	62.10	18.75	5.51	2.32
7	762.80	193.98	208.75	17.85	207.81	320.04	741.43	14.44	3.88	29.22	2.50	29.14	28.32	84.00	3.48	0.04	0.05	15.62	6.02	399.19	62.13	20.51	5.52	2.32
8	762.80	193.97	208.63	17.84	207.69	320.04	741.56	14.50	5.82	31.29	2.68	31.77	28.32	84.00	3.49	0.04	0.05	15.63	6.02	407.08	62.56	22.31	5.53	2.32
9	762.80	193.97	208.58	17.83	207.64	320.04	741.62	14.57	5.82	35.46	3.03	34.51	28.32	84.00	3.50	0.04	0.05	15.66	6.03	415.13	62.94	24.13	5.53	2.32
10	762.80	193.97	208.57	17.83	207.63	320.04	741.63	14.66	5.82	37.54	3.21	37.19	28.32	84.00	3.51	0.04	0.05	15.69	6.04	423.19	63.05	26.02	5.53	2.32
11	762.80	193.97	208.57	17.83	207.63	320.04	741.64	14.74	5.82	39.63	3.39	39.87	28.32	84.00	3.52	0.04	0.05	15.73	6.04	431.24	63.05	27.89	5.53	2.32
12	762.80	193.97	208.57	17.83	207.63	320.04	741.64	14.81	5.82	43.80	3.57	42.56	28.32	84.00	3.53	0.04	0.05	15.75	6.05	439.30	63.05	29.76	5.53	2.32
13	762.80	193.97	208.57	17.83	207.63	320.04	741.64	14.88	5.82	45.89	3.92	45.25	28.32	84.00	3.53	0.04	0.05	15.78	6.05	447.36	63.05	31.63	5.53	2.32
14	762.80	193.97	208.57	17.83	207.63	320.04	741.64	14.90	5.82	50.06	4.28	50.32	28.32	84.00	3.53	0.04	0.05	15.78	6.05	449.48	63.05	32.68	5.53	2.32
15	762.80	193.97	208.57	17.83	207.63	320.04	741.64	14.90	5.82	56.31	4.81	56.25	28.32	84.00	3.53	0.04	0.05	15.78	6.05	449.48	63.05	33.91	5.53	2.32
16	762.80	193.97	208.57	17.83	207.63	320.04	741.64	14.90	5.82	62.57	5.35	62.17	28.32	84.00	3.53	0.04	0.05	15.78	6.05	449.48	63.05	34.95	5.53	2.32
17	762.80	193.97	208.57	17.83	207.63	320.04	741.64	14.90	5.82	68.83	5.88	68.08	28.32	84.00	3.53	0.04	0.05	15.78	6.05	449.48	63.05	35.98	5.53	2.32
18	762.80	193.97	208.57	17.83	207.63	320.04	741.64	14.90	5.82	75.08	6.42	74.01	28.32	84.00	3.53	0.04	0.05	15.78	6.05	449.48	63.05	37.01	5.53	2.32
19	762.80	193.97	208.57	17.83	207.63	320.04	741.64	14.90	5.82	79.26	6.95	79.94	28.32	84.00	3.53	0.04	0.05	15.78	6.06	449.48	63.05	38.04	5.53	2.32

Description of Variables:

CN2	Runoff curve number, antecedent moisture condition 2
COTP	Crop yield for picker cotton (t/ha)
DN	N loss by denitrification (kg/ha)
DRNN	Mineral N loss in subsurface drain flow (kg/ha)
DRT	Drain time, days required for drainage to reduce plant stress (days)
ET	Evapotranspiration (mm)
FNH3	Fertilizer N applied in the form NH₃-N (kg/ha)
FNO3	Fertilizer N applied in the form NO₃-N (kg/ha)
GRSG	Crop yield for grain sorghum (t/ha)
IRGA	Irrigation water applied (mm)
MUSS	Soil loss from water erosion using a modified MUSLE option for small watersheds
PRCP	Precipitation (mm)
PRK	Percolation below the root zone (mm)
PRKN	Mineral N loss in percolate (kg/ha)
PRKP	Percolation of P below the root zone (kg/ha)
Q	Runoff (mm)
QDRN	Subsurface drain flow (mm)
SSF	Lateral subsurface flow (mm)
SSFN	Mineral N loss in subsurface flow (kg/ha)
UNO3	N uptake by the crop (kg/ha)
UPP	P uptake by the crop (kg/ha)
WNO3	Initial nitrate concentration in the soil (ppm)
YAP	Soluble P loss in runoff (kg/ha)
YNO3	NO3 loss in surface runoff (kg/ha)
YON	Organic N loss with sediment (kg/ha)
YP	P loss with sediment (kg/ha)
YW	Soil loss from wind erosion (t/ha)

EPIC Variable WNO3, Initial Nitrate Concentration (ppm) in Soil Layers 1 - 3
% Change

WNO3	PRCP	Q	SSF	PRK	QDRN	IRGA	ET	YON	YNO3	SSFN	PRKN	DRNN	FNO3	FNH3	YP	YAP	PRKP	MUSS	YW	UNO3	UPP	DN	GRSG	COTP
-88%	0.0%	0.0%	0.2%	0.2%	0.2%	0.0%	-0.1%	-10.5%	-33.3%	-53.3%	-53.3%	-53.9%	0.0%	0.0%	-10.1%	-16.5%	0.2%	-10.1%	-5.5%	-20.9%	-3.4%	-52.4%	-8.1%	0.0%
-75%	0.0%	0.0%	0.2%	0.2%	0.2%	0.0%	-0.1%	-7.8%	-33.3%	-46.6%	-46.6%	-47.0%	0.0%	0.0%	-7.1%	-11.0%	0.2%	-7.1%	-3.9%	-17.4%	-2.1%	-45.9%	-4.6%	0.0%
-63%	0.0%	0.0%	0.2%	0.2%	0.2%	0.0%	-0.1%	-5.7%	-33.3%	-39.9%	-39.9%	-39.8%	0.0%	0.0%	-4.9%	-5.5%	0.2%	-4.8%	-2.6%	-13.9%	-1.4%	-39.1%	-2.5%	0.0%
-50%	0.0%	0.0%	0.2%	0.2%	0.2%	0.0%	-0.1%	-3.1%	-33.3%	-33.2%	-33.2%	-32.2%	0.0%	0.0%	-2.4%	-5.5%	0.2%	-2.1%	-1.3%	-10.2%	-1.0%	-31.8%	-1.3%	0.0%
-38%	0.0%	0.0%	0.2%	0.2%	0.2%	0.0%	-0.1%	-1.6%	-33.3%	-19.9%	-19.9%	-24.2%	0.0%	0.0%	-1.0%	-5.5%	0.2%	-0.6%	-0.5%	-6.4%	-0.8%	-23.9%	-0.7%	0.0%
-25%	0.0%	0.0%	0.2%	0.2%	0.2%	0.0%	0.0%	-0.9%	-33.3%	-13.2%	-13.2%	-16.1%	0.0%	0.0%	-0.5%	-5.5%	0.2%	-0.1%	-0.3%	-3.8%	-0.7%	-15.9%	-0.3%	0.0%
-13%	0.0%	0.0%	0.1%	0.1%	0.1%	0.0%	0.0%	-0.4%	-33.3%	-6.6%	-6.6%	-8.3%	0.0%	0.0%	-0.3%	0.0%	0.0%	-0.1%	-0.1%	-1.9%	-0.7%	-8.1%	0.0%	0.0%
0%	0.0%	0.0%	0.0%	0.0%	0.0%	0.0%	0.0%	0.0%	0.0%	0.0%	0.0%	0.0%	0.0%	0.0%	0.0%	0.0%	0.0%	0.0%	0.0%	0.0%	0.0%	0.0%	0.0%	0.0%
13%	0.0%	0.0%	0.0%	0.0%	0.0%	0.0%	0.0%	0.5%	0.0%	13.3%	13.3%	8.6%	0.0%	0.0%	0.3%	5.5%	0.2%	0.2%	0.1%	2.0%	0.6%	8.2%	0.0%	0.0%
25%	0.0%	0.0%	0.0%	0.0%	0.0%	0.0%	0.0%	1.1%	0.0%	20.0%	20.0%	17.1%	0.0%	0.0%	0.6%	5.5%	0.2%	0.4%	0.2%	4.0%	0.8%	16.6%	0.0%	0.0%
38%	0.0%	0.0%	0.0%	0.0%	0.0%	0.0%	0.0%	1.6%	0.0%	26.6%	26.6%	25.5%	0.0%	0.0%	0.8%	5.5%	0.2%	0.6%	0.3%	5.9%	0.8%	25.0%	0.0%	0.0%
50%	0.0%	0.0%	0.0%	0.0%	0.0%	0.0%	0.0%	2.1%	0.0%	40.0%	33.3%	34.0%	0.0%	0.0%	1.0%	5.5%	0.2%	0.8%	0.4%	7.9%	0.8%	33.4%	0.0%	0.0%
63%	0.0%	0.0%	0.0%	0.0%	0.0%	0.0%	0.0%	2.6%	0.0%	46.6%	46.6%	42.4%	0.0%	0.0%	1.1%	5.5%	0.2%	0.9%	0.5%	9.9%	0.8%	41.8%	0.0%	0.0%
75%	0.0%	0.0%	0.0%	0.0%	0.0%	0.0%	0.0%	2.7%	0.0%	60.0%	60.0%	58.4%	0.0%	0.0%	1.1%	5.5%	0.2%	1.0%	0.5%	10.4%	0.8%	47.4%	0.0%	0.0%
88%	0.0%	0.0%	0.0%	0.0%	0.0%	0.0%	0.0%	2.7%	0.0%	79.9%	79.9%	77.1%	0.0%	0.0%	1.2%	5.5%	0.2%	1.0%	0.5%	10.4%	0.8%	52.0%	0.0%	0.0%
100%	0.0%	0.0%	0.0%	0.0%	0.0%	0.0%	0.0%	2.7%	0.0%	99.9%	99.9%	95.7%	0.0%	0.0%	1.2%	5.5%	0.2%	1.0%	0.5%	10.4%	0.8%	56.7%	0.0%	0.0%
113%	0.0%	0.0%	0.0%	0.0%	0.0%	0.0%	0.0%	2.7%	0.0%	119.9%	119.9%	114.3%	0.0%	0.0%	1.2%	5.5%	0.2%	1.0%	0.5%	10.4%	0.8%	61.3%	0.0%	0.0%
125%	0.0%	0.0%	0.0%	0.0%	0.0%	0.0%	0.0%	2.7%	0.0%	139.9%	139.9%	133.0%	0.0%	0.0%	1.2%	5.5%	0.2%	1.0%	0.5%	10.4%	0.8%	65.9%	0.0%	0.0%
138%	0.0%	0.0%	0.0%	0.0%	0.0%	0.0%	0.0%	2.7%	0.0%	153.3%	159.9%	151.6%	0.0%	0.0%	1.2%	5.5%	0.2%	1.0%	0.5%	10.4%	0.8%	70.5%	0.0%	0.0%

EPIC Variable CN2, Runoff Curve Number - Antecedent Moisture Condition 2

CN2	PRCP mm	Q mm	SSF mm	PRK mm	QDRN mm	IRGA mm	ET mm	YON Kg/ha	YNO3 Kg/ha	SSFN Kg/ha	PRKN Kg/ha	DRNN Kg/ha	FNO3 Kg/ha	FNH3 Kg/ha	YP Kg/ha	YAP Kg/ha	PRKP Kg/ha	MUSS t/ha	YW t/ha	UNO3 Kg/ha	UPP Kg/ha	DN Kg/ha	GRSG t/ha	COTP t/ha
74	762.80	131.41	244.51	20.90	243.35	320.04	758.59	10.10	1.31	29.34	2.51	30.09	28.32	84.00	2.43	0.02	0.05	9.83	5.05	371.75	60.75	17.19	5.49	2.21
75	762.80	128.90	246.58	21.08	245.40	320.04	759.03	10.06	1.29	29.59	2.53	30.42	28.32	84.00	2.42	0.02	0.06	9.86	5.05	371.98	60.78	17.14	5.49	2.22
76	762.80	131.34	244.65	20.91	243.49	320.04	758.86	10.19	1.31	29.36	2.51	30.14	28.32	84.00	2.45	0.02	0.06	10.06	5.06	372.21	60.81	17.17	5.49	2.22
77	762.80	133.79	242.85	20.76	241.71	320.04	758.51	10.32	1.34	29.14	2.49	29.88	28.32	84.00	2.49	0.02	0.05	10.27	5.07	372.41	60.84	17.18	5.49	2.22
78	762.80	136.27	241.20	20.62	240.07	320.04	757.98	10.45	1.36	28.94	2.47	29.64	28.32	84.00	2.52	0.02	0.05	10.48	5.06	372.61	60.87	17.20	5.49	2.22
79	762.80	140.21	239.27	20.45	238.16	320.04	756.30	10.72	1.40	28.71	2.45	29.35	28.32	84.00	2.59	0.03	0.05	10.84	5.07	372.82	60.90	17.23	5.49	2.23
80	762.80	142.78	237.78	20.33	236.68	320.04	755.52	10.87	1.43	28.53	2.44	29.13	28.32	84.00	2.62	0.03	0.05	11.06	5.08	373.04	60.93	17.24	5.49	2.23
81	762.80	145.07	236.62	20.23	235.52	320.04	754.68	10.98	1.45	28.39	2.43	28.97	28.32	84.00	2.65	0.03	0.05	11.26	5.08	373.28	60.97	17.25	5.49	2.23
82	762.80	147.22	235.32	20.12	234.23	320.04	754.13	11.10	1.47	28.24	2.41	28.78	28.32	84.00	2.68	0.03	0.05	11.44	5.09	373.52	61.00	17.25	5.49	2.23
83	762.80	149.14	234.17	20.02	233.10	320.04	753.30	11.15	1.49	28.10	2.40	28.63	28.32	84.00	2.69	0.03	0.05	11.59	5.02	373.33	60.98	17.26	5.49	2.23
84	762.80	151.00	233.09	19.93	232.02	320.04	752.30	11.20	1.51	27.97	2.39	28.49	28.32	84.00	2.70	0.03	0.05	11.74	4.94	372.89	60.91	17.27	5.49	2.23
85	762.80	152.84	232.29	19.86	231.23	320.04	751.20	11.25	1.53	27.87	2.38	28.39	28.32	84.00	2.72	0.03	0.05	11.89	4.90	372.70	60.88	17.27	5.49	2.22
86	762.80	186.19	213.89	18.29	212.93	320.04	743.47	13.65	3.72	25.67	2.19	24.73	28.32	84.00	3.30	0.03	0.05	14.81	5.67	380.57	62.00	17.18	5.49	2.32
87	762.80	188.78	212.10	18.13	211.15	320.04	742.83	13.85	3.78	25.45	2.18	24.46	28.32	84.00	3.35	0.03	0.05	15.05	5.75	380.61	62.00	17.18	5.49	2.32
88	762.80	191.38	210.36	17.99	209.42	320.04	742.17	14.00	3.83	25.24	2.16	24.31	28.32	84.00	3.39	0.03	0.05	15.29	5.79	380.73	62.01	16.98	5.49	2.32
89	762.80	193.99	208.97	17.87	208.03	320.04	741.17	14.27	3.88	25.08	2.14	24.09	28.32	84.00	3.46	0.03	0.05	15.53	5.99	380.90	62.04	16.98	5.49	2.32
90	762.80	196.60	207.56	17.75	206.63	320.04	740.19	14.07	3.93	24.91	2.13	23.87	28.32	84.00	3.41	0.03	0.05	15.77	5.45	381.13	62.07	16.98	5.49	2.32
91	762.80	199.20	205.93	17.61	205.01	320.04	739.43	14.08	3.98	24.71	2.11	23.63	28.32	84.00	3.41	0.03	0.05	16.02	5.24	381.26	62.09	16.96	5.49	2.33
92	762.80	201.61	204.40	17.48	203.49	320.04	738.74	14.17	6.05	24.53	2.10	23.40	28.32	84.00	3.43	0.03	0.05	16.25	5.18	381.40	62.11	16.96	5.49	2.33

Description of Variables:

CN2	Runoff curve number, antecedent moisture condition 2
COTP	Crop yield for picker cotton (t/ha)
DN	N loss by denitrification (kg/ha)
DRNN	Mineral N loss in subsurface drain flow (kg/ha)
DRT	Drain time, days required for drainage to reduce plant stress (days)
ET	Evapotranspiration (mm)
FNH3	Fertilizer N applied in the form NH₃-N (kg/ha)
FNO3	Fertilizer N applied in the form NO₃-N (kg/ha)
GRSG	Crop yield for grain sorghum (t/ha)
IRGA	Irrigation water applied (mm)
MUSS	Soil loss from water erosion using a modified MUSLE option for small watersheds
PRCP	Precipitation (mm)
PRK	Percolation below the root zone (mm)
PRKN	Mineral N loss in percolate (kg/ha)
PRKP	Percolation of P below the root zone (kg/ha)
Q	Runoff (mm)
QDRN	Subsurface drain flow (mm)
SSF	Lateral subsurface flow (mm)
SSFN	Mineral N loss in subsurface flow (kg/ha)
UNO3	N uptake by the crop (kg/ha)
UPP	P uptake by the crop (kg/ha)
WNO3	Initial nitrate concentration in the soil (ppm)
YAP	Soluble P loss in runoff (kg/ha)
YNO3	NO₃ loss in surface runoff (kg/ha)
YON	Organic N loss with sediment (kg/ha)
YP	P loss with sediment (kg/ha)
YW	Soil loss from wind erosion (t/ha)

EPIC Variable CN2, Runoff Curve Number - Antecedent Moisture Condition 2
% Change

CN2	PRCP	Q	SSF	PRK	QDRN	IRGA	ET	YON	YNO3	SSFN	PRKN	DRNN	FNO3	FNH3	YP	YAP	PRKP	MUSS	YW	UNO3	UPP	DN	GRSG	COTP
-9%	0.0%	-9.4%	3.3%	3.3%	3.3%	0.0%	0.5%	-8.1%	-9.4%	3.3%	3.3%	3.9%	0.0%	0.0%	-8.3%	-9.4%	3.4%	-12.7%	-0.6%	-0.4%	-0.4%	-0.3%	0.0%	-0.9%
-7%	0.0%	-11.1%	4.2%	4.2%	4.2%	0.0%	0.6%	-8.4%	-11.1%	4.2%	4.2%	5.0%	0.0%	0.0%	-8.7%	-11.1%	4.3%	-12.4%	-0.5%	-0.3%	-0.3%	-0.6%	0.0%	-0.7%
-6%	0.0%	-9.5%	3.4%	3.4%	3.4%	0.0%	0.6%	-7.2%	-9.5%	3.4%	3.4%	4.1%	0.0%	0.0%	-7.4%	-9.5%	3.6%	-10.6%	-0.3%	-0.3%	-0.3%	-0.5%	0.0%	-0.6%
-5%	0.0%	-7.8%	2.6%	2.6%	2.6%	0.0%	0.5%	-6.0%	-7.8%	2.6%	2.6%	3.2%	0.0%	0.0%	-6.2%	-7.8%	2.8%	-8.8%	-0.2%	-0.2%	-0.2%	-0.4%	0.0%	-0.5%
-4%	0.0%	-6.1%	1.9%	1.9%	1.9%	0.0%	0.4%	-4.9%	-6.1%	1.9%	1.9%	2.3%	0.0%	0.0%	-5.0%	-6.1%	2.1%	-6.9%	-0.3%	-0.2%	-0.2%	-0.3%	0.0%	-0.4%
-2%	0.0%	-3.4%	1.1%	1.1%	1.1%	0.0%	0.2%	-2.4%	-3.4%	1.1%	1.1%	1.3%	0.0%	0.0%	-2.4%	-3.4%	1.1%	-3.7%	-0.1%	-0.1%	-0.1%	-0.1%	0.0%	-0.3%
-1%	0.0%	-1.6%	0.5%	0.5%	0.5%	0.0%	0.1%	-1.1%	-1.6%	0.5%	0.5%	0.6%	0.0%	0.0%	-1.1%	-1.6%	0.6%	-1.7%	0.1%	-0.1%	-0.1%	-0.1%	0.0%	-0.1%
0%	0.0%	0.0%	0.0%	0.0%	0.0%	0.0%	0.0%	0.0%	0.0%	0.0%	0.0%	0.0%	0.0%	0.0%	0.0%	0.0%	0.0%	0.0%	0.0%	0.0%	0.0%	0.0%	0.0%	0.0%
1%	0.0%	1.5%	-0.6%	-0.5%	-0.5%	0.0%	-0.1%	1.1%	1.5%	-0.6%	-0.5%	-0.6%	0.0%	0.0%	1.1%	1.5%	-0.6%	1.6%	0.2%	0.1%	0.1%	0.0%	0.0%	0.1%
2%	0.0%	2.8%	-1.0%	-1.0%	-1.0%	0.0%	-0.2%	1.5%	2.8%	-1.0%	-1.0%	-1.2%	0.0%	0.0%	1.6%	2.8%	-0.9%	3.0%	-1.2%	0.0%	0.0%	0.1%	0.0%	0.0%
4%	0.0%	4.1%	-1.5%	-1.5%	-1.5%	0.0%	-0.3%	1.9%	4.1%	-1.5%	-1.5%	-1.6%	0.0%	0.0%	2.0%	4.1%	-1.5%	4.3%	-2.6%	-0.1%	-0.1%	0.1%	0.0%	-0.2%
5%	0.0%	5.4%	-1.8%	-1.8%	-1.8%	0.0%	-0.5%	2.5%	5.4%	-1.8%	-1.8%	-2.0%	0.0%	0.0%	2.6%	5.4%	-1.9%	5.6%	-3.6%	-0.2%	-0.1%	0.1%	0.0%	-0.3%
6%	0.0%	28.3%	-9.6%	-9.6%	-9.6%	0.0%	-1.5%	24.3%	156.7%	-9.6%	-9.6%	-14.6%	0.0%	0.0%	24.7%	21.2%	-9.8%	31.5%	11.6%	2.0%	1.7%	-0.4%	0.0%	3.9%
7%	0.0%	30.1%	-10.4%	-10.4%	-10.3%	0.0%	-1.6%	26.1%	160.3%	-10.4%	-10.4%	-15.5%	0.0%	0.0%	26.5%	22.9%	-10.5%	33.7%	13.3%	2.0%	1.7%	-0.4%	0.0%	3.9%
9%	0.0%	31.9%	-11.1%	-11.1%	-11.1%	0.0%	-1.7%	27.5%	163.8%	-11.1%	-11.1%	-16.1%	0.0%	0.0%	27.9%	24.6%	-11.3%	35.8%	13.9%	2.0%	1.7%	-1.5%	0.0%	4.0%
10%	0.0%	33.7%	-11.7%	-11.7%	-11.7%	0.0%	-1.8%	29.9%	167.4%	-11.7%	-11.7%	-16.8%	0.0%	0.0%	30.4%	26.3%	-11.9%	38.0%	18.0%	2.0%	1.8%	-1.6%	0.0%	4.1%
11%	0.0%	35.5%	-12.3%	-12.3%	-12.3%	0.0%	-1.9%	28.1%	171.0%	-12.3%	-12.3%	-17.6%	0.0%	0.0%	28.5%	28.0%	-12.6%	40.1%	7.3%	2.1%	1.8%	-1.5%	0.0%	4.1%
12%	0.0%	37.3%	-13.0%	-13.0%	-13.0%	0.0%	-2.0%	28.2%	174.6%	-13.0%	-13.0%	-18.4%	0.0%	0.0%	28.7%	29.7%	-13.2%	42.3%	3.2%	2.1%	1.8%	-1.6%	0.0%	4.2%
14%	0.0%	39.0%	-13.6%	-13.6%	-13.6%	0.0%	-2.1%	29.0%	316.9%	-13.6%	-13.6%	-19.2%	0.0%	0.0%	29.5%	31.3%	-13.9%	44.4%	2.0%	2.2%	1.9%	-1.7%	0.0%	4.3%

Representative Crop Management Schedules

Furrow Irrigated Cotton - Baseline BMP, Current Conditions

D=Dry year N=Normal year W=Wet year		Picker Cotton EPIC Crop # in USDACROP DAT... S, PHU 2900		EPIC Tillage #	Irrigation Volume		EPIC Pesticide #	Pesticide Trade Name (Common Name)	Pesticide Appl. Rates (Active Ingredient)		N Application Rates		P Application Rates (as P) P₂O₅ = 2.27P	
	Mo	Day	Operation		mm	in.			kg/ha	lb/ac	kg/ha	lb/ac	kg/ha	lb/ac
D,N,W	1	10	Apply preemergent herbicide, soil incorporated (top 2")	6			255	Treflan (Trifluralin)	1.68	1.50				
D,N,W	1	20	Apply fertilizer (dry, surface applied)	10							67.25	60	29.59	26.4
D	2	1	Border Ditching, forming block ends in preparation for furrow irrigation	80										
D	2	2	Furrow Irrigation	72	152	6								
D,N,W	2	10	Cultivate	19										
D,N,W	2	20	Plant picker cotton with row planter, Potential Heat Units for crop = 2900	2										
D,N,W	3	15	Cultivate	19										
D,N,W	3	15	Border Ditching, forming block ends in preparation for furrow irrigation	80										
D,N,W	3	16	Furrow Irrigation	72	152	6								
N,W	4	5	Apply insecticide to control overwintering/inseason cotton boll weevils	11			122	Guthion (Azinphos-methyl)	0.28	0.25				
D,N	4	14	Border Ditching, forming block ends in preparation for furrow irrigation	80										
D,N	4	15	Furrow Irrigation	72	152	6								
D,N,W	4	20	Apply insecticide to control overwintering/inseason cotton boll weevils	11			122	Guthion (Azinphos-methyl)	0.28	0.25				
D,N,W	5	14	Cultivate	19										
D,N	5	14	Border Ditching, forming block ends in preparation for furrow irrigation	80										
D,N	5	15	Furrow Irrigation	72	152	6								
D,N,W	5	20	Apply insecticide to control inseason cotton boll weevils	11			122	Guthion (Azinphos-methyl)	0.28	0.25				
D,N,W	6	5	Apply dual purpose insecticide to control weevils	11			122	Guthion (Azinphos-methyl)	0.28	0.25				
D,N,W	6	14	Border Ditching, forming block ends in preparation for furrow irrigation	80										
D,N,W	6	15	Furrow Irrigation	72	152	6								
D,N,W	6	15	Apply dual purpose insecticide to control weevils	11			122	Guthion (Azinphos-methyl)	0.28	0.25				
D,N,W	6	20	Apply dual purpose (pyrethroid) insecticide to control both weevils and worms	11			130	Karate (Cyhalothrin)	0.03	0.03				
D,N,W	7	5	Apply dual purpose (pyrethroid) insecticide to control both weevils and worms	11			130	Karate (Cyhalothrin)	0.03	0.03				
D	7	14	Border Ditching, forming block ends in preparation for furrow irrigation	80										
D	7	15	Furrow Irrigation	72	152	6								
D	7	15	Apply dual purpose insecticide to control weevils	11			122	Guthion (Azinphos-methyl)	0.28	0.25				
W	7	20	Apply dual purpose (pyrethroid) insecticide to control both weevils and worms	11			130	Karate (Cyhalothrin)	0.03	0.03				
D,N,W	8	5	Apply defoliant (29% use Dropp/ 71% use DEF)	11			96	Dropp (Thidiazuron)	0.17	0.15				
D,N,W	8	5	Apply defoliant (29% use Dropp/ 71% use DEF)	11			83	DEF (Tribufos or Phosphorotrithioate)	1.23	1.10				
D,N,W	8	20	Harvest - picker cotton	51										
D,N,W	8	20	Kill cotton crop	41										
D,N,W	8	25	Shredding	57										
D,N,W	9	1	Plowing	24										
D,N,W	9	5	Sweep-Chisel	32										
D,N,W	9	10	Discing-offset	33										
D,N,W	9	15	Discing-offset	33										
D,N,W	9	20	Discing-offset	33										
D,N,W	12	15	Bedding	15										

Changes in pesticide applications or irrigations due to rainfall conditions
Under normal rainfall conditions, denoted (N), 8 insecticide applications are generally sufficient to control cotton pests.
    Four irrigations of 6" each supply 24" of irrigation water at 2/3 efficiency = 16" of water supplied to crop
    One preplant herbicide application for weed control
During wet years, denoted with a (W), two additional applications, (1) of Guthion and (1) of Karate, may be required
    Two irrigations of 6" each supply 12" of irrigation water at 2/3 efficiency = 8" of water supplied to crop
During dry years (D), one less Guthion application may be sufficient
    Six irrigations of 6" each supply 36" of irrigation water at 2/3 efficiency = 24" of water supplied to crop

This represents IPM (Full Implementation)
For mid-level IPM, add 1 Guthion and 1 Karate application (6/1 and 6/10)
For low-level IPM, add 2 more Guthion applications (7/1 and 7/10)
and 1 Orthene application for aphids at 0.4 lb/acre (5/1)

Dryland Cotton - Baseline BMP, Current Conditions

D=Dry year N=Normal year W=Wet year			Picker Cotton - EPIC Crop # in USDACROP.DAT = 5, PHU=2900	EPIC Tillage #	Irrigation Volume		EPIC Pesticide #	Pesticide Trade Name (Common Name)	Pesticide Application Rates (Active Ingredient)		N Application Rates		P Application Rates (as P) P₂O₅ = 2.27P	
	Month	Day	Operation		mm	in.			kg/ha	lb/ac	kg/ha	lb/ac	kg/ha	lb/ac
D,N,W	1	10	Apply fertilizer (dry, surface applied)	10							33.6	30	14.8	13
D,N,W	2	10	Cultivate	19										
D,N,W	2	15	Plant picker cotton with row planter, Potential Heat Units for crop = 2900	2										
D,N,W	2	15	Apply preemergent herbicide, soil incorporated (top 2")	6			255	Treflan (Trifluralin)	1.68	1.50				
D,N,W	3	15	Cultivate	19										
D,N,W	4	20	Apply insecticide to control cotton fleahoppers	11			43	Bidrin (Dicrotophos)	0.22	0.20				
D,N,W	5	20	Cultivate	19										
N,W	6	1	Apply insecticide to control overwintering/inseason cotton boll weevils	11			122	Guthion (Azinphos methyl)	0.28	0.25				
D,N,W	6	20	Apply dual purpose (pyrethroid) insecticide to control both weevils and worms	11			122	Guthion (Azinphos-methyl)	0.28	0.25				
D,N,W	7	5	Apply dual purpose (pyrethroid) insecticide to control both weevils and worms	11			130	Karate (Cyhalothrin)	0.03	0.03				
D,N,W	8	5	Apply defoliant (29% use Dropp/ 71% use DEF)	11			96	Dropp (Thidiazuron)	0.17	0.15				
D,N,W	8	5	Apply defoliant (29% use Dropp/ 71% use DEF)	11			83	DEF (Tribufos or Phosphorotrithioate)	1.23	1.10				
D,N,W	8	20	Harvest - picker cotton	51										
D,N,W	8	20	Kill cotton crop	41										
D,N,W	8	25	Shredding	57										
D,N,W	9	1	Plowing	24										
D,N,W	9	5	Sweep-Chisel	32										
D,N,W	9	10	Discing-offset	33										
D,N,W	9	15	Discing-offset	33										
D,N,W	9	20	Discing-offset	33										
D,N,W	12	15	Bedding	15										

Changes in pesticide applications due to rainfall conditions

Under normal rainfall conditions, denoted with an (N), four insecticide applications are generally sufficient to control cotton pests

   One preemergent herbicide application for weed control at planting

During dry years, denoted with a (D), one less Guthion application may be sufficient

Dryland Cotton - Baseline BMP, Current Conditions

D=Dry year N=Normal year W=Wet year	Picker Cotton - EPIC Crop # in USDACROP.DAT = 5, PHU=2900			EPIC Tillage #	Irrigation Volume		EPIC Pesticide #	Pesticide Trade Name (Common Name)	Pesticide Application Rates (Active Ingredient)		N Application Rates		P Application Rates (as P) $P_2O_5 = 2.27P$	
	Month	Day	Operation		mm	in.			kg/ha	lb/ac	kg/ha	lb/ac	kg/ha	lb/ac
D,N,W	1	10	Apply fertilizer (dry, surface applied)	10							33.6	30	14.8	13
D,N,W	2	10	Cultivate	19										
D,N,W	2	15	Plant picker cotton with row planter. Potential Heat Units for crop = 2900	2										
D,N,W	2	15	Apply preemergent herbicide, soil incorporated (top 2")	6			255	Treflan (Trifluralin)	1.68	1.50				
D,N,W	3	15	Cultivate	19										
D,N,W	4	20	Apply insecticide to control cotton fleahoppers	11			43	Bidrin (Dicrotophos)	0.22	0.20				
D,N,W	5	20	Cultivate	19										
N,W	6	1	Apply insecticide to control overwintering/inseason cotton boll weevils	11			122	Guthion (Azinphos-methyl)	0.28	0.25				
D,N,W	6	20	Apply dual purpose (pyrethroid) insecticide to control both weevils and worms	11			122	Guthion (Azinphos-methyl)	0.28	0.25				
D,N,W	7	5	Apply dual purpose (pyrethroid) insecticide to control both weevils and worms	11			130	Karate (Cyhalothrin)	0.03	0.03				
D,N,W	8	5	Apply defoliant (29% use Dropp/ 71% use DEF)	11			96	Dropp (Thidiazuron)	0.17	0.15				
D,N,W	8	5	Apply defoliant (29% use Dropp/ 71% use DEF)	11			83	DEF (Tribufos or Phosphorotrithioate)	1.23	1.10				
D,N,W	8	20	Harvest - picker cotton	51										
D,N,W	8	20	Kill cotton crop	41										
D,N,W	8	25	Shredding	57										
D,N,W	9	1	Plowing	24										
D,N,W	9	5	Sweep-Chisel	32										
D,N,W	9	10	Discing-offset	33										
D,N,W	9	15	Discing-offset	33										
D,N,W	9	20	Discing-offset	33										
D,N,W	12	15	Bedding	15										

Changes in pesticide applications due to rainfall conditions
Under normal rainfall conditions, denoted with an (N), four insecticide applications are generally sufficient to control cotton pests
   One preemergent herbicide application for weed control at planting
During dry years, denoted with a (D), one less Guthion application may be sufficient

Furrow Irrigated Grain Sorghum - Baseline BMP, Current Conditions

D=Dry year N=Normal year W=Wet year			Grain Sorghum - EPIC Crop # in USDACROP.DAT = 3, PHU=2000	EPIC Tillage #	Irrigation Volume		EPIC Pesticide #	Pesticide Trade Name (Common Name)	Pesticide Application Rates (Active Ingredient)		N Application Rates		P Application Rates (as P) P₂O₅ = 2.27P	
	Month	Day	Operation		mm	in.			kg/ha	lb/ac	kg/ha	lb/ac	kg/ha	lb/ac
D,N,W	1	10	Apply fertilizer (dry, surface applied)	10							135	120	29.6	26
D,N,W	1	15	Cultivate	19										
D,N,W	2	10	Border Ditching, forming block ends in preparation for furrow irrigation	80										
D,N,W	2	10	Cultivate	19										
D,N,W	2	15	Plant grain sorghum with row planter, Potential Heat Units for crop = 2000	2										
D,N,W	3	15	Apply post emergent herbicide, incorporated (culti-spray)	6			255	Treflan (Trifluralin)	0.78	0.70				
D,N,W	3	15	Cultivate	19										
D	3	15	Border Ditching, forming block ends in preparation for furrow irrigation	80										
D	3	16	Furrow Irrigation	72	152	6								
D,N,W	4	14	Cultivate	19										
D,N	4	14	Border Ditching, forming block ends in preparation for furrow irrigation	80										
D,N	4	15	Furrow Irrigation	72	152	6								
D,N	5	14	Border Ditching, forming block ends in preparation for furrow irrigation	80										
D,N	5	15	Furrow Irrigation	72	152	6								
D,N,W	7	20	Harvest - grain sorghum	51										
D,N,W	9	10	Kill sorghum crop	41										
D,N,W	9	10	Shredding	57										
D,N,W	9	15	Sweep-chisel	32										
D,N,W	9	20	Discing-offset	33										
D,N,W	10	15	Discing-offset	33										
D,N,W	11	15	Discing-offset	33										
D,N,W	12	15	Bedding	15										

Changes in pesticide applications or irrigations due to rainfall conditions
Under normal rainfall conditions,
   Grain sorghum crops in the area typically do not receive insecticide applications
   One preemergent herbicide application at planting
   Two irrigations (Denoted with N) of 6" each supply 12" of irrigation water at 2/3 efficiency = 8" of water supplied to crop
During wet years,
   Irrigation not required
During dry years,
   Three irrigations (Denoted with D) of 6" each supply 18" of irrigation water at 2/3 efficiency = 12" of water supplied to crop

Dryland Grain Sorghum - Baseline BMP, Current Conditions

D=Dry year N=Normal year W=Wet year			Grain Sorghum - EPIC Crop # in USDACROP.DAT = 3, PHU=2000	EPIC Tillage #	Irrigation Volume		EPIC Pesticide #	Pesticide Trade Name (Common Name)	Pesticide Application Rates (Active Ingredient)		N Application Rates		P Application Rates (as P) P₂O₅ = 2.27P	
	Month	Day	Operation		mm	in.			kg/ha	lb/ac	kg/ha	lb/ac	kg/ha	lb/ac
D,N,W	1	15	Apply fertilizer (dry, surface applied)	10							33.63	30		
D,N,W	2	10	Cultivate	19										
D,N,W	2	15	Plant grain sorghum with row planter. Potential Heat Units for crop = 2000	2										
D,N,W	3	15	Cultivate	19										
D,N,W	5	15	Cultivate	19										
D,N,W	7	20	Harvest - grain sorghum	51										
D,N,W	9	10	Kill sorghum crop	41										
D,N,W	9	10	Shredding	57										
D,N,W	9	15	Plowing	24										
D,N,W	9	16	Sweep-chisel	32										
D,N,W	9	20	Discing-offset	33										
D,N,W	10	15	Discing-offset	33										
D,N,W	11	15	Bedding	15										

Changes in management due to rainfall conditions
Under normal rainfall conditions.
   Grain sorghum crops in the area typically do not receive insecticide applications
   No herbicide or insecticide applications under normal conditions

Furrow Irrigated Corn - Baseline BMP, Current Conditions

D=Dry year N=Normal year W=Wet year	Corn - EPIC Crop # in USDACROP.DAT = 2, PHU=1950			EPIC Tillage #	Irrigation Volume		EPIC Pesticide #	Pesticide Trade Name (Common Name)	Pesticide Application Rates (Active Ingredient)		N Application Rates		P Application Rates (as P) P₂O₅ = 2.27P	
	Month	Day	Operation		mm	in.			kg/ha	lb/ac	kg/ha	lb/ac	kg/ha	lb/ac
D,N,W	1	15	Apply fertilizer (dry, surface applied)	10							168	150	24.7	22
D,N,W	2	10	Cultivate	19										
D,N,W	2	10	Border Ditching, forming block ends for furrow irrigation	80										
D,N,W	2	15	Plant corn with row planter, Potential Heat Units for crop = 1950	2										
D,N,W	2	15	Apply preemergent herbicide, surface applied	6			255	Prowl (Pendimethalin)	0.78	0.70				
D,N,W	3	10	Cultivate	19										
D	3	15	Border Ditching, forming block ends for furrow irrigation	80										
D	3	15	Furrow Irrigation	72	152	6								
D,N,W	4	10	Cultivate	19										
D,N	4	15	Border Ditching, forming block ends for furrow irrigation	80										
D,N	4	15	Furrow Irrigation	72	152	6								
D,N	5	15	Border Ditching, forming block ends for furrow irrigation	80										
D,N	5	15	Furrow Irrigation	72	152	6								
D,N,W	6	20	Harvest - Corn	51										
D,N,W	9	10	Kill corn crop	41										
D,N,W	9	10	Shredding	57										
D,N,W	9	15	Sweep-chisel	32										
D,N,W	9	20	Discing-offset	33										
D,N,W	10	15	Discing-offset	33										
D,N,W	11	15	Discing-offset	33										
D,N,W	12	15	Bedding	15										

Changes in irrigations due to rainfall conditions
Under normal rainfall conditions (denoted with N).
  Two irrigations of 6" each supply 12" of irrigation water at 2/3 efficiency = 8" of water supplied to crop
During wet years (denoted with W).
  Irrigation not required
During dry years (denoted with D).
  Three irrigations of 6" each supply 18" of irrigation water at 2/3 efficiency = 12" of water supplied to crop

Pesticide Applications
  One preemergent herbicide application at planting.

Dryland Corn - Baseline BMP, Current Conditions

D=Dry year N=Normal year W=Wet year	Corn - EPIC Crop # in USDACROP.DAT = 2, PHU=1950			EPIC Tillage #	Irrigation Volume		EPIC Pesticide #	Pesticide Trade Name (Common Name)	Pesticide Application Rates (Active Ingredient)		N Application Rates		P Application Rates (as P) P₂O₅ = 2.27P	
	Month	*Day*	*Operation*		*mm*	*in.*			*kg/ha*	*lb/ac*	*kg/ha*	*lb/ac*	*kg/ha*	*lb/ac*
D,N,W	1	15	Apply fertilizer (dry, surface applied)	10							84.07	75		
D,N,W	2	10	Cultivate	19										
D,N,W	2	15	Plant corn with row planter. Potential Heat Units for crop = 1950	2										
D,N,W	3	10	Cultivate	19										
D,N,W	4	10	Cultivate	19										
D,N,W	6	20	Harvest - Corn	51										
D,N,W	9	10	Kill corn crop	41										
D,N,W	9	10	Shredding	57										
D,N,W	9	15	Plowing	24										
D,N,W	9	16	Sweep-chisel	32										
D,N,W	9	20	Discing-offset	33										
D,N,W	10	15	Discing-offset	33										
D,N,W	11	15	Bedding	15										

Assumed the same management for wet, normal and dry years

Furrow Irrigated Sugarcane (Plant Cane) - Baseline BMP, Current Conditions

D=Dry year N=Normal year W=Wet year	Sugarcane (Plant Cane) - EPIC Crop # in USDACROP.DAT = 77			EPIC Tillage #	Irrigation Volume		EPIC Pesticide #	Pesticide Trade Name (Common Name)	Pesticide Application Rates (Active Ingredient)		N Application Rates		P Application Rates (as P) P₂O₅ = 2.27P	
	Month	Day	Operation		mm	in.			kg/ha	lb/ac	kg/ha	lb/ac	kg/ha	lb/ac
D,N,W	9	1	weed disking or shredding or previous crop	57										
D,N,W	9	3	Plowing or deep subsoil ripping	34										
D,N,W	9	4	Surface disking	33										
D,N,W	9	5	Land planing (laser leveling)	-										
D,N,W	9	13	drawing of plant furrows	15										
D,N,W	9	14	fertilizer application (fertilizer #64)	10							89.6	80		
D,N,W	9	14	fertilizer application (fertilizer #65)	10									49.28	44
D,N,W	9	15	planting/seed covering (4-6 tons/acre)	2										
D,N,W	9	16	herbicide application (pre-emergence)	11			3	Aatrex (Atrazine)	2.24	2.00				
D,N,W	9	16	herbicide application (pre-emergence)	11			194	Prowl (Pendimethalin)	2.31	2.06				
D,N,W	9	17	build borders	80										
D,N,W	9	18	furrow irrigation	72	152.4	6								
D	10	18	furrow irrigation (dry years only)	72	152.4	6								
D,N,W	11	20	knock down borders	77										
D,N,W	11	21	cultivate and reshape cane rows	19										
D,N,W	12	21	cultivate and reshape cane rows	19										
D,N,W	1	25	cultivate interrows	19										
D,N,W	2	10	herbicide application (post-emergence)	11			3	Aatrex (Atrazine)	2.24	2.00				
D,N,W	2	10	herbicide application (post-emergence)	11			194	Prowl (Pendimethalin)	2.31	2.06				
D,N,W	4	13	rebuild borders	80										
D,N,W	4	15	furrow irrigation	72	152.4	6								
D,N,W	5	10	spot spray or aerial application of herbicides	11			32	Banvel (Dicambra Soluble Salt)	0.56	0.50				
D,N,W	5	10	spot spray or aerial application of herbicides	11			204	Roundup (Glyphosate Amine)	2.24	2.00				
D,N,W	5	10	spot spray or aerial application of herbicides	11			109	Evik (Ametryn)	1.792	1.60				
D	5	22	furrow irrigation (dry years only)	72	152.4	6								
D,N	6	15	furrow irrigation	72	152.4	6								
D,N	7	1	furrow irrigation	72	152.4	6								
D,N,W	7	14	knock down and rebuild weedy borders	80										
D,N,W	7	15	furrow irrigation	72	152.4	6								
D,N	8	1	furrow irrigation	72	152.4	6								
D,N,W	8	15	furrow irrigation	72	152.4	6								
D,N	9	1	furrow irrigation	72	152.4	6								
D,N,W	1	3	knock down borders (pre-harvest preparation)	77										
D,N,W	1	4	harrow furrows (pre-harvest preparation)	25										
D,N,W	1	5	burn & harvest	53										

Changes in irrigations due to rainfall conditions
Under normal rainfall conditions (denoted with N),
 Eight irrigations of 6" each supply 42" of irrigation water at 2/3 efficiency = 28" of water supplied to crop
During wet years (denoted with W),
 Four irrigations of 6" each supply 24" of irrigation water at 2/3 efficiency = 16" of water supplied to crop
During dry years (denoted with D),
 Ten irrigations of 6" each supply 60" of irrigation water at 2/3 efficiency = 40" of water supplied to crop

Herbicide Applications (3 applications/year)
Fall pre-emergence applications (9/16) of
 Aatrex (Atrazine) & Prowl (Pendimethalin)
Winter post-emergence applications (2/10)
 of the same two herbicides
Spring spot sprays (5/10) for misses

Furrow Irrigated Sugarcane (Plant Cane) - BMP #1, Nutrient Management

D=Dry year N=Normal year W=Wet year	Sugarcane (Plant Cane) - EPIC Crop # in USDACROP.DAT = 77			EPIC Tillage #	Irrigation Volume		EPIC Pesticide #	Pesticide Trade Name (Common Name)	Pesticide Application Rates (Active Ingredient)		N Application Rates		P Application Rates (as P) P₂O₅ = 2.27P	
	Month	Day	Operation		mm	in.			kg/ha	lb/ac	kg/ha	lb/ac	kg/ha	lb/ac
D,N,W	9	1	weed disking or shredding or previous crop	57										
D,N,W	9	3	Plowing or deep subsoil ripping	34										
D,N,W	9	4	Surface disking	33										
D,N,W	9	5	Land planing (laser leveling)	.										
D,N,W	9	13	drawing of plant furrows	15										
D,N,W	9	14	fertilizer application 11-37-0 (200 lbs/acre) fertilizer #52	10							24.64	22	82.88	74
D,N,W	9	15	planting/seed covering (4-6 tons/acre)	2										
D,N,W	9	16	herbicide application (pre-emergence)	11			3	Aatrex (Atrazine)	2.24	2.00				
D,N,W	9	16	herbicide application (pre-emergence)	11			194	Prowl (Pendimethalin)	2.31	2.06				
D,N,W	9	17	build borders	80										
D,N,W	9	18	furrow irrigation	72	152.4	6								
D	10	18	furrow irrigation (dry years only)	72	152.4	6								
D,N,W	11	20	knock down borders	77										
D,N,W	11	21	cultivate and reshape cane rows	19										
D,N,W	12	21	cultivate and reshape cane rows	19										
D,N,W	1	25	cultivate interrows	19										
D,N,W	2	10	herbicide application (post-emergence)	11			3	Aatrex (Atrazine)	2.24	2.00				
D,N,W	2	10	herbicide application (post-emergence)	11			194	Prowl (Pendimethalin)	2.31	2.06				
D,N,W	4	13	rebuild borders	80										
D,N,W	4	15	furrow irrigation	72	152.4	6								
D,N,W	5	10	spot spray or aerial application of herbicides	11			32	Banvel (Dicamba Soluble Salt)	0.56	0.50				
D,N,W	5	10	spot spray or aerial application of herbicides	11			204	Roundup (Glyphosate Amine)	2.24	2.00				
D,N,W	5	10	spot spray or aerial application of herbicides	11			109	Evik (Ametryn)	1.79	1.60				
D	5	22	furrow irrigation (dry years only)	72	152.4	6								
D,N	6	15	furrow irrigation	72	152.4	6								
D,N	7	1	furrow irrigation	72	152.4	6								
D,N,W	7	14	knock down and rebuild weedy borders	80										
D,N,W	7	15	furrow irrigation	72	152.4	6								
D,N,W	8	1	furrow irrigation	72	152.4	6								
D,N,W	8	15	furrow irrigation	72	152.4	6								
D,N	9	1	furrow irrigation	72	152.4	6								
D,N,W	1	3	knock down borders (pre-harvest preparation)	77										
D,N,W	1	4	harrow turnrows (pre-harvest preparation)	25										
D,N,W	1	5	burn & harvest	53										

Changes in irrigations due to rainfall conditions
Under normal rainfall conditions (denoted with N).
  Eight irrigations of 6" each supply 42" of irrigation water at 2/3 efficiency = 28" of water supplied to crop
During wet years (denoted with W).
  Four irrigations of 6" each supply 24" of irrigation water at 2/3 efficiency = 16" of water supplied to crop
During dry years (denoted with D).
  Ten irrigations of 6" each supply 60" of irrigation water at 2/3 efficiency = 40" of water supplied to crop

Herbicide Applications (3 applications/year)
Fall pre-emergence applications (9/16) of
  Aatrex (Atrazine) & Prowl (Pendimethalin)
Winter post-emergence applications (2/10)
  of the same two herbicides
Spring spot sprays (5/10) for misses

Representative Management for Furrow Irrigated Sugarcane (Ratoon Cane) - Baseline BMP, current conditions

D=Dry year N=Normal year W=Wet year	Sugarcane (Ratoon Cane) - EPIC Crop # in USDACROP.DAT = 77			EPIC Tillage #	Irrigation Volume		EPIC Pesticide #	Pesticide Trade Name (Common Name)	Pesticide Application Rates (Active Ingredient)		N Application Rates		P Application Rates (as P) P₂O₅ = 2.27P	
	Month	Day	Operation		mm	in.			kg/ha	lb/ac	kg/ha	lb/ac	kg/ha	lb/ac
D,N,W	1	13	interrow gang harrow	25										
D,N,W	1	14	subsoil	34										
D,N,W	1	15	fertilize (liquid N-32, incorporated)	13							201.6	180	-	-
D,N,W	1	15	cultivation - reshape	19										
D,N,W	1	20	herbicide application (sprayer)	11			3	Aatrex (Atrazine)	2.24	2.00				
D,N,W	1	20	herbicide application (sprayer)	11			194	Prowl (Pendimethalin)	2.31	2.06				
D,N,W	1	23	border building	80										
D,N,W	1	24	furrow irrigation	72	152	6								
D	3	15	furrow irrigation	72	152	6								
D,N,W	4	12	knock down borders	77										
D,N,W	4	12	cultivate weeds	19										
D,N,W	4	13	herbicide application (sprayer)	11			3	Aatrex (Atrazine)	2.24	2.00				
D,N,W	4	13	herbicide application (sprayer)	11			194	Prowl (Pendimethalin)	2.31	2.06				
D,N,W	4	14	rebuild borders	80										
D,N,W	4	15	furrow irrigation	72	152	6								
D	5	1	furrow irrigation	72	152	6								
D,N,W	5	20	spot spray or aerial application of herbicides	11			32	Banvel (Dicambra Soluble Salt)	0.56	0.50				
D,N,W	5	20	spot spray or aerial application of herbicides	11			204	Roundup (Glyphosate Amine)	2.24	2.00				
D,N,W	5	20	spot spray or aerial application of herbicides	11			109	Evik (Ametryn)	1.792	1.60				
D,N	5	22	furrow irrigation	72	152	6								
D,N,W	6	15	furrow irrigation	72	152	6								
D,N,W	7	1	furrow irrigation	72	152	6								
D,N,W	7	14	rebuild borders	80										
D,N	7	15	furrow irrigation	72	152	6								
D,N	8	1	furrow irrigation	72	152	6								
D,N,W	8	15	furrow irrigation	72	152	6								
D,N,W	12	3	knock down borders (pre-harvest preparation)	77										
D,N,W	12	3	harrow turnrows (pre-harvest preparation)	25										
D,N,W	1	6	burn & harvest	53										

Changes in irrigations due to rainfall conditions
Under normal rainfall conditions (denoted with N).
  Eight irrigations of 6" each supply 42" of irrigation water at 2/3 efficiency = 28" of water supplied to crop
During wet years (denoted with W).
  Four irrigations of 6" each supply 24" of irrigation water at 2/3 efficiency = 16" of water supplied to crop
During dry years (denoted with D).
  Ten irrigations of 6" each supply 60" of irrigation water at 2/3 efficiency = 40" of water supplied to crop

Three herbicide applications (1/20, 4/13, and 5/20)

Furrow Irrigated Sugarcane (Ratoon Cane) - BMP #1, Nutrient Management

D=Dry year N=Normal year W=Wet year	Month	Day	Sugarcane (Ratoon Cane) - EPIC Crop # in USDACROP.DAT = 77 — Operation	EPIC Tillage #	Irrigation Volume mm	in.	EPIC Pesticide #	Pesticide Trade Name (Common Name)	Pesticide Application Rates (Active Ingredient) kg/ha	lb/ac	N Application Rates kg/ha	lb/ac	P Application Rates (as P) P₂O₅ = 2.27P kg/ha	lb/ac
D,N,W	1	13	interrow gang harrow	25										
D,N,W	1	14	subsoil	34										
D,N,W	1	15	fertilize (liquid N-32, incorporated)	13							**	**	-	-
D,N,W	1	15	cultivation - reshape	19										
D,N,W	1	20	herbicide application (sprayer)	11			3	Aatrex (Atrazine)	2.24	2.00				
D,N,W	1	20	herbicide application (sprayer)	11			194	Prowl (Pendimethalin)	2.31	2.06				
D,N,W	1	23	border building	80										
D,N,W	1	24	furrow irrigation	72	152.4	6								
D	3	15	furrow irrigation	72	152.4	6								
D,N,W	4	12	knock down borders	77										
D,N,W	4	12	cultivate weeds	19										
D,N,W	4	13	herbicide application (sprayer)	11			3	Aatrex (Atrazine)	2.24	2.00				
D,N,W	4	13	herbicide application (sprayer)	11			194	Prowl (Pendimethalin)	2.31	2.06				
D,N,W	4	14	rebuild borders	80										
D,N,W	4	15	furrow irrigation	72	152.4	6								
D	5	1	furrow irrigation	72	152.4	6								
D,N,W	5	20	spot spray or aerial application of herbicides	11			32	Banvel (Dicambra Soluble Salt)	0.56	0.50				
D,N,W	5	20	spot spray or aerial application of herbicides	11			204	Roundup (Glyphosate Amine)	2.24	2.00				
D,N,W	5	20	spot spray or aerial application of herbicides	11			109	Evik (Ametryn)	1.792	1.60				
D,N	5	22	furrow irrigation	72	152.4	6								
D,N	6	15	furrow irrigation	72	152.4	6								
D,N,W	7	1	furrow irrigation	72	152.4	6								
D,N,W	7	14	rebuild borders	80										
D,N	7	15	furrow irrigation	72	152.4	6								
D,N	8	1	furrow irrigation	72	152.4	6								
D,N	8	15	furrow irrigation	72	152.4	6								
D,N,W	12	3	knock down borders (pre-harvest preparation)	77										
D,N,W	12	3	harrow turnrows (pre-harvest preparation)	25										
D,N,W	1	6	burn & harvest	53										

Changes in irrigations due to rainfall conditions

Under normal rainfall conditions (denoted with N),
  Eight irrigations of 6" each supply 42" of irrigation water at 2/3 efficiency = 28" of water supplied to crop
During wet years (denoted with W),
  Four irrigations of 6" each supply 24" of irrigation water at 2/3 efficiency = 16" of water supplied to crop
During dry years (denoted with D),
  Ten irrigations of 6" each supply 60" of irrigation water at 2/3 efficiency = 40" of water supplied to crop

Three herbicide applications (1/20, 4/13, and 5/20)

** Fertilizer application rate depends on ratoon cycle
1st Year Ratoon Cane
100 lbs/ac N (112.09 kg/ha)
2nd Year Ratoon Cane
140 lbs/ac N (156.93 kg/ha)
3rd - 5th Year Ratoon Cane
150 lbs/ac N (168.14 kg/ha)

Flood Irrigated Citrus (Level Border Irrigation) - Baseline BMP, Current Conditions

D=Dry year N=Normal year W=Wet year	Month	Day	Irrigated Citrus - EPIC Crop # in USDACROP DAT = 83 / Non-Temik Program. 100% trunk-to-trunk herbicide program — Operation	EPIC Tillage #	Irrigation Volume (mm)	Irrigation Volume (in.)	EPIC Pesticide #	Pesticide Trade Name (Common Name)	Pesticide Application Rates (Active Ingredient) kg/ha	lb/ac	N Application Rates kg/ha	lb/ac	P Application Rates (as P) P_2O_5 = 2.27P kg/ha	lb/ac
D,N,W	11	15	Flood Irrigation	72	127	5								
D,N,W	2	10	Border Ditching, forming border in preparation for flood irrigation	82										
D,N,W	2	15	Fertilizer application (Ammonium Sulfate, 21-0-0, Fert #68)	10							•	•		
D	2	20	Flood Irrigation	72	127	5								
D,N,W	3	15	Apply selective herbicide (preemergent)	11			192	Princep (Simazine)	3.53	3.15				
D,N,W	3	15	Apply selective herbicide (preemergent)	11			126	Hyvar X (bromacil)	3.14	2.80				
D,N,W	3	15	Apply contact herbicide	11			204	Roundup (Glyphosate isopropyl amine salt)	1.79	1.60				
D,N	3	20	Flood Irrigation	72	127	5								
D,N,W	4	15	Apply miticide, sprayer	11			262	Vendex (Fenbutatin oxide)	1.12	1.00				
D,N,W	4	15	Apply fungicide, sprayer	11			272	Kocide (Copper hydroxide)	4.31	3.85				
D,N,W	4	20	Flood Irrigation	72	127	5								
D,N,W	6	20	Apply contact herbicide	11			204	Roundup (Glyphosate isopropyl amine salt)	0.28	0.25				
D,N,W	6	20	Apply miticide, sprayer	11			267	Vydate (Oxamyl)	0.21	0.19				
D,N,W	6	20	Apply citrus spray oil	11			265	Petroleum Spray Oil	4.48	4.00				
D,N,W	6	20	Apply fungicide, sprayer	11			272	Kocide (Copper hydroxide)	4.31	3.85				
D,N,W	6	25	Flood Irrigation	72	127	5								
D,N,W	7	20	Flood Irrigation	72	127	5								
D,N,W	8	15	Apply selective herbicide (preemergent)	11			192	Princep (Simazine)	3.53	3.15				
D,N,W	8	15	Apply selective herbicide (preemergent)	11			126	Hyvar X (bromacil)	3.14	2.80				
D,N,W	8	15	Apply contact herbicide	11			204	Roundup (Glyphosate isopropyl amine salt)	1.79	1.60				
D,N,W	8	15	Apply scalicide	11			145	Lorsban (Chlorpyrifos)	2.24	2.00				
D,N,W	8	15	Apply miticide, sprayer	11			133	Kelthane (Dicofol)	2.24	2.00				
D,N,W	8	15	Apply fungicide, sprayer	11			39	Benlate (Benomyl)	1.79	1.60				
D,N,W	10	5	Harvest - Ring Pick	50										

Changes in pesticide applications or irrigations due to rainfall conditions

Under normal rainfall conditions, five irrigations (Denoted with N) of 5" each supply 25" of irrigation water at 95% efficiency = 24" of water supplied to crop
During wet years, four irrigations (Denoted with W) of 5" each supply 20" of irrigation water at 95% efficiency = 19" of water supplied to crop
During dry years, six irrigations (Denoted with D) of 5" each supply 30" of irrigation water at 95% efficiency = 29" of water supplied to crop
Herbicide Applications (3 Applications/year)
Spring application (3/15) of 2 selective herbicides and a contact post-emergent herbicide
Treat again in early summer (6/20) and again in late summer (8/15)
Scalicide/Miticide/Fungicide Applications (3 applications)
Spring application (4/15) of miticide (Vendex) and fungicide (Kocide 101 for control of melanose)
Summer (6/20) application of miticide (Vydate), spray oil and fungicide (Kocide)
Late Summer (8/15) application of miticide (Kelthane), scalicide (Lorsban) and fungicide (Benlate)

*Fertilizer Application Rates depend on tree age

Tree Age	Fertilizer Application Rates — One Appl kg/ha	Split Appl. (kg/ha) 2/3	1/3	Nitrogen Rates lb/ha	kg/ha
1 yr	186.7	124.4	62.2	35	39.2
2 yr	266.7	177.8	88.9	50	56.0
3 yr	400.0	266.7	133.3	75	84.0
4 yr	533.3	355.6	177.8	100	112.0
5 yr	560.0	373.3	186.7	105	117.6
6 yr	586.7	391.1	195.6	110	123.2
7 yr	613.3	408.9	204.4	115	128.8
8 yr	666.7	444.4	222.2	125	140.0
9 yr	746.7	497.8	248.9	140	156.8
10+ yr	800.0	533.3	266.7	150	168.0

Flood Irrigated Citrus (Level Border Irrigation) - Baseline BMP, Current Conditions

D=Dry year N=Normal year W=Wet year		Irrigated Citrus - EPIC Crop # in USDACROP.DAT = 83 Temik Program, 100% trunk-to-trunk herbicide program		EPIC Tillage #	Irrigation Volume		EPIC Pesticide #	Pesticide Trade Name (Common Name)	Pesticide Application Rates (Active Ingredient)		N Application Rates		P Application Rates (as P) P₂O₅ = 2.27P	
	Month	Day	Operation		#in	in.			kg/ha	lb/ac	kg/ha	lb/ac	kg/ha	lb/ac
D,N,W	11	15	Flood Irrigation	72	127	5								
D,N,W	2	10	Border Ditching, forming border in preparation for flood irrigation	82										
D,N,W	2	15	Fertilizer application (Ammonium Sulfate, 21-0-0, Fert.#68)	10							*	*		
D	2	20	Flood Irrigation	72	127	5								
D,N,W	3	15	Apply selective herbicide (preemergent)	11			192	Princep (Simazine)	3.53	3.15				
D,N,W	3	15	Apply selective herbicide (preemergent)	11			126	Hivar X (Bromacil)	3.14	2.80				
D,N,W	3	15	Apply contact herbicide	11			204	Roundup (Glyphosate isopropyl amine salt)	1.79	1.60				
D,N	3	20	Flood Irrigation	72	127	5								
D,N,W	4	1	Apply pesticide, sprayer	11			236	Temik (Aldicarb)	5.54	4.95				
D,N,W	4	15	Flood Irrigation	72	127	5								
D,N,W	6	15	Apply contact herbicide	11			204	Roundup (Glyphosate isopropyl amine salt)	0.28	0.25				
D,N,W	6	20	Flood Irrigation	72	127	5								
D,N,W	7	20	Flood Irrigation	72	127	5								
D,N,W	8	15	Apply scalicide	11			145	Lorsban (Chlorpyrifos)	2.24	2.00				
D,N,W	8	15	Apply fungicide	11			39	Benlate (Benomyl)	1.79	1.60				
D,N,W	8	15	Apply miticide, sprayer	11			133	Kelthane (Dicofol)	2.24	2.00				
D,N,W	8	15	Apply selective herbicide (preemergent)	11			192	Princep (Simazine)	3.53	3.15				
D,N,W	8	15	Apply selective herbicide (preemergent)	11			126	Hyvar X (bromacil)	3.14	2.80				
D,N,W	8	15	Apply contact herbicide	11			204	Roundup (Glyphosate isopropyl amine salt)	1.79	1.60				
D,N,W	10	5	Harvest - Ring Pick	50										

Changes in pesticide applications or irrigations due to rainfall conditions
Under normal rainfall conditions, five irrigations (Denoted with N) of 5" each supply 25" of irrigation water at 95% efficiency = 24" of water supplied to crop
During wet years, four irrigations (Denoted with W) of 5" each supply 20" of irrigation water at 95% efficiency = 19" of water supplied to crop
During dry years, six irrigations (Denoted with D) of 5" each supply 30" of irrigation water at 95% efficiency = 29" of water supplied to crop
Herbicide Applications (3 Applications/year)
Spring application (3/15) of 2 selective herbicides and a contact post-emergent herbicide
Treat again in early summer (6/15) and again in late summer (8/15)
Scalicide/Miticide/Fungicide Applications under Temik Program (2 applications/yr)
Single application of Temik in spring (4/1) at 30 lb/acre
Late Summer (8/15) application of miticide (Kelthane), scalicide (Lorsban) and fungicide (Benlate)

*Fertilizer Application Rates depend on tree age

	Fertilizer Application Rates			Nitrogen Rates	
	One Appl.	Split Appl. (kg/ha)		Nitrogen	
Tree Age	kg/ha	2/3	1/3	lb/ac	kg/ha
1 yr	186.7	124.4	62.2	35	39.2
2 yr	266.7	177.8	88.9	50	56.0
3 yr	400.0	266.7	133.3	75	84.0
4 yr	533.3	355.6	177.8	100	112.0
5 yr	560.0	373.3	186.7	105	117.6
6 yr	586.7	391.1	195.6	110	123.2
7 yr	613.3	408.9	204.4	115	128.8
8 yr	666.7	444.4	222.2	125	140.0
9 yr	746.7	497.8	248.9	140	156.8
10+ yr	800.0	533.3	266.7	150	168.0

Micro-Spray Irrigated Citrus - BMP #4, Improved Irrigation Technology

D=Dry year N=Normal year W=Wet year	Irrigated Citrus - EPIC Crop # in USDACROP.DAT = 83 Temik Program, 100% trunk-to-trunk herbicide program			EPIC Tillage #	Irrigation Volume		EPIC Pesticide #	Pesticide Trade Name (Common Name)	Pesticide Application Rates (Active Ingredient)		N Application Rates		P Application Rates (as P) $P_2O_5 = 2.27P$	
	Month	Day	Operation		mm	in			kg/ha	lb/ac	kg/ha	lb/ac	kg/ha	lb/ac
D,N,W	10	7	Weekly Irrigation	72	23.8	0.94								
D,N,W	10	21	Weekly Irrigation/Fertilizer application (N32, 32-0-0)	72/13	23.8	0.94					*	*		
D,N,W	11	4	Weekly Irrigation	72	23.8	0.94								
D,N,W	11	18	Weekly Irrigation/Fertilizer application (N32, 32-0-0)	72/13	23.8	0.94					*	*		
D,N,W	2	15	Weekly Irrigation/Fertilizer application (N32, 32-0-0)	72/13	17.3	0.68					*	*		
D,N,W	2	22	Weekly Irrigation	72	17.3	0.68								
D,N,W	3	1	Weekly Irrigation	72	17.3	0.68								
D,N,W	3	8	Weekly Irrigation	72	17.3	0.68								
D,N,W	3	15	Apply selective herbicide (preemergent)	11			192	Princep (Simazine)	3.53	3.15				
D,N,W	3	15	Apply selective herbicide (preemergent)	11			126	Hyvar X (bromacil)	3.14	2.80				
D,N,W	3	15	Apply contact herbicide	11			204	Roundup (Glyphosate isopropyl amine salt)	1.79	1.60				
D,N,W	3	15	Weekly Irrigation/Fertilizer application (N32, 32-0-0)	72/13	17.3	0.68					*	*		
D,N,W	3	22	Weekly Irrigation	72	17.3	0.68								
D,N,W	3	29	Weekly Irrigation	72	17.3	0.68								
D,N,W	4	1	Apply pesticide, sprayer	11			236	Temik (Aldicarb)	5.04	4.95				
D,N,W	4	5	Weekly Irrigation	72	19.5	0.77								
D,N,W	4	12	Weekly Irrigation/Fertilizer application (N32, 32-0-0)	72/13	19.5	0.77					*	*		
D,N,W	4	15	Inject selective herbicide (preemergent)	11			223	Surflan (Oryzalin)	2.24	2.00				
D,N,W	4	19	Weekly Irrigation	72	19.5	0.77								
D,N,W	4	26	Weekly Irrigation	72	19.5	0.77								
D,N,W	5	2	Weekly Irrigation	72	19.5	0.77								
D,N,W	5	9	Weekly Irrigation	72	19.5	0.77								
D,N,W	5	16	Weekly Irrigation/Fertilizer application (N32, 32-0-0)	72/13	19.5	0.77					*	*		
D,N,W	5	23	Weekly Irrigation	72	19.5	0.77								
D,N,W	5	30	Weekly Irrigation	72	19.5	0.77								
D,N,W	6	6	Weekly Irrigation	72	21.7	0.85								
D,N,W	6	13	Weekly Irrigation/Fertilizer application (N32, 32-0-0)	72/13	21.7	0.85								
D,N,W	6	19	Apply contact herbicide	11			204	Roundup (Glyphosate isopropyl amine salt)	0.28	0.25				
D,N,W	6	20	Weekly Irrigation	72	21.7	0.85								
D,N,W	6	27	Weekly Irrigation	72	21.7	0.85								
D,N,W	7	1	Apply citrus spray oil	11			265	Petroleum Spray Oil	3.36	4.00				
D,N,W	7	1	Apply miticide, sprayer	11			262	Vendex (Fenbutatin oxide)	1.12	1.00				
D,N,W	7	1	Apply fungicide, sprayer	11			272	Kocide (Copper hydroxide)	4.32	3.85				
D,N,W	7	4	Weekly Irrigation	72	23.8	0.94								
D,N,W	7	11	Weekly Irrigation	72	23.8	0.94								
D,N,W	7	18	Weekly Irrigation/Fertilizer application (N32, 32-0-0)	72/13	23.8	0.94					*	*		
D,N,W	7	25	Weekly Irrigation	72	23.8	0.94								
D,N,W	8	1	Weekly Irrigation	72	26	1.03								
D,N,W	8	8	Weekly Irrigation	72	26	1.03								
D,N,W	8	12	Apply selective herbicide (preemergent)	11			192	Princep (Simazine)	3.53	3.15				
D,N,W	8	12	Apply selective herbicide (preemergent)	11			126	Hyvar X (bromacil)	3.14	2.80				
D,N,W	8	12	Apply contact herbicide	11			204	Roundup (Glyphosate isopropyl amine salt)	1.79	1.60				
D,N,W	8	15	Weekly Irrigation/Fertilizer application (N32, 32-0-0)	72/13	26	1.03					*	*		
D,N,W	8	20	Apply scalicide	11			145	Lorsban (Chlorpyrifos)	2.24	2.00				
D,N,W	8	20	Apply miticide, sprayer	11			133	Kelthane (Dicofol)	2.24	2.00				
D,N,W	8	20	Apply fungicide, sprayer	11			39	Benlate (Benomyl)	1.79	1.60				
D,N,W	8	22	Weekly Irrigation/Fertilizer application (N32, 32-0-0)	72/13	26	1.03					*	*		
D,N,W	9	15	Inject selective herbicide (preemergent)	11			110	Solicam (Norflurazon)	2.24	2.00				
D,N,W	10	5	Harvest - Ring Pick	48										

	Monthly Application Rates		
Tree Age	N	N	Fert. Rate
	lb/acre	kg/ha	kg/ha
1 yr	2.8	3.136	9.80
2 yr	4	4.48	14.00
3 yr	6	6.72	21.00
4 yr	8	8.96	28.00
5 yr	8.4	9.408	29.40
6 yr	8.8	9.856	30.80
7 yr	9.2	10.3	32.20
8 yr	10	11.2	35.00
9 yr	11.2	12.54	39.20
10+ yr	12	13.44	42.00

Herbicide Applications (5 Applications/year)
Use less leachable herbicides such as Surflan and Solicam
Treat in the spring (3/15 and 4/15), early summer (6/19), late summer (8/12), and early fall (9/15)
Scalicide/Miticide/Fungicide Applications under Temik Program (3 applications/yr)
Single application of Temik in spring (4/1) at 30 lb/acre
Summer (7/1) application of miticide (Vendex), spray oil and fungicide (Kocide)
Late Summer (8/20) application of miticide (Kelthane), scalicide (Lorsban) and fungicide (Benlate)

* Fertilizer Application Rates depend on tree age
Liquid Fertilizer (80% of that applied to flood irrigated groves)
applied monthly (10 months)
N32 applied with irrigation water monthly (10 months)